
**University of Natural Resources and Life Sciences, Vienna**

Department for Agrobiotechnology Tulln, Center for Analytical Chemistry

# Elucidation of $\beta$-Lactam Conjugates and a $\beta$-Lactam Receptor Protein for their Application in Lateral Flow Devices for the Detection of Antibiotic Residues

**Master Thesis**

submitted in partial fulfillment of the requirements for the degree

Diplomingenieur (Dipl.-Ing.)

under supervision of

**Univ.Prof. Dipl.-Ing. Dr.techn. Rudolf Krska**

and under co-supervision of

**Ass.Prof. Dipl.-Ing. Dr.nat.techn. Sabine Baumgartner**

by

**Eva Esther König B.Sc.**

- Tulln, August 2012 -

# Abstract

To avoid using labor- and instrumental-intensive methods to detect residues of antibiotics in liquid samples, a competitive lateral flow device was developed using a commercially purchased polyclonal antibody raised against ampicillin-BSA. $\beta$-lactam-protein conjugates, employing bovine serum albumin, ovalbumin, and keyhole limpet hemocyanin as carrier proteins, and tetracycline-BSA bioconjugates intended for use as test line capture reagent were synthesized. Those were characterized by LDS-PAGE and the 2,4,6-trinitrobenzene sulfonic acid assay in this research. Haptens were coupled to carrier proteins via the N-hydroxysuccinimide active ester method, the carbamate linkage method, or the diazonium conjugation method. Penicillin G-BSA conjugates with a coupling ratio of 1:50 were used to set up the competitive antibody-based lateral flow device. Initial experiments resulted in a detection limit of 0.3 ppb and a limit of quantification of 0.6 ppb using penicillin G as analyte. Thus, the polyclonal antibody against ampicillin-BSA could be the basis for further investigations.

As detector reagent, 40 nm gold nanoparticles with an UV/Vis absorption spectroscopy maximum of 529 nm were used. Gold solution titration experiments figured out that coupling of 8 µg anti-ampicillin-BSA antibody/mL colloidal gold resulted in stable gold conjugates. By contrast, the commercially obtained protein A purified anti-tetracycline antibody was not able to stabilize colloidal gold particles.

Moreover, a soluble derivative of the penicillin binding protein 2x from *Streptococcus pneumonia* was expressed as a recombinant glutathione S-transferase fusionprotein in *Escherichia coli* BL21(DE3) in order to design a receptor-based strip test. Nevertheless, it was figured out that the unstable fusionprotein did not lead to PBP2x* or PBP2x*-GST labeled gold nanoparticles, since only the GST-tag moiety of the fusionprotein preferably bound to gold nanoparticles.

# Kurzfassung

Der Einsatz von Lateral Flow Devices hat für das Monitoring von Kontaminationen in der Tierproduktion große Bedeutung erlangt. Ziel dieser Masterarbeit war es, die unterschiedlichen Grundbausteine eines LFDs zum Nachweis von Antibiotikarückständen zu produzieren und zu evaluieren.

$\beta$-Lactam Konjugate mit bovinem Serumalbumin, Ovalbumin und Keyhole Limpet Hemocyanin als Trägerprotein und Tetracycline-BSA Konjugate wurden synthetisiert und als Testlinenreagenzien eingesetzt. Folgende Kopplungsverfahren wurden angewandt: die Aktivester-Methode mit N-Hydroxysuccinimid, die Carbamat-Verknüpfungsmethode und die Diazoniumkonjugation. Die synthetisierten Hapten-Protein-Konjugate wurden mittels LDS-PAGE und dem 2,4,6-Trinitrobenzolsulfonsäure Assay charakterisiert. Als Detektionsreagenz wurde kolloidales Gold mit einer Partikelgröße von 40 nm eingesetzt. Die Koppelung von 8 µg des anti-Ampicillin-BSA Antikörpers/mL kolloidalem Gold resultierte in stabilen Goldkonjugaten. Hingegen konnte der ebenfalls kommerziell erhältliche, Protein A gereinigte anti-Tetracycline Antikörper die Goldnanopartikel nicht stabilisieren. Penicillin G-BSA Konjugate mit einer Kopplungsdichte von 1:50 wurden im Prototyp eingesetzt um den kommerziell erhältlichen polyklonalen Antikörper (Immunogen: Ampicillin-BSA) zu evaluieren. Der entwickelte Prototyp hat eine Nachweisgrenze von 0.3 ppb und ein Quantifikationsgrenze von 0.6 ppb bei der Verwendung von Penicillin G als Analyt. Demnach ist dieser polyklonale Antikörper für den Einsatz in einem LFD für die Detektion von $\beta$-lactam Rückständen geeignet.

Außerdem wurde ein lösliches Derivative des Penicillin-bindenden Proteins 2x von *Streptococcus pneumonia* als Glutahion S-transferase Fusionsprotein in *E. coli* BL21(DE3) exprimiert um einen Rezeptor-basierenden LFD zu entwickeln. Aufgrund der stabileren Kopplung des GST-tags an Goldpartikel war es nicht möglich PBP2x*-AuC oder PBP2x*-GST-AuC Konjugate zu erhalten, wenn eine Proteinlösung des instabilen Fusionsprotein eingesetzt wurde.

# Acknowledgements

First, I would like to express my gratitude to Univ.Prof. Dipl.-Ing. Dr. techn. Rudolf Krska for the opportunity to write my diploma thesis at the Department for Agrarbiotechnology, Tulln.

I want to thank my supervisor Ass. Prof. Dipl.-Ing. Dr. Sabine Baumgartner and my co-supervisor Dipl.-Ing. Barbara Cvak for their enduring support during my master thesis. The doors to their offices were always open whenever I ran into a trouble spot or had a question about our research or writing.

As, my studies were performed in cooperation with Romer Labs Division Holding GmbH, I would like to acknowledge Dr. Hannes Binder for making this thesis possible.

I am grateful to Romer Labs Division Holding GmbH and the Austrian Research Promotion Agency (FFG) (FEMtech program of the Federal Ministry for Transport, Innovation and Technology (BMVIT), FFG project number 825151/F4S) for financial support.

Thanks are also due to Prof. Dr. Regine Hackenbeck and due to Dr. Patrick Maurer from the University of Kaiserslautern for providing us the plasmid 'pGEX-6P1-tet-PBP2x*'.

I would also like to acknowledge the staff and colleagues (Antonia, Brigitte, Jenny, Judith, Kathi, Manuela and Parisa) at the Christian Doppler Laboratory for Rapid Test Systems for Allergenic Food Contaminants for their precious help and the kind working atmosphere.

Moreover, I give my thanks to all my colleagues at RomerLabs Diagnostic GmbH for their assistance. Especially, I am grateful to Dipl.-Ing. Georg Häubl for his support with conjugate synthesis, to Ass. Prof. Dipl.-Ing. Dr. Roman Labuda for his assistance with fermentation and to Mag. Andreas Firzinger for performing agarose gel electrophoreses. Additionally, I want to thank our research technician Julia and both trainees, Bernadette and Bernhard.

Further, I wish to extend special thanks to Dr. Dieter Moll and Alex Frank (Biomin Holding

GmbH) for their cooperative work in cloning and expression of PBP2x* and providing chemically competent cells.

Moreover, I would like to thank Dipl.-Ing. Dr. Alexandra Molinelli for taking time to read and comment my thesis.

Above all, I am deeply indebted to my parents, my sister Lisa, and my 'sunshine' Florian, who supported and believed in me.

# Contents

# List of Figures

# List of Tables

# Abbreviations

Abbreviations for chemicals are given in the Method section.

| | |
|---|---|
| Aa | amino acid |
| Ab | antibody |
| Abs | absorption |
| BB | borate buffer |
| CO | cut-off |
| Conc. | concentration |
| CV | column volumes |
| Da | dalton |
| EC | European commission |
| Hmw | high-molecular-weight |
| LB | Luria-Bertani |
| LFD | lateral flow device |
| lmw | low-molecular-weight |
| Max | maximum |
| MCR | molecular coupling ratio (protein:hapten) |
| MTP | used assay buffer, composition is given in the Materials section 3.5 |
| MW | molecular weight |
| MRL | maximum residue limits |
| NC | nitrocellulose |

| | |
|---|---|
| PAGE | polyacrylamide gel electrophoresis |
| PB | penicillin-binding |
| PBS | phosphate buffered saline |
| pGEX | plasmid for glutathion S-transferease expression |
| Ppb | part per billion, $10^{-9}$ $\mu g\,kg^{-1}$ |
| Ppm | part per million, $10^{-6}$ $mg\,kg^{-1}$ |
| Rpm | Revolutions per minute |
| SBGT | used assay buffer, composition is given in the Materials section 3.5 |
| *S.* | *Streptococcus* |
| St. dev. | standard deviation |
| SOC | super optimal broth with catabolite repression |
| SPR | surface plasmon resonance |
| Tet | tetracycline (supplemented to media) |
| TL | test line |
| TP | DD-transpeptidase |
| UV/Vis | ultraviolet/visible |
| X-buffer | used assay buffer, composition is given in the Materials section 3.5 |

# 1 Introduction

$\beta$-lactam antibiotics, i.e. penicillins and cephalosporins, are among the most widely used antibiotics for the treatment of bacterial infections (e.g. mastitis, an inflammation of the udder) in lactating dairy cows. Passage of antibiotics into milk from medicated animals is of great concern regarding the quality of milk and public health [1]. In the dairy industry, antibiotics can inhibit starter cultures used in the production of fermented products, such as yoghurt and cheese [1, 2]. This may result in a considerable economic loss as product batches may be downgraded or discarded. Further, antibiotic residues from animal-based food can affect human health. $\beta$-lactams are not toxic to humans, but they can provoke an allergic immune response in sensitized individuals [2, 3]. Nevertheless, it is unlikely that antibiotic residues would cause allergic responses, because of the low drug concentration in contaminated food [4]. The rarity of reported cases shows that the risk is small [5]. Additionally, antibiotic residues can impact microflora in the human gastrointestinal tract [6]. Since the continuous exposure may lead to an increase in the number of individuals resistant to antibiotics [7], the emergence of antibiotic-resistant strains of bacteria should be prevented by manufacturing food products without any antibiotic residues. Actually, the correlation between antibiotic applications in food-producing animals and the increase of antibiotic resistance strains of human-pathogenic bacteria is discussed [8]. Resumed, consumers should be insured to consume non-contaminated products, free from antibiotic residues [2].

Thus, maximum residue limits (MRLs) have been specified by the European Union for $\beta$-lactams and other veterinarian drugs, which are approved for use in food-producing animals [9]. To meet the requirements of the dairy industry, several rapid tests for the detection of $\beta$-lactams or cephalosporins residues in milk at or below their MRL values are commercially available. These tests are easy and rapid (approx. 10 min) to perform, sensitive, and specific.

One aim of the FFG project 825151/F4S is to develop a lateral flow device for the detection of $\beta$-lactam and tetracycline antibiotic residues in raw commingled bovine milk. This thesis

focuses on the synthesis of hapten-protein conjugates used as capture reagent, the recombinant expression of the soluble derivative of the penicillin binding protein PBP2x of *Streptococcus pneumoniae* (PBP2x*) as glutathione S-transferase (GST) fusionprotein, the production of colloidal gold (AuC) sol, and labeling AuC with PBP2x*-GST fusionprotein and a commercially purchased anti-$\beta$-lactam antibody. Further, the influence of different assay conditions on the assay performance are discussed.

# 2 Literature review

## 2.1 Antimicrobial residues in milk

The major reason for the use of anti-infectious agents in dairy cattle is the control of bovine mastitis. The pharmacokinetics of antibiotics in the lactating cow are mainly referred to the route of administration, the dose and the number of treatments, physicochemical properties of the excipient, the milk production, and the condition of the udder. Because of drawbacks of residues of veterinarian drugs in milk [10], which are already discussed above, milk from animals under antibiotic treatment or in the withdrawal period must not enter the food chain. For this purpose, European legislation requires the food business operators to test a representative number of random samples of raw milk to monitor the effectiveness of the initiated procedures and withdrawal periods, as explained in Section 2.1.2.

### 2.1.1 Milk as sample

Milk is a translucent white liquid, produced by the mammary glands of mammals. Since milk contains significant amounts of fat, protein, lactose, calcium, and vitamin C, its nutritional value is high. The composition of milk, regarding different animal species and breed variations, is given by Reybroeck [10]. The primary group of milk proteins (approx. 80%) are the caseins, which form micellar structures by noncovalent aggregations. All other proteins, grouped together as whey proteins, are more water-soluble than the caseins and do not aggregate into micelles. Concentration, molecular weight, and potential biological function of major bioactive protein components of bovine milk are given by Park *et al.* [11, Table 2.1]. The milk lipids form fat globules surrounded by a membrane of phospholipids and proteins [10].

Different stability studies of antibiotics and chemotherapeutics in milk have been published. A summary can be found in Reybroeck [10]. It was figured out that storage of milk at 4 °C resulted in a great measurable loss of $\beta$-lactams, whereas storage at −76 °C did not. In case of tetracyclines, published degradation studies were divergent.

### 2.1.2 Legislative Aspects

To guarantee that food of animal origin is free from antimicrobial residues, regulations were set by the European Union. Regulation EC 853/2004 laying down specific hygiene rules for food of animal origin [12]: According to regulation EC 853/2004, food business operators must initiate procedures to ensure that raw milk is not placed on the market, if it contains antibiotic residues in excess of the maximum residue limit. Furthermore, it requires that a representative number of random samples of raw milk must be tested to monitor the effectiveness of the initiated procedures. These random tests may be performed at various points of the supply chain, such as producers (on farm), collectors, or processors. Here, the MRLs are set for raw milk and not for processed milk or dairy products. Note that the regulation does not apply to milk of animals that have not been treated with antibiotics, unless the milk is mixed with milk from animals that have been treated with antibiotics. Regulation EC 1774/2002 laying down health rules concerning animal by-products not intended for human consumption [13]: milk samples with antibiotic residues above the MRLs should be disposed of as a category 2 animal by-product. Either the positive result of the primary screening test (test fail) is accepted or a second quantitative sample measurement is performed to identify antibiotics and determine their concentration. Note that the time between the primary screening test and the verification test should be less than 24 h [14]. Council Directive 96/23/EC on measures to monitor certain substances and residues thereof in live animals and animal products [15], lays down measures to monitor the substances and groups of residues listed in Annex 1. Regulation EC 470/2009 laid down Community procedures for the establishment of residue limits of pharmacologically active substances in foodstuffs of animal origin (repealing Council Regulation EEC 2377/90 and amending Directive 2001/82/EC and Regulation EC 726/2004) [16]. In regulation 37/2010 on pharmacologically active substances and their classification regarding maximum residue limits in foodstuffs of animal origin [9], all the pharmacologically active substances were listed in one Annex in alphabetical order. MRLs have been established in different matrices for sulfonamides, $\beta$-lactams, tetracyclines, macrolides, quinolones, and aminoglycosides, while the use of chloramphenicol and nitrofurans was prohibited in the EC.

The MRL, expressed in $\mu g\,kg^{-1}$, is the maximum concentration of residues in a product (milk, meat, egg and so on) considered by the authorities as without sanitary hazard for the consumer

and without effect on the manufacturing process. In Table 2.1 the EU MRLs for $\beta$-lactams and tetracyclines in milk are outlined.

Table 2.1: Pharmacologically active substances and their classification regarding MRL [9].

| Group | Pharmacologically active substance | Marker residue | MRL ($\mu g\,kg^{-1}$) |
|---|---|---|---|
| Penicillins | Benzylpenicillin | Benzylpenicillin | 4 |
| | Ampicillin | Ampicillin | 4 |
| | Amoxicillin | Amoxicillin | 4 |
| | Oxacillin | Oxacillin | 30 |
| | Cloxacillin | Cloxacillin | 30 |
| | Dicloxacillin | Dicloxacillin | 30 |
| | Nafcillin | Nafcillin | 30 |
| | Penethamate | Benzylpenicillin | 4 |
| Cephalosporins | Ceftiofur | Sum of all residues retaining the $\beta$-lactam structure expressed as desfuroylceftiofur | 100 |
| | Cefquinome | Cefquinome | 20 |
| | Cefazolin | Cefazolin | 50 |
| | Cephapirin | Sum of cephaprin and desacetyl-cephapirin | 60 |
| | Cefacetrile | Cefacetrile | 125 |
| | Cefoperazone | Cefoperazone | 50 |
| | Cefalexin | Cefalexin | 100 |
| | Cefalonium | Cefalonium | 20 |
| Tetracyclines | Tetracycline | Sum of parent drug and its 4-epimer | 100 |
| | Oxytetracycline | Sum of parent drug and its 4-epimer | 100 |
| | Chlortetracycline | Sum of parent drug and its 4-epimer | 100 |

### 2.1.3 Assays for the control of antibiotic residues in milk

Samples (e.g. milk) suspected to contain antibiotic residues can be analyzed by rapid screening tests, which are shortly discussed below. In order to confirm the residue presence in the sample, physicochemical analysis such as HPLC or LC-MS/MS are employed [10, 17]. In recent years, surface plasmon resonance (SPR) biosensors were investigated for the detection of $\beta$-lactam antibiotics [1, 2, 8]. Generally, four types of rapid screening tests are mostly used and currently commercially available:

- Enzyme-linked immunosorbent assays (ELISA) for monitoring single veterinary milk drug residues such as chloramphenicol as well as multi-screening ELISAs are offered by e.g. EuroProxima, EuroClone SpA, Tecna Srl, BioControl Systems Inc., R-Biopharm AG, BiooScientific Corporation, and Randox Laboratories Ltd.
- Lateral flow devices (LFD) are available from Charm Sciences Inc., Twinsensor$^{BT}$, Tetrasensor$^{BT}$, Neogen Corporation, IDEXX Laboratories Inc., and BiooScientific Corporation. These products cover most of the commonly tested antibiotic groups in milk which are $\beta$-lactams and tetracyclines and further the single antibiotic tests for sulfamethazine, sulfadimethoxine, enrofloxacin, and gentamicin.
- Microbial inhibition tests can be purchased from DSM Food Specialties B.V., Charm Sciences Inc., Zeu-Inmunotec S.L., EuroClone SpA, and Copan Italia SpA.
- A enzymatic colorimetric assay is offered by UCB Bioproducts Belgium.

Navrátilová [18] summarized in detail the commercially available screening methods used for the detection of veterinary drug residues in raw cow milk. Here, a short overview about the principles is given.

Enzyme-linked immunosorbent assays are well-established tools for analyzing antibiotic residues. Mostly, the direct competitive assay format is used, $\beta$-lactams, if present in the standard and sample, compete for example with horseradish peroxidase labeled conjugate for capture antibody binding sites on the microtiter plate. Hence, the measured absorbance is inversely proportional to the concentration of the analyte. Beside antibodies raised against $\beta$-lactams (e.g. available from Randox), the penicillin binding protein 2x* (see Section 2.2.6) was used in a microtiter plate test [19].

The principle of lateral flow devices is briefly described in Section 2.3. Generally, lateral flow devices can be divided into immunoassays using antibodies and receptor/enzyme-based assays employing enzymes. To our knowledge, each commercially available lateral flow device for detection of $\beta$-lactam antibiotics employs a receptor-based assay format by means of applying a penicillin binding protein. Commercial LFDs for milk, animal tissues, and honey are reviewed by Wang *et al.* [17]. An overview about enzyme-based LFDs employing penicillin binding proteins is given by Cacciatore [8, Table 2].

Microbiological screening is based on the property of antibiotics to inhibit the growth of the test organism. Microorganisms employed as test bacteria are not equally sensitive to all antibiotics. As a consequence, they detect some substances better than others. Combinations of different test bacteria, each in an optimal medium, are applied to detect a large range of antibiotics up to the MRL levels [10]. Time is here a factor since the sample is incubated for 3 h in the ampule containing the agar medium at an appropriate temperature.

The enzymatic colorimetric assay is based on the inactivation of the DD-carboxypeptidase enzyme by $\beta$-lactams followed by the addition of its natural substrate. The degree of inactivation is determined by an organic redox indicator detecting the not cleaved natural substrate. For further explanation see Navrátilová [18].

While microbial inhibition tests and LFDs may be used on-site (farm, raid tankers, storage silos, milk reception sites), ELISA tests and confirmatory tests are restricted to laboratory use.

### 2.1.4 Anti-infectious agents

Tetracyclines are next to $\beta$-lactam antibiotics, macrolides, and sulfonamide the most commonly used antibiotics for the treatment of farm animals in Austria [20]. Here, $\beta$-lactam and tetracyclines should be discussed shortly.

The antibacterial effect of *$\beta$-lactam antibiotics*, i.e. penicillins and cephalosporins, is owing to their inhibition of bacterial cell wall synthesis (see Section 2.2). Those antibiotics consist of a four-membered $\beta$-lactam ring, which is fused to either a five- or a six-membered sulfur-containing heterocyclic ring (Figure 2.1) in case of penicillins or cephalosporins, respectively. An overview about chemical properties, reactivity, and chemical structures of $\beta$-lactam antibiotics, which are

relevant for residue testing, are given by e.g. Lamer [19] and Cacciatore [8].

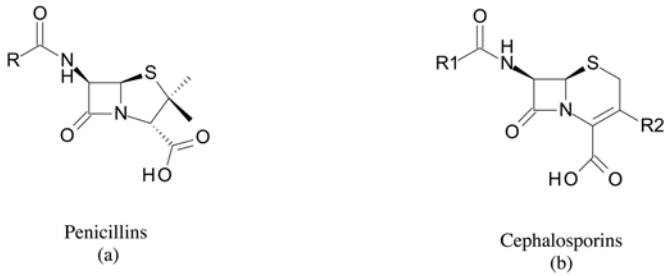


Figure 2.1: Penicillin and cephalosporin core structures, where 'R' are the variable groups.

*Tetracyclines* (TCs) are broad spectrum antibiotics, showing a great activity against a variety of gram-positive and gram-negative bacteria. TCs act through inhibition of protein synthesis by binding to the small ribosomal subunit at the A site. Tetracycline, oxytetracycline, and chlortetracycline are natural products [10]. The core structure of TCs is illustrated in Figure 2.2. An overview about chemical properties and chemical structures of all TC is given by Möller [21].

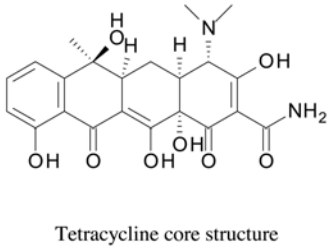


Figure 2.2: Tetracycline core structure.

## 2.2 Penicillin binding protein

Penicillin binding proteins (PBPs) catalyze the last stages in the polymerization of peptidoglycan (also known as murein), the major compound of the cell wall in gram-positive bacteria. Murein is essential in cell division and protects bacteria from osmotic shock and lysis. The antibacterial effect of $\beta$-lactam antibiotics, like penicillins and cephalosporins, is based upon the inhibition of those proteins. This results in a weak cell wall, causing the microbe to swell and burst. $\beta$-lactams are most effective on rapidly multiplying bacteria [22]. Intense research has been carried out on PBPs, particularly on their role in the resistance to $\beta$-lactams of some important pathogens such as *S. pneumoniae* [23], causing pneumonia. The resistance to $\beta$-lactams in *Streptococcus pneumoniae*, for example, occurs from the alteration of the sequence and structure of its PBPs [24]. A review on PBP-based $\beta$-lactam resistance is published by Zapun *et al.* [23].

PBPs are used as receptor proteins for detection of the active form of the $\beta$-lactam structure, e.g. in milk. PBPs have been applied in commercially available receptor-based lateral flow devices (e.g. DD-carboxylase from *Streptomyces* is used in the enzyme-based Penzym test [18]) as well as in SPR biosensor analysis of $\beta$-lactam antibiotics in milk [1, 2, 8]. Generally, the advantage of using PBPs compared to antibodies in methods for residue detection is that PBPs specifically interact with the active form of the $\beta$-lactams. The $\beta$-lactam ring structure is easily hydrolyzed, whereby the substance becomes inactivated. MRLs are set for the pharmacologically active substance (see Table 2.1), it is important that only these forms are detected. Taking the instability of the $\beta$-lactam structure into account, the production of group-specific antibodies against the active $\beta$-lactam structure is complex [2].

### 2.2.1 Classification

PBPs can be classified into high-molecular-weight (hmw) PBPs and low-molecular-weight (lmw) PBPs [25, 26]. Hmw PBPs can be further divided into class A and class B, depending on the structure and the activity of the N-terminal domain [26]. Both classes carry a C-terminal penicillin binding (PB) domain with a transpeptidase activity. Because of the glycosyltransferase activity of the N-terminal domain of class A PBPs, those proteins are bifunctional enzymes, which are responsible for both polymerization of the glycan strain and peptide crosslinking. Whereas, class B PBPs are monofunctional transpeptidases with a non-catalytic periplasmic N-terminal domain whose function is unknown [27]. For more detailed information, a clearly represented classification of a complete set of PBPs from 10 bacteria is given by Sauvage *et al.* [28, Figure 1].

### 2.2.2 Mureinsynthesis

PBPs are involved in the synthesis of Murein, a mesh net-like product that surrounds and protects bacteria [28]. Murein consists of glycan chains of alternating *N*-Acetylglucosamine (GlcNAc) and *N*-acetylmuramic acid (MurNAc) crosslinked by peptides attached to N-acetylmuramic acid. PBPs catalyze the polymerization of the glycan strains (transglycosylase) and the crosslinking between glycan chains (transpeptidase). Some PBPs can hydrolyze the last D-alanine of stem pentapeptides (DD-carboxypeptidase) or hydrolyze the peptide bond joining two glycan strains (endopeptidase). A basic reaction scheme of the biosynthesis of murein is given in various

textbooks, e.g. Fuchs and Schlegel [29]. Sauvage *et al.* [28] reviewed the structure and role of PBPs regarding their implication in peptidoglycan synthesis.

### 2.2.3 Penicillin binding domain

PBPs are characterized by a common DD-peptidase activity, whether a DD-carboxypeptidase, a DD-transpeptidase, or a DD-endopeptidase activity [25, 26]. These enzymatic activities are catalyzed by a common penicillin binding (PB) domain [28]. The PB domain consists of an $\alpha$-helical subdomain and an $\alpha/\beta$ subdomain and harbors three highly conserved motifs: SXXK, (S/Y)XN, and (K/H)(S/T)G. This distinctive feature is characteristic to the family of penicillin-recognizing active-site serine enzymes (ASPRE) [25], to which PBPs and $\beta$-lactamases are constituted. The topology of PBP2x of *S. pneumoniae*, a transpeptidase, is shown in Figure 2.3. The SXXK motif is on the N-terminus of helix $\alpha$2 of the helical subdomain. The second SXN motif is on a loop between helix 4 and 5 of the helical subdomain. The KTG motif is located on strand $\beta$3 of the $\alpha/\beta$ sub-domain.

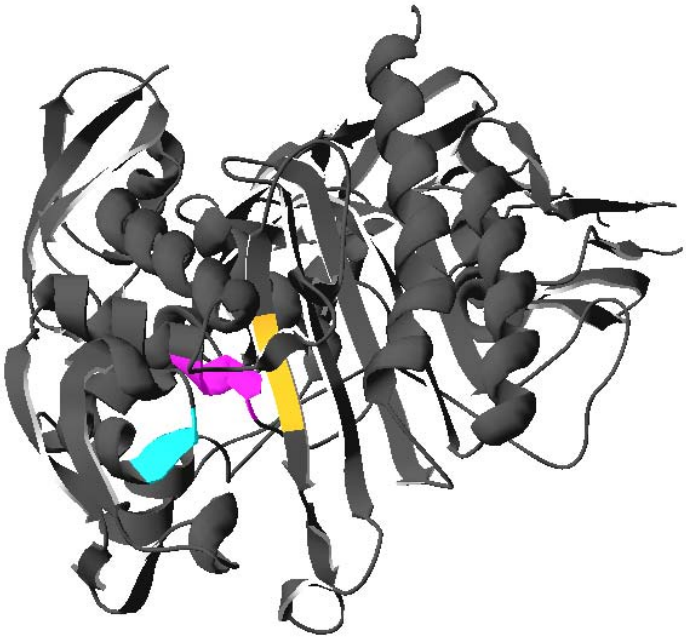

Figure 2.3: Topology of the penicillin-binding domain of PBP2x (PDB-Code: 1QME). The SXXK motif (purple) is on the bottom of the active-site groove in this representation. The KTG motif (yellow) and the SXN motif (turquoise) are located on the right side and on the left side of the active side, respectively.

### 2.2.4 Catalytic mechanism of DD-transpeptidase

The transpeptidation, the major target of $\beta$-lactam antibiotics, has been accurately analyzed. This reaction occurs in two steps as outlined in Figure 2.4. First, there is a nucleophilic attack by the hydroxyl group of the serine residue in the active site (in the SXXK motif) on the carbonyl carbon of the penultimate D-Ala amino acid of the stem peptide, resulting in the removal of the last D-Ala and the formation of a covalent acyl-enzyme intermediate between the 'donor' stem peptide and the transpeptidase. Then, the newly formed ester bond between the D-Ala and the active-site serine is subjected to a nucleophilic attack by the primary amine of the third residue of a second 'acceptor' stem peptide. The newly formed amide bond crosslinks both stem peptides. Further, the hydroxyl group in the active-site serine is regenerated [23, 30]

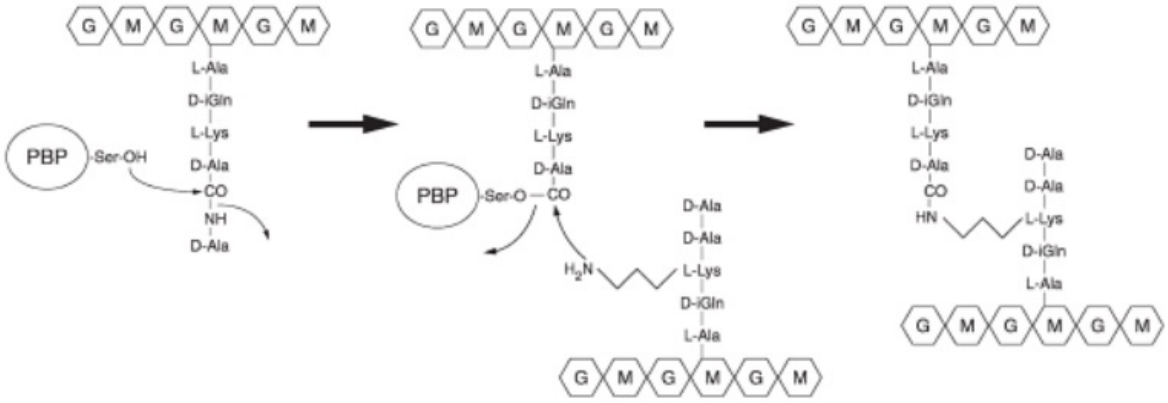


Figure 2.4: Transpeptidation reaction. The glycan strains are depicted by chains of hexagons standing for the hexoses GluNAc (G) and MurNAc (M). The 'donor' peptide is bound to the upper glycan strand, whereas the 'acceptor' peptide is depicted here on the lower strand. The peptides shown are those from *S. pneumoniae* [23, Figure 2].

### 2.2.5 Interaction of DD-transpeptidase with $\beta$-lactams

Because of the structural similarity between $\beta$-lactams and the natural substrate, D-Ala-D-Ala, of TPs (Figure 2.5), PBPs are inhibited by $\beta$-lactams by forming a relatively stable, covalent penicilloyl-enzyme-complex. The bound $\beta$-lactam sterically hampers the access path of acceptor molecules with the result that no $\beta$-lactam can be transfered to the acceptor peptide. Bound $\beta$-lactams can only be released by water molecules, because they are able to enter into the active site [19]. The inhibition mechanism is schematically presented in Figure 2.6.

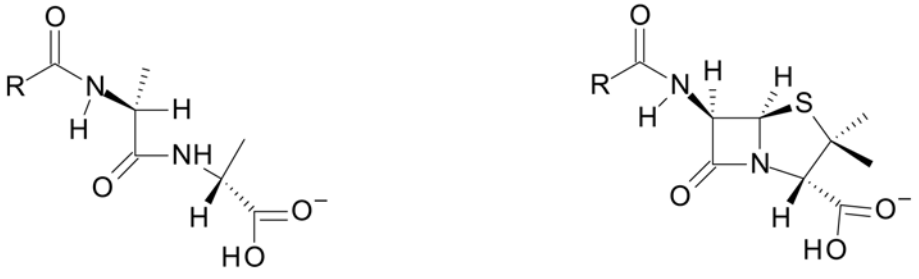

N-acyl-D-alanyl-D-alanine peptide (a)

Penicillin-backbone (b)

Figure 2.5: Structural similarity between $\beta$-lactams and the natural substrate of PBPs, adapted from Mayers *et al.* [23].

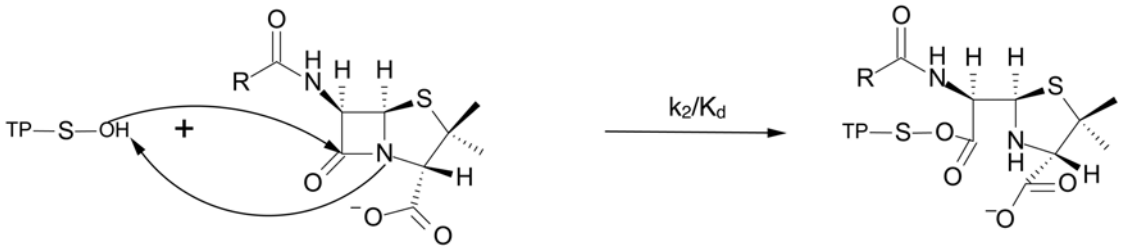


Figure 2.6: The penicillin-interactive, serine active site of PBPs. Adapted from Mascaretti [31].

PBSs kinetically interact with $\beta$-lactams in the following scheme: After forming a noncovlaent complex EI between the enzyme E and the inhibitor I with the dissociation constant $K_d$, acylation occurs to form the covalent complex EI* with the rate $k_2$. Finally, EI* is hydrolyzed with the rate $k_3$ to E and the inactivated product P (penicilloate). The $k_3$ constant is very low and a very slow breakdown of the acyl-protein or even complete inertness occurs [31]. Both $k_2$ and $k_3$ are first-order rate constants. The second order rate constant $k_2/K_d$ ($M^{-1}$ $s^{-1}$) describes the efficiency of acylation, allowing for the calculation of the overall acylation range at a given concentration of antibiotics [23]. Hence, the inhibition efficiency increases with the increased $k_2/K_d$ constant value. Kinetic parameters of PBP2x*, a soluble derivative of the PBP2x from *S. pneumoniae*, are outlined in Table 2.2.

$$E + I \underset{k_{-1}}{\overset{k_1}{\rightleftharpoons}} EI \xrightarrow{k_2} EI^* \xrightarrow{k_3} E + P \tag{2.1}$$

### 2.2.6 PBP2x of *Streptococcus pneumoniae*

*S. pneumonia* contains five hmw PBPs (1a, 1b, 2x, 2a, and 2b) [32] and a lmw PBP (3) [33]. PBP2x is a hmw class B PBPs with a molecular weight of 82.35 kDa [34]. A schematic overview of the PBP2x from *S. pneumoniae* penicillin-susceptible R6 strain is shown in Figure 2.7. Relevant elements of secondary structure are represented above the open boxes. Amino acids belonging to conserved sequence motifs characteristic of ASPRE family are indicated below the open boxes together with their position in the amino acid sequence. PBP2x consists of a short cytoplasmic region (aa 1-18), a transmembrane region (aa 19-49), a non-penicillin-binding domain (nPB domain; aa 50-266), a penicillin-binding transpeptidase domain (TP domain; 267-616), and a COOH-terminal domain (C-ter.; aa 617-750). Amino acids most frequently replaced in clinical isolates or laboratory mutants are indicated below the open box [35].

In this thesis, the soluble PBP2x derivative (PBP2x*) - lacking the hydrophobic transmembrane domain (delta amino acids 10 to 48) [36] - was under investigation. PPB2x* possesses high affinities to penicllins and cephalosporins (Table 2.2) [37, 38]. Further, the soluble PBP2x* is stable over several months, which substantiate the structural independence of the hydrophilic main part of PBP [36]. Therefore, PBP2x* might be suitable for the application in a receptor-based strip test.

Table 2.2: Kinetic parameters for the interaction between $\beta$-lactam antibiotics and PBP2x* from *S. pneumoniae* [37, 38]. Kinetic parameters are described above.

| $\beta$-lactams | $k_2/K$ ($M^{-1}$ $s^{-1}$) |
|---|---|
| Benzylpenicillin | 58,000 |
| Ampicillin | 67,000 |
| Oxacillin | 21,000 |
| Cephalexine | 1,400 |

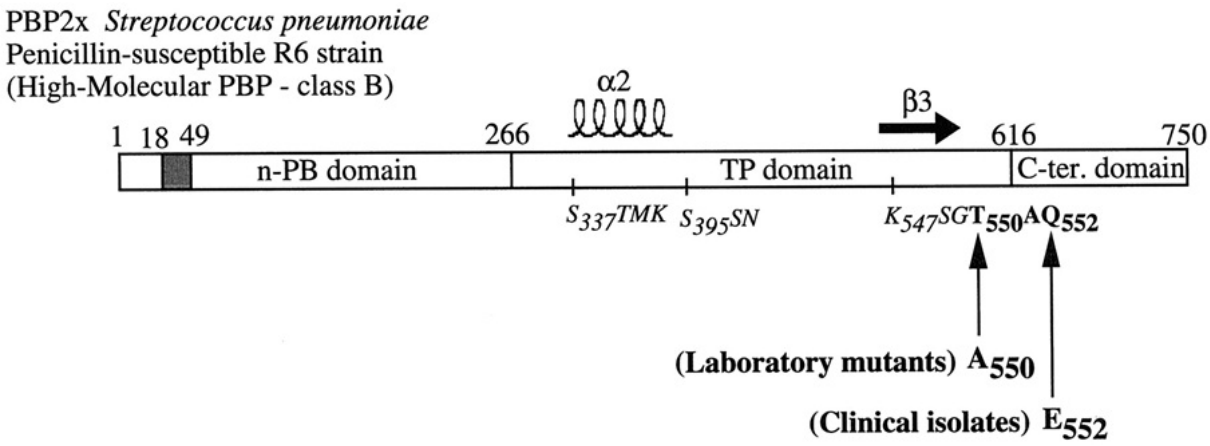


Figure 2.7: Schematic representation of the hmw PBP2x. class B of *S. pneumoniae* penicillin-susceptible R6 strain. This Figure is taken form Mouz *et al.* [35]. Explanations see text.

## 2.3 Lateral flow devices (LFDs)

Lateral flow devices (LFD), also known as 'lateral flow immunoassay', 'dip-stick immunoassay', or simply 'strip tests' are membrane-based immunochromatographic tests. LFD technology is widely used in point-of-care (POC) or field use applications (e.g. medical diagnostic, blood banking, agriculture, forensic science, and food safety). Especially in the food safety area, residue detection should be user-friendly, accurate, rapid, inexpensive, and feasible regarding to field or on-site applications.

Although dipstick assays are easy to perform, even for untrained users, the technology behind is advanced and elaborated [17]. Since the LFD technology becomes prevalent in various applications, a considerable number of articles, books, and technical publications dealing with the LFD technology have been published in recent years. Both Millipore´s [39] and GE Healthcare´s [40] technical publications on LFD thoroughly describe the properties and specification of various membrane, sample pad, and conjugate pad materials and provide a guide for product development. Further, several articles [41–45] concerning LFD development, trouble shooting, and processing methods are published in the IVD (Technology for in vitro diagnostics development and manufacturing) online magazine. Posthuma-Trumpie *et al.* [46] presented a literature survey concerning LFD discussing numerous aspects of this technology. 'Immunoassays in Agricultural Biotechnology' by Shan [47] and 'Chemical Analysis of Antibiotic Residues in Food' by Wang *et al.* [17], outlining various aspects of LFD technology and applications in food

safety, were recently published.

### 2.3.1 Architecture of a lateral flow device

A typical test strip is composed of multiple component parts, each serving one or more purposes [17, 48]. The employed materials can be classified into three categories [49]:

1. Porous materials are layered onto an adhesive backing card. The pads and membranes have to overlap one another in order to maintain a continuous flow path for the sample [39].
   a) The sample pad is an absorbent pad placed at one end of the strip onto which the sample is applied. Impregnation with components such as proteins, detergents, viscosity enhancers, and buffer salts can lead to filtration of unwanted sample components [47], increased sample viscosity, and/or to a modified chemical nature of the sample so that it is compatible with immunocomplex formation [39].
   b) The conjugate or reagent pad, located adjacent to the sample pad, contains labeled analyte or analyte-specific antibodies depending on the applied assay format [17, 47] and is ordinarily made from glass fibers, cellulose filters, or surface-modified polyesters [39].
   c) The reaction membrane, where the test line reagent (e.g. analyte-protein conjugate, anti-target analyte antibodies) and the control line reagent (e.g. anti-species specific antibody) are immobilized, are mostly made from nitrocellulose. However, various polymers such as nitrocellulose, cellulose acetate, nylon, and polysulfones may be used as well [47]. The two key parameters for the membrane selection are: capillary flow characteristics and the ability to irreversibly bind capture reagents at the test and control lines [39, 47].
   d) The wick pad, a further absorbent pad, is designed to draw excess buffer and reagent in order to avoid back-flow onto the reaction membrane and to enhance flow through the membrane.
2. Various reagents, depending on the assay format and requirements, are used.
   a) Antibodies may be employed as a capture reagent at the test line, as a conjugate on the detector particle, or both [39]. Additionally, antibodies may be used as capture reagent at the control line.

b) In case of an independent control line, e.g. Biotin-BSA (CL) and Streptavidin-AuC conjugates are used.

c) Bioconjugates (analyte-protein conjugates, hapten-protein conjugates) are applied as test line in case of competitive reaction schemes.

d) Detector particles (e.g. latex beads, colloidal gold particles) are used for the visualization of the signal.

e) Reagents such as blocking agents, detergents, surfactants, stabilizer, and/or buffer salts [49] are added to the assay buffer or impregnated onto the sample or conjugate pad in order to accomplish the performance requirements regarding to wettability, capillary flow rate, protein binding, stability, and so on.

3. Housing and lamination materials:

a) Backing cards are used to properly align pads and membranes in a test strip.

b) An optional laminate tap may be used as 'splash guard' or to hamper evaporation and back-migration of detector reagent [49].

c) The components of the strip may be presented in a simple dipstick format or optionally, within a plastic casing with a sample port and reaction window showing the capture and control lines [39, 49].

Figure 2.8 shows a schematic view of the simplified LFD format used during this work. A porous nitrocellulose membrane and a wick pad are layered onto a plastic adhesive backing card.

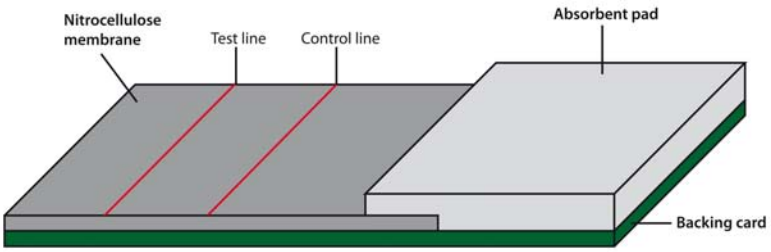


Figure 2.8: Architecture of a lateral flow device.

### 2.3.2 LFD format

Apart from serum assays, which are designed to detect antibodies as an indicator of various diseases, there are two main types of LFDs: non-competitive (double antibody sandwich) and competitive (competitive inhibition) format assay [46]. Both principles are described in detail

by Wang *et al.* [17].

Generally, sandwich assays are used for the detection of higher-molecular-weight analytes (macromolecules such as human chorionic gonadotropin (hCG), which is produced during pregnancy [39], and such as various allergens [50]), which comprises multiple epitops. Briefly, the sample first encounter labeled analyte-specific antibodies and the target analyte (if present) will bind to the detector conjugate. The test line will also contain antibodies raised against the target analyte, although these antibodies may bind to a different epitope on the analyte. Hence, the presence of the analyte in the sample leads to a visible test line. If no analyte is present in the test solution, only the control line appears [17, 47].

The competitive lateral flow format is commonly used to analyze low-molecular-weight molecules [17], which often possess a single-epitope region [17, 47] such as mycotoxins, drugs (antibiotics, drug abuse tests) [39] drugs metabolites, and hormones [51]. In this assay format, the target analytes bind to the reporter (colored particle labeled analyte-specific antibodies) and block these reporters from binding to the immobilized ligand at the test line. Here, a competitive colloidal gold based assay (Figure 2.9) should be described in more detail, as it is used in this study. The liquid sample and a ready gold mix, containing AuC labeled analyte-specific antibodies, are mixed together in a microtiter well and are briefly incubated to allow the antibodies to interact with any analyte present in the sample. Then, the test strip is inserted into the sample well and the fluid mixture migrates across the membrane due to the capillary action. The membrane contains a test line and a control line, onto which an analyte-protein conjugate and an anti-species specific antibody are immobilized, respectively. The antigen-protein conjugate in the test line can capture any free anti-analyte antibody gold particle conjugate, allowing color particles to form a visible line. Thus, a positive sample with an analyte concentration greater than or equal to the assay cut-off level will result in no visible line in the test zone. On the contrary, a negative sample with an analyte concentration less than the cut-off level will form a visible line in the test zone. Excess buffer along with any reagents not captured at the test or control line will then be entrapped in the absorbent pad.

Considering the competitive assay format, the color intensity of the test line inversely correlates with the analyte concentration in the sample, which means, the greater the reduction in signal intensity at the test line, the greater the concentration of the analyte present in the sample. The

smallest amount of analyte that results in no color development at the test line can be considered the cut-off value. In case of qualitative tests (is the analyte present), a single control line on the membrane is a positive result. Two visible lines in the capture and control zone is a negative result. However, if an excess of target analyte is not present, a weak line may be produced in the capture zone, indicating an ambiguous result. Semi-quantitative results (what amount of the analyte is present) can be achieved by the determination of the intensity of the test line, which can be related to the concentration of the analyte (see next section).

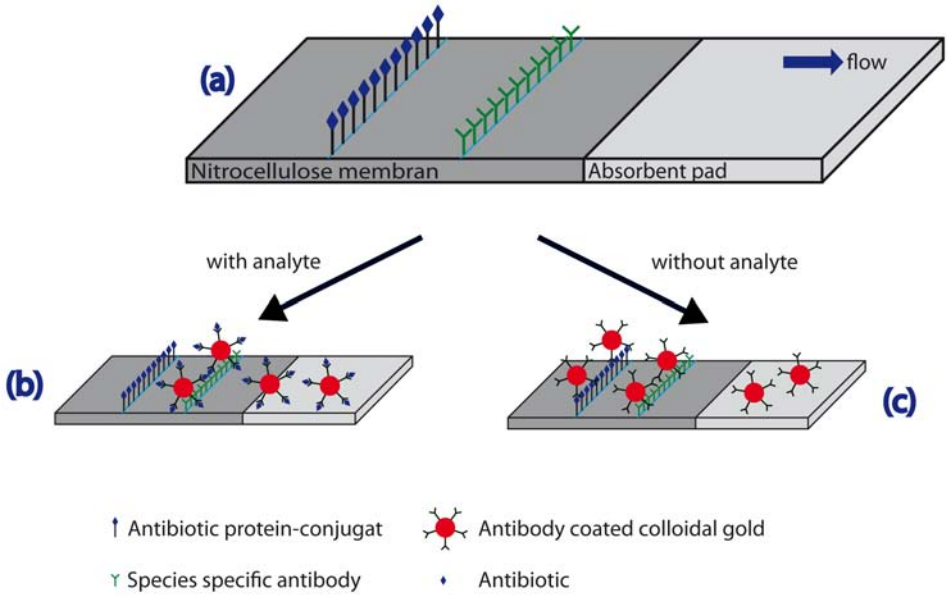


Figure 2.9: Principle of the competitive assay.

### 2.3.3 Analytical aspects of screening tests

Commission Decision 2002/657/EC [52] establishes criteria and procedures for the validation of analytical methods. Since the scope of Commission Decision 2002/657/EC on the validation of screening methods is limited, the CRL document of 20/1/2010 Guidelines for the validation of screening methods for residues of veterinary medicines-initial validation and transfer [53] was drafted.

Lateral flow devices give qualitative (yes/no) or semi-quantitative results of the target analyte in the sample. In case of qualitative assays, the preferable screening test provides a positive result with a cut-off near the MRL, or previously defined level of interest. A test which only yields to negative results at values well below the MRL will lead to a number of samples which require confirmatory testing in a regulatory program [10]. According to the above mentioned new document a cut-off level is defined as the level which indicates that a confirmatory test has

to be performed. For MRL substances the cut-off has to be preferably around 1/2 MRL. Hence, very low LODs need to be obtained with the developed method to obtain the required cut-off levels. Further, it is possible to obtain semi-quantitative results by measuring the amount of gold-conjugate bound to the capture zone. This can be done by using a dedicated reader to measure the intensity of the colored test line.

### 2.3.4 Protein binding to nitrocellulose

For lateral flow devices, the nitrocellulose membrane must irreversibly bind capture reagents at the test and control lines, because the test results thoroughly depend on it [39, 44]. Although, the nature of the binding of proteins to nitrocellulose is not well understood [44, 47], it is widely accepted that hydrophobic interactions, hydrogen bonding, and electrostatic interactions play a role in the binding mechanism [44, 45, 54]. Various factors that influence protein binding to nitrocellulose membranes are summarized by Jones [44, 45]:

1. Properties of the capture reagent application buffer (e.g. salt concentration, pH, addition of alcohol, or crosslinking-agents to the application buffer) may decrease or increase the binding forces.

2. Three main factors affecting membrane performance: pore size, post-treatments, and membrane type (e.g. nitrocellulose, nylon, polysulfones).

3. The capture reagent itself and its way of synthesis (carrier protein, coupling ratio) are crucial for their application.

4. Ambient humidity at the time of protein application may influence the binding.

5. Agents that interfere with protein binding by inhibiting one or more of the essential binding forces are:

   a) Formamide and urea disrupt hydrogen bondings between the reagent and the NC.

   b) Tween, Triton, and Brij may interfere with hydrophobic bonding between the capture line reagent and the NC.

   c) Polymers such as polyvinyl alcohol (PVA), polyethylene glycol (PEG), polyvinyl pyrrolidone (PVP) interfere through a combination of effects.

   d) Non-specific proteins may compete for binding sites, e.g. BSA.

# 3 Materials

The practical work was carried out at the Center for Analytical Chemistry of the Boku-Department IFA-Tulln and at the Romer Labs Division Holding GmbH research laboratories. All buffers and media were prepared with deionized water. All media were autoclaved at 121 °C for 20 min. The media was allowed to cool down to at least 50 °C before adding the antibiotic (filter sterilized). Solid media (media for plates) was cooled down to approximately 50 °C before pouring into sterile petri dishes. Media plates were aseptically prepared in a sterile bench. The solid and liquid media were stored at 4 °C until further use. All buffers used for affinity chromatography were filtered and degassed before usage.

## 3.1 Protein determination

The bicinchoninic acid (BCA) protein assay kit (Pierce) was performed in non-binding 96-well microtiter plates (Greiner) and spectrophotometrically read on a Sunrise™ plate reader with Magellan5 software, which were obtained from Tecan.

## 3.2 Lithium dodecyl sulphate polyacrylamide gel electrophoresis (LDS-PAGE)

2-(N-morpholino) ethane sulfonic acid (MES Pufferan®), 3-(N-Morpholino)-propanesulfonic acid (MOPS Pufferan®), sodium dodecyl sulfate (SDS), and N-Tris-(hydroxymethyl)-methyl-glycin (Tricine Pufferan®) were obtained from Roth. Ethylenediaminetetraacetate (EDTA) and Trisbase were obtained from Sigma-Aldrich. NuPAGE® Novex 3-8% Tris-acetate Gel (1.5 mm $x$ 15 well; used with Tris-acetate SDS running buffer, separation range from 40 kDa to 500 kDA), NuPage® Novex 4-12% Bis-Tris Gel (1.0 mm $x$ 15 well; used with MOPS running buffer: separation range from 15 kDa to 260 kDa; used with MES running buffer: separation range form 3.5 kDA to 160 kDa), NuPage® LDS sample buffer (4x), HiMark™ prestained standard (1x), SeeBlue® prestained standard (1x), XCell SureLock™ Mini Cell and

SimplyBlue™ SafeStain (Coomassie® G-250) were purchased from Invitrogen.

The Tris-acetate (TA) SDS running buffer (20 x) contains: 50 mM Tricine, 50 mM Tris base, 0.1% SDS, pH 8.24. The MES SDS running buffer pH 7.3 (20 x) contains: 50 mM MES, 50 mM Tris base, 0.1% SDS, and 1 mM EDTA. The MOPS SDS running buffer (20 x) contains: 50 mM MOPS, 50 mM Tris base, 0.1% SDS, 1 mM EDTA, pH 7.7.

### 3.2.1 Silverstaining of LDS-PAGE gels

Further chemicals were needed for silverstaining: Glycerol was purchased from Roth. Formaldehyde, acetic acid, glycine, glutardialdehyde, sodium thiosulfate*5 $H_2O$, sodium acetate and carbonate, and silver nitrate were bought from Merck. Ethanol was received from J.T. Baker.

For silverstaing following solutions were freshly prepared: The fixing solution consisted of 30% (v/v) ethanol and 10% (v/v) acetic acid. The sensitizing solution contained 0.05 M sodium acetate, 0.8 mM sodium thiosulfate pentahydrate, 30% (v/v) ethanol, and 0.5% (v/v) glutardialdehyde. The silverstaining solution contained 0.2% (w/v) silver nitrate and 0.02% (v/v) formaldehyde. The developing solution consisted of 0.02 M sodium carbonate and 0.01% (v/v) formaldehyde. The stop solution contained 1% (v/v) glycerin in deionized water. To preserve the gel, a solution with 10% (v/v) glycerol was used.

## 3.3 Bioconjugate synthesis and characterization

Penicillin G potassium salt was provided by Riedel-de-Haën. Ampicillin trihydrate (Amp), cefalexin (Cef), N,N-dimethylformamide (DMF), 4-aminobenzoic acid (APA), sodium hydroxide (NaOH), 1,1-carbonyldiimidazole (CDI), sodium chloride, disodium hydrogen phosphate dehydrate, and sodium nitrite were purchased from Fluka. Acetone, HCl 37%, dimethyl sulfoxide (DMSO), and sodium dihydrogen phosphate monohydrate were obtained from Merck. Boric acid, bovine serum albumin (BSA; essentially globulin and protease free, ≥98%), tetracycline hydrochloride (TC), 1-ethyl-3-(dimethylaminopropyl)-carbodiimide hydrochloride (EDC), keyhole limpet hemocyanin from *Megathura crenulata* (KLH) in PBS solution, and ovalbumin were from Sigma-Aldrich. N,N'-Dicyclohexylcarbodiimide (DCC) was from Aldrich. N-Hydroxysuccinimide (NHS) and borax were purchased from Sigma. Agron was from Messer. 2,4,6-trinitrobenzene sulfonic acid (TNBSA) was obtained from Thermo Scientific.

Sodium borate buffer (pH 8.5) consisted of 150 mM NaCl and 500 mM sodium borate. 0.2 M phosphate buffered saline (PBS) buffer containing 0.36 M NaCl, pH 7.5 was prepared by dissolving 32.22 g $Na_2HPO_4$, 2.62 g $NaH_2PO_4$ and 21.18 g NaCl in deionized water. The PBS buffer was diluted to lower molarities, if required.

Rotary evaporation was carried out with the rotary evaporator from Büchner. Centrifugation was performed using a Beckman GS-6KR centrifuge. UV/Vis spectrophotometry data were collected on a Lambda 16 UV/Vis spectrometer from Perkin Elmer.

## 3.4 Antibodies

Polyclonal anti-$\beta$-lactam antibody (PAS 9567, 10.31 mg mL$^{-1}$, immunogen: ampicillin-BSA), abbreviated $\beta$-lactam ab, and monoclonal antibody to Tetracycline (MAB9258, 1.82 mg mL$^{-1}$, immunogen: tetracycline(amide)-BTG), shortened TC ab, were purchased from Randox Sciences. The monoclonal antibody was purified with protein A affinity chromatography. In case of the polyclonal antibody no purification procedure was mentioned in the certificate.

## 3.5 Lateral flow devices

Instruments used for strip production were BioDot ZX1000 dispensing platform with frontline contact tips and BioDot CM4000 guillotine cutter. Nitrocellulose membranes (FF 85/100, AE 98 FAST, AE 99, AE 100, and Immunopore RP) and the wick pad were purchased from Whatman GE Healthcare. Nitrocellulose nitrate membrane (UniSart CN 95) was from Satorius. Citric acid and methanol were from Fluka. Disodium hydrogen phosphate and sodium carbonate were purchased from Merck. Ficoll®, polyvinyl alcohol (PVA), Polyvinylpyrrolidon (PVP), and SDS were obtained from Roth. BSA (≥96%) was from Sigma-Aldrich. Tween® 20, Span™ 80, Triton® X-114, and Brij® 58 were from VWR. Penicillin G potassium salt was provided by Riedel-de-Haën. The photometric reflectance strip reader AgraStrip® XReader from Romer Labs Division Holding GmbH was used. The 'Die leichte Muh Frühstücksmilch' with a fat content of 0.9% was used as milk sample.

SBGT buffer consisted of 10 mM $Na_2HPO_4$, 24 mM NaCl, 58 mM sucrose, 2% BSA, 0.8 M glycerol, and 1 mL L$^{-1}$ Triton X-100. This buffer was prepared to a slightly modified

protocol by Franse *et al.* [55]. The SGT buffer is equal to the SBGT buffer, but without BSA. MTP buffer consisted of 5%(w/v) Tween$^{\text{textregistered}}$ 20 and 4% (v/v) methanol in 0.1 M PBS buffer. X-buffer consisted of 1% Tween$^{\text{textregistered}}$ 20 in 0.1 M PBS buffer.

## 3.6 Recombinant production of the PBP2x*-GST fusionprotein

Agar-Agar Kolbe I, dithiothreitol (DTT), isopropyl-$\beta$-D-1-thiogalactopyranoside (IPTG), phenylmethylsulfonyl fluoride (PMSF), reduced glutathione, tetracycline hydrochloride (TC.HCl), and tris(hydroxymethyl)aminomethane (Trizma® base) were obtained from Roth. Peptone (pancreatic) for bacteriology, D-glucose monohydrate, and natrium chloride were purchased from VWR (BDH Prolabo). Yeast extract for microbiology, magnesium sulfate heptahydrate, and potassium chloride were purchased from Fluka. Magnesium chloride hexahydrate, disodium hydrogen orthophosphate, glycerol, and potassium dihydrogen phosphate were from Merck. Plasmid pGEX-6P1-tet-PBP2x* was provided by Prof. Dr. Hakenbeck (TU Kaiserslautern) and chemically competent *E. coli* BL21(DE3) cells were prepared by Patricia Fajtl (Biomin Tulln) according to Sambrook *et al.* [54].

Following media were used for transformation and expression of PBP2x*-GST fusionprotein: SOC medium contained 2% peptone, 0.5% yeast extract, 10 mM NaCl, 2.5 mM KCl, 10 mM $MgCl_2$, 10 mM $MgSO_4$, 20 mM glucose (filter sterilized). LB medium was composed of 1% peptone, 0.5% yeast extract, 0.5% NaCl, and for plates 1.5% Agar-Agar was added. 2xTY broth contained 1.6% peptone, 1% yeast extract, and 0.5% NaCl. Both LB and 2xTY media were supplemented with 15 µg mL$^{-1}$.

The QIAprep spin miniprep kit from Qiagen was used for plasmid isolation. An horizontal electrophoreses system with a power supply MP250 (Omnipac) was used. For visualizing, BioDoc-It® (UPV) was employed. All buffers and agarose gels were already prepared by Mag. Andreas Firzinger (RomerLabs). GeneRuler™ 1 kb DNA ladder (Fermentas) was used as standard. A KS 4000i control shaker (IKA®-Werke) was used for fermentation and a high pressure batch-liquid expansion French Press (Thermo Electron) for disruption of bacterial cells. For cell harvest Beckman Avanti™ J-25 and for removing cell debris Beckman Allegra™ X-22 were employed. GSTrap FF HiTrap™ column, 5 mL, with a binding capacity of approx. 50 mg GST-fusionprotein per 5 mL gel and PD-10 desalting columns were obtained from GE Healthcare. FPLC (Fast Protein Liquid Chromatography) system for affinity chromatographic

purification was purchased from Pharmacia: Pharmacia LKB pump P-500, Pharmacia LKB FRAC-100 (collector), Pharmacia LKB optical unit UV-1 (detector), Pharmacia LKB controller LCC-501 Plus, FPLCdirector™ version 1.03 (software). Amicon ultra-2 centrifugal filter unit with a cut-off of 50 kDa was from Millipore.

Following buffers were used for affinity chromatography: Binding buffer, pH 7.3, was composed of 140 mM NaCl, 2.7 mM KCl, 10 mM $Na_2HPO_4$, 1.8 mM KH2PO4, and 5 mg DTT. Elution buffer, pH 8.0, contained 50 mM Tris-HCl, 10 mM reduced glutathione.

## 3.7 Colloidal gold production

Tetrachloroauric(III)acid trihydrate ($HAuCl_4$*3 $H_2O$), ACS reagent, and potassium carbonate anhydrous ($K_2CO_3$), p.a. were purchased from Sigma Chemical Co. Trisodium citrate ($C_6H_5Na_3O_7$*2$H_2O$), p.a. was from Merck. For all preparations only Milli-Q water (18.2 mΩ) (Millipore) was used. All glassware employed was cleaned with aqua regia, rinsed with ultrapure water, and used only for preparing colloidal gold solutions.

## 3.8 Software

ISIS Draw was used to draw chemical structures, SigmaPlot to analyze and graph data, pDRAW32 for drawing the plasmid construct, and Adobe Illustrator CS5 was employed for graphics. SPDBV was used for illustrating protein crystal structures. ClustalW2 provided by EMBL-EBI was used for sequence alignement.

# 4 Methods

## 4.1 Determination of the protein concentration

**Theory**—The BCA assay [56, 57] is based on the biuret reaction, which is the peptide-induced reduction of $Cu^{2+}$ to $Cu^{+}$ in an alkaline solution combined with the concentration-dependent detection of monovalent copper ions. Bicinchoninic acid is a chromogenic reagent that chelates the reduced copper (Figure 4.1), producing a purple complex with strong absorbance at 562 nm.

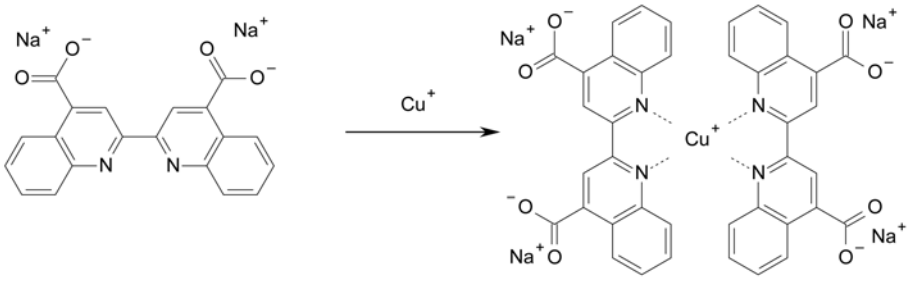


Bicinchoninic acid (BCA)

BCA-copper complex

Figure 4.1: The reaction of BCA with cupric ion. Two molecules of BCA bind to each molecule of copper that had been reduced by a peptide-mediated biuret reaction.

The Pierce® BCA protein assay was carried out according to the manufacturer´s protocol [58]. Briefly, standards of BSA were prepared at eight concentrations in 0.01 M PBS buffer ranging from 25 µg mL$^{-1}$ to 2000 µg mL$^{-1}$ and unknown samples were appropriately diluted in the same buffer. 20 µL of each standard or diluted sample were pipetted into the wells of a non-binding microtiter plate and 200 µL of coloring reagent were added to each well. Then, the plate was mixed thoroughly on a plate shaker for 30 s and the covered plate was incubated at 37 °C for 30 min. The reaction mixture was allowed to cool down to room temperature and the plate was read out at 562 nm on an ELISA plate reader. The data for the standard curve were fit to a quadratic equation, and the amount of protein in the samples was calculated from the fit parameters.

## 4.2 LDS-PAGE

**Theory**—Denaturing sodium dodecyl sulphate polyacrylamide gel electrophoresis (SDS-PAGE) is an electrophoretic method for separating proteins by their molecular weight, based on their diverging rates of migration through a sieving matrix in an applied electric field. The anionic detergent, SDS, denatures secondary and non–disulfide–linked tertiary structures and confers a uniform negative charge to the polypeptide in proportion to its length (electrophoretic mobility only depends on size) [59]. Compared to the Laemmli system [60], lithium dodecyl sulfate (LDS) replaces SDS but functions equally. A loading dye is added to the protein solution to track the progress of the protein solution through the gel during the electrophoretic run.

Lithium dodecyl sulphate polyacrylamide gel electrophoresis (LDS-PAGE) was carried out according to the manufacturer´s instructions [61]. Protein concentration was determined using the BCA assay, as described in chapter 4.1. About 5 µg to 6 µg protein provided with 2.5 µL sample buffer per lane were applied onto the gel. Samples were heated before electrophoresis to 70 °C for 10 min under non-reducing conditions. Running conditions were set to 200 V and 1 h at 4 °C. Proteins were visualized either by staining with Coomassie® or silver nitrate.

### 4.2.1 Staining of LDS-PAGE gels

**Theory**—Classical coomassie blue staining of the gel can usually detect a 50 ng protein band. Silverstaining enhances the sensitivity by 50 times [62]. In acidic conditions, the dye Coomassie Brilliant Blue G-250 primarily binds to proteins through basic amino acids (arginine, lysine and histidine). It also binds weakly to the aromatic amino acids, tyrosine, tryptophan, and phenylalanine via van der Waals forces and hydrophobic interactions [63]. The principles of silverstaining are summarized by Poland *et al.* [64]. Basically, the staining depends on the complexation of $Ag^+$ ions with glutamic acid, aspartic acid, and cysteine residuals [65].

For staining with Coomassie Blue, the gel was washed three times in deionized water and then stained with coomassie blue overnight while shaking. It was destained in deionized water for several hours. To increase the sensitivity of detection, silverstaining was performed according to a modified protocol of Heukeshoven and Dernick [66]. First, the gel was transferred into a glass tray containing the fixing solution and incubated for 30 min at room temperature, followed by

sensitizing solution for 30 min. After washing the gel three times with 100 mL dd$H_2O$ for 5 min each time, the silver nitrate solution was added and incubated for 20 min. The development took 8 min and stopping was done after 10 min. Then, the gel was washed three times for five minutes in deionized water and preserved in glycerol solution for 30 min.

### 4.2.2 Monitoring of PBP2x*-GST fusionprotein expression by LDS-PAGE

In order to monitor the expression of PBP2x*-GST protein, 500 µL samples of the fermentation broth, before and after induction, were spinned down, resuspended in 40 µL of 4x LDS-Sample buffer, heated to 70 °C for 10 min and stored at −4 °C. For electrophoresis, the samples were again heated as stated before and 10 µL of each sample were applied onto the gel. 7.5 µL of the cell free lysate were mixed with 2.5 µL of the loading buffer, heated as mentioned above, and loaded onto the gel.

### 4.2.3 Analysis of the supernatant after labeling PBP2x*-GST fusionprotein with colloidal gold

In order to analyze the coupling efficiency of the PBP2x*-GST fusionprotein to AuC, 1 mL of 40 nm colloidal gold sol was spinned down and redissolved in 500 µL of MQ-water, and then, 40 µL of fraction 4 containing GST-tag, PBP2x* and PBP2x*-GST fusionprotein were added. The mixture was incubated by overhead-shaking at 7 rpm for 30 min and was centrifuged (10,000 $x$ g, 10 min, 4 °C). Subsequently, 35 µL of sample buffer were added to 175 µL of the supernatant and heated at 70 °C for 15 min. Evaporation was possible due to a hole in the lid of the reaction tube (final volume approx. 50 µL). 10 µL to 12 µL of the mixture were evaluated by LDS-PAGE. Hence, no quantification of the protein amount in the obtained gel was possible.

## 4.3 Size exclusion chromatography

**Theory**—Size exclusion chromatography, also known as gel filtration, separates molecules based on molecular size. The larger molecules flow through the resin and are collected first, while the smaller molecules take longer to flow through, because they are held up within the pores of the resins. Hence, the sample passes through the resin in decreasing molecular weight. Commonly, gravity size exclusion is used for desalting and buffer exchange.

Gel filtration was used to desalt and remove small molecules (MW $\leq$5000 g mol$^{-1}$) from

protein-conjugates and to remove GSH from affinity chromatographic purified PBP2x*-GST fusionprotein. The disposable PD-10 desalting columns were equilibrated with 2 CV of 0.01 M PBS or 0.1 M BB buffer, 2.5 mL of the sample was applied onto the column and then, the sample was eluted with 3.5 mL of the same buffer in one fraction.

## 4.4 Analyte-protein conjugates

**Theory**—In competitive immunoassays, a protein conjugate of a small molecule (homologous to the analyte) is applied at the test line as capture reagent [47]. Conjugation may be accomplished either by direct conjugation between an existing functional group on the hapten and the carrier protein or by more complex methods entailing modifications of the hapten to generate appropriate coupling groups and/or to add an additional spacer arm between two conjugated molecules [67]. Pastor-Navarro *et al.* [68] reviewed the immunoanalysis methods for the determination of tetracycline in food products with emphasis on syntheses of haptens and their coupling to carrier-proteins. For $\beta$-lactam-protein conjugates various synthesis procedures are published ([69–71]). Since bovine serum albumin (BSA), ovalbumin (OVA), and keyhole limpet hemocyanin (KLH) were used as carrier protein, they should be shortly discussed here.

*BSA* is a highly soluble plasma protein from cattle with a molecular mass of 67 kDa. BSA contains various functional groups suited for conjugation, e.g. BSA possesses a total of 59 lysine $\epsilon$-amine groups (only 30-35 of these are available for derivatization) [67]. The crystal structure of BSA is not available, hence, the structure of human serum albumin HSA is shown in Figure 4.2a. Sequence alignment employing ClustalW results in 76% sequence homology between HSA and BSA (Annex A.2).

*OVA*, a protein isolated from hen egg whites, with a MW of 43 kDa contains 20 lysine residues suitable for conjugation. The majority of acidic groups gives the protein a pI of 4.63. OVA is sensitive to temperature above 56 °C and vigorous mixing.

*KLH* is a copper-containing protein that belongs to a family of non-heme proteins found in mollusks. KLH is an extremely large, multimeric protein that dissociates reversibly into subunits. The molecular mass of KLH is about $4.5\,x10^5$ Da to $1.3\,x10^7$ Da. KLH possess over 2,000 amines from lysine residues calculated on a per-mole basis using an average multi-subunit MW of 5,000 kDa [67].

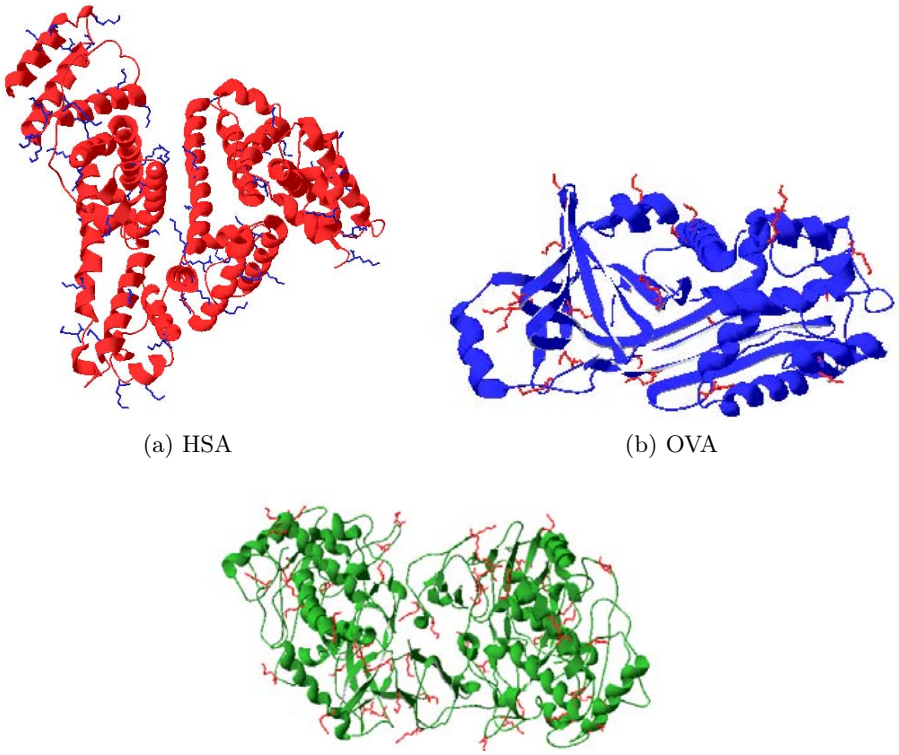

(a) HSA (b) OVA

(c) KLH

Figure 4.2: Crystal structures of (a) human serum albumin (PDB-Code: 1GNJ), (b) ovalbumin (PDB-Code: 1OVA), and (c) of the functional unit KLH1-H of keyhole limpet hemocyanin (PDB-Code: 3QJO). Lysine residues are highlighted in blue or red.

### 4.4.1 Synthesis of $\beta$-lactam-protein conjugates

**Theory**—$\beta$-lactam-protein conjugates may be produced by the formation of an amide linkage made by the condensation of a primary amine group (-$NH_2$) with a carboxylic acid (-COOH) using carbodiimides (e.g. DCC, and EDC) as zero-length crosslinkers [67]. This type of reaction is known as active ester method. Carbodiimides react with carboxylic acids to create an active ester intermediate (*o*-acylisourea), which is too slow to react with amines. Hence, a two-step protocol, including carbodiimides in combination with NHS, is often used to improve efficiency. In the reaction illustrated in Figure 4.3, the carboxyl group of the hapten is activated with DCC and further transformed to a N-hydroxysuccinimide ester. The reaction releases dicyclohexylisourea. Further, NHS activated haptens react with primary amines in slightly alkaline conditions yielding in amid bond formations with release of N-hydroxysuccinimides [67]. Though, this synthetic procedure can give rise to unwanted side reactions such as crosslinking of the protein and N-acylurea formation on the protein [72]. Allowing the reaction to proceed under mildly alkaline

pH conditions, may limit the polymerization of proteins, while still facilitating the coupling reaction [67].

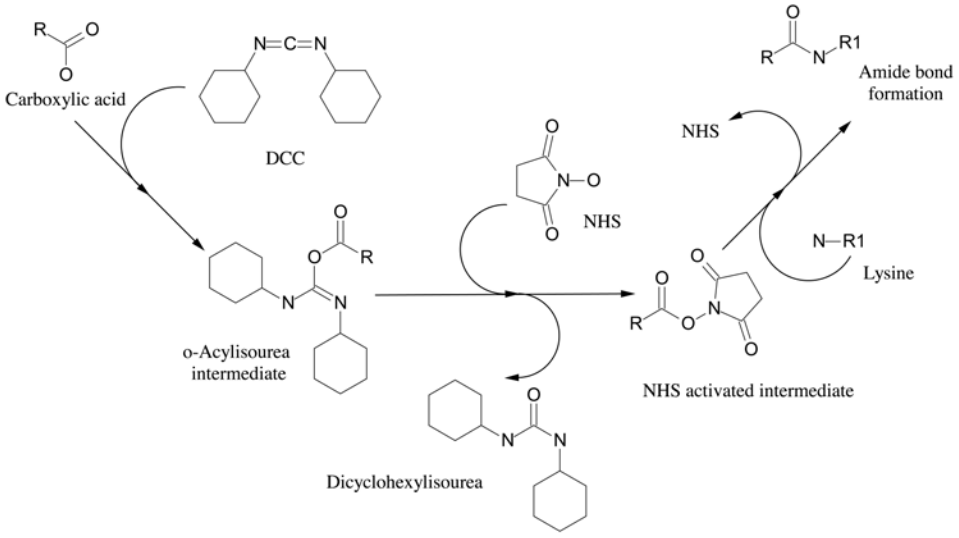


Figure 4.3: Coupling of hapten to BSA using the active ester method. The carboxyl group of the hapten is activated with DCC, further transformed to a N-hydroxysuccinimide ester, and finally, a stable amide linkage is formed [67].

#### 4.4.1.1 Synthesis of $\beta$-lactam-BSA/KLH conjugates

The haptens penicillin G potassium salt, ampicillin, and cefalexin were covalently bound through their carboxylic acid moiety to the lysine group of BSA with a coupling ratio of 1:50 (protein:hapten) on basis of a modification of the active ester method [67]. Additionally, penicillin G potassium salt was coupled to BSA with coupling ratios of 1:15 and 1:10 (protein:hapten). The molar volume of hapten:NHS:DCC was always 1:1.5:1.5. NHS, DCC, and hapten stock solutions (at least 0.5 mL) were freshly prepared using dry DMF. Then, the required volume of hapten was transferred into a 4 mL glass vial with screw cap. NHS and DCC were added to a 75-fold molar excess over the amount of protein. Further, DMF was added to a final volume of 500 µL. Subsequently, the mixture was stirred at room temperature for 1 h. In the meantime, the required amount of BSA was dissolved in 1 mL of 0.1 M sodium bicarbonate buffer or 0.1 M borate buffer and cooled on ice. After the activation reaction time was completed, the NHS activated intermediate was added to the BSA solution under stirring. The solution was gently shaken overnight at 4 °C employing an overhead shaker. Excess reagents of conjugation were removed with gel chromatography (Section 4.3) employing 0.1 M PBS or

0.1 M BB buffer as equilibration and elution buffer. Molar ratios and the applied amounts of the reagents are outlined in Table 4.1.

Table 4.1: Molar coupling ratios used for synthesis of $\beta$-lactam-BSA/KLH conjugates.

| | Penicillin G-BSA 1:50 | | | Penicillin G-BSA 1:25 | | | Penicillin G-BSA 1:10 | | |
|---|---|---|---|---|---|---|---|---|---|
| | MCR* | µmol | mg | MCR | µmol | mg | MCR | µmol | mg |
| Hapten | 50 | 8.96 | 3.34 | 25 | 4.48 | 1.67 | 10 | 1.79 | 0.67 |
| NHS | 75 | 13.43 | 1.55 | 37.5 | 6.72 | 0.77 | 15 | 2.69 | 0.31 |
| DCC | 75 | 13.43 | 2.77 | 37.5 | 6.72 | 1.39 | 15 | 2.69 | 0.55 |
| Protein | 1 | 0.18 | 12.00 | 1 | 0.18 | 12.00 | 1 | 0.18 | 12.00 |
| | Ampicillin-BSA 1:50 | | | Cefalexin-BSA 1:50 | | | Penicillin G-KLH 1:50 | | |
| | MCR | µmol | mg | MCR | µmol | mg | MCR | nmol | µg |
| Hapten | 50 | 8.96 | 2,59 | 50 | 7.46 | 2.59 | 50 | 33.33 | 12.42 |
| NHS | 75 | 13.43 | 1.29 | 75 | 11.19 | 1.29 | 75 | 50.00 | 5.76 |
| DCC | 75 | 13.43 | 2.31 | 75 | 11.19 | 2.31 | 75 | 50.00 | 10.32 |
| Protein | 1 | 0.18 | 10.00 | 1 | 0.15 | 10.00 | 1 | 0.67 | 5000 |

*The molar coupling ratio (MCR) is defined as the moles of hapten per mole of protein in the initial reaction mixture.

#### 4.4.1.2 Synthesis of the Penicillin G-OVA conjugate

The synthesis was performed according to a slightly modified protocol of Knecht *et al.* [69]. The penicillin ovalbumin conjugate was produced employing a solution of 20.9 mg (56 µmol) of penicillin G potassium salt, 6.45 mg (56 µmol) of NHS, and 26.7 mg (139 µmol) of EDC hydrochloride in 1 mL of 0.01 M PBS buffer. After stirring the mixture in an ice bath for 25 min, dissolved OVA (10 mg (0.23 µmol) in 1 mL 0.01 M PBS) was added. Then, the reaction mixture was brought to room temperature and stirred for another 3 h. Excess reagents were removed by size exclusion chromatography as described in Section 4.3.

### 4.4.2 Synthesis of tetracycline-protein conjugates

In literature, protocols of tetracycline-protein conjugates following a direct coupling procedure of TC to the carrier protein via the Mannich condensation using homobifunctional aldehydes, the carbodiimide method or diazonium conjugation methods are described. In addition, TC derivatives as haptens have been synthesized and coupled to different carrier proteins [68]. In this work, the TC-4-BSA (TC-ABA-BSA) conjugate and the TC-CDI-BSA conjugate were synthesized according to Pastor-Navarro *et al.* and Zhang *et al.* [73], respectively.

#### 4.4.2.1 Synthesis of TC-4-BSA conjugate

**Theory**—Figure 4.4 illustrates the synthetic procedure of TC-4-BSA conjugate production. First, the linking reagent APA is diazotized and coupled to TC to introduce a carboxylic acid group. Afterwards, the modified hapten is attached to BSA via the diazo spacer arm on the ring D by means of the active ester method. In this reaction, the carbodiimide EDC is used as zero-length crosslinker and an amide linkage between the inserted carboxylic group and the primary amine groups of lysines in BSA is formed.

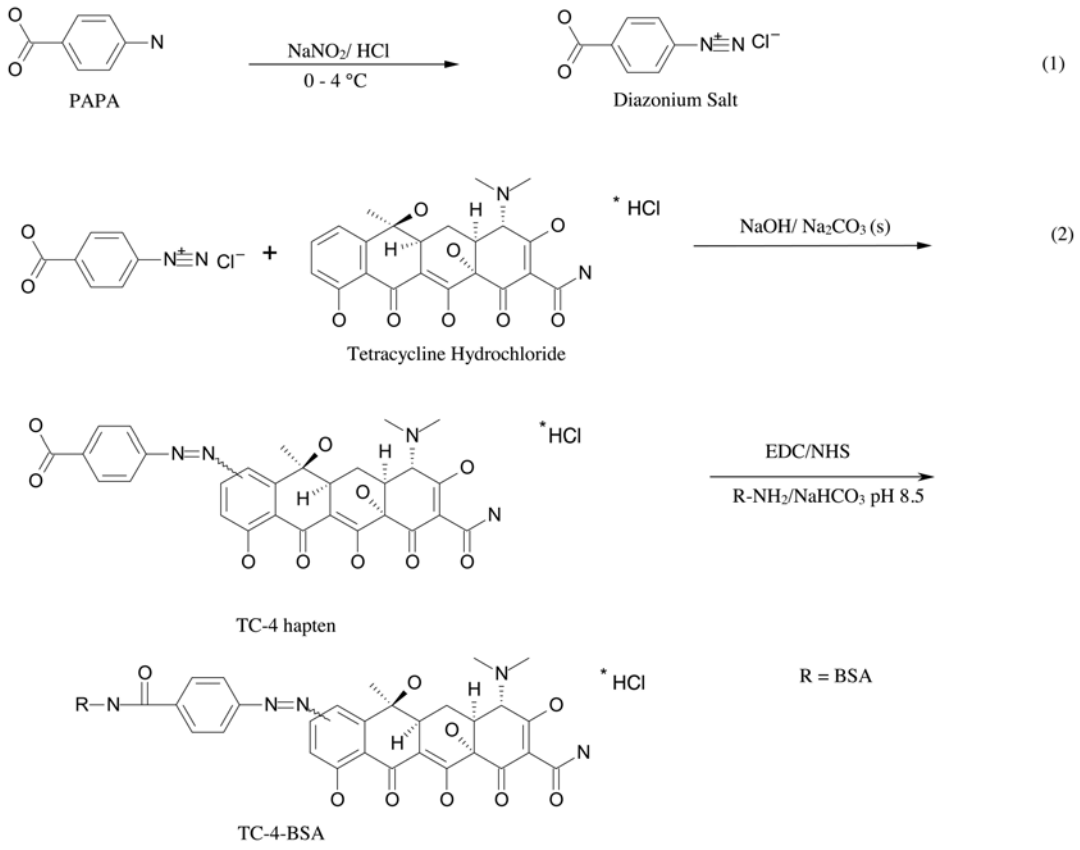


Figure 4.4: Synthesis of the TC-4-BSA conjugate through the ABA method [73, 74].

The TC-4-BSA conjugate was produced according to a slightly modified protocol by Pastor-Navarro *et al.* [74] and Zhang *et al.* [73]. APA (1.12 g) was dissolved in 16 mL of 2 M HCl and cooled in an ice bath. Subsequently, 1 mL of sodium nitrite in water (0.61 g, 8.82 mmol) was added dropwise to the cooled solution and the resulting diazonium salt was stirred for 10 min. The mixture was dropwise added to a solution of TC HCl (3.75 g, 7.8 mmol) in 60 mL of 0.2 M NaOH. Solid sodium carbonate was added to keep the pH at 9 to 10. Subsequently, the mixture was stirred for 2 h at 10 °C, brought to room temperature and acidified with 6 M

HCl. To separate the remaining tetracycline hydrochloride, the solution was centrifuged (10 min, 20000 *x* g). After the pale-red to colorless supernatant (pH 2) was discarded, the pellet was washed three times with 20 mL cold distilled water and dried at reduced pressure. The 7 or 9-(4´-carboxyphenylazo)tetracycline hydrochloride (TC-4, calculated MW 593.55 g mol$^{-1}$) was attained as a dark red solid (3.28 g). Further, TC-4 haptens were covalently attached through their carboxylic acid moiety to the lysine group of BSA by means of a modification of the active ester method (EDC/NHS) [67] in a ratio of 1:50. First, NHS and EDC stock solutions were freshly dissolved in DMSO. The conjugation was induced by the addition of EDC to a 125-fold and NHS to a 50-fold molar excess over the amount of BSA, to 8.85 mg TC-4 hapten. Afterwards, the reaction was allowed to stand for 1 h at room temperature. Meanwhile, 20 mg of BSA were dissolved in 0.1 M $NaHCO_3$ buffer (pH 8.1) and stored on ice. The EDC/NHS activated hapten solution was added dropwise to the cooled BSA solution under stirring. The mixture was gently shaken overnight at 4 °C using an overhead shaker. The protein-conjugate was purified by size exclusion chromatography (Section 4.3) with 0.01 M PBS buffer, aliquoted and stored at −20 °C.

#### 4.4.2.2 Synthesis of TC-CDI-BSA conjugate

**Theory**—Carbonylating reagents such as CDI can produce stable carbamate linkages after subsequent conjugation with an amine containing molecule. When CDI is used as linking and activation reagent, the nucleophilic hydroxyl group of TC at C-6 attacks the carbonyl carbon of CDI resulting in an active imidazolyl carbamate. The subsequent attack by the amine containing BSA releases the imidazole, but not the carbonyl. Thereby, TC may be coupled to an $\epsilon$-amine group of BSA via an one-carbon spacer, forming the TC-CDI-BSA conjugate [67, 68, 73].
TC-CDI-BSA conjugate was produced following a slightly modified protocol of Zhang *et al.* [73]. In this procedure (Figure 4.5), 43.2 mg of Tetracycline hydrochloride (90 µmol) was dissolved in 8 mL acetone. Then, 29.2 mg of CDI (180 µmol) was added to the solution in one step and the reaction mixture was incubated at room temperature (instead of 37 °C) in the dark, under argon for 3 h. Afterwards, acetone was evaporated employing a rotary evaporator under vacuum and the residue was re-dissolved in 15 mL of sodium borate (0.5 M, pH 8.5). Subsequently, 201 mg of BSA (3 µmol) were added and the solution was allowed to stand at room temperature for 48 h in the dark under argon. The mixture was dialyzed (MWCO 15 kDa) under stirring against PBS (0.01 M, pH 7.3) for 3 days with frequent changes of the PBS buffer to remove the uncoupled free hapten. The yellow TC-CDI-BSA conjugate with a molecular coupling ratio of 1:30 was stored at −20 °C until further use.

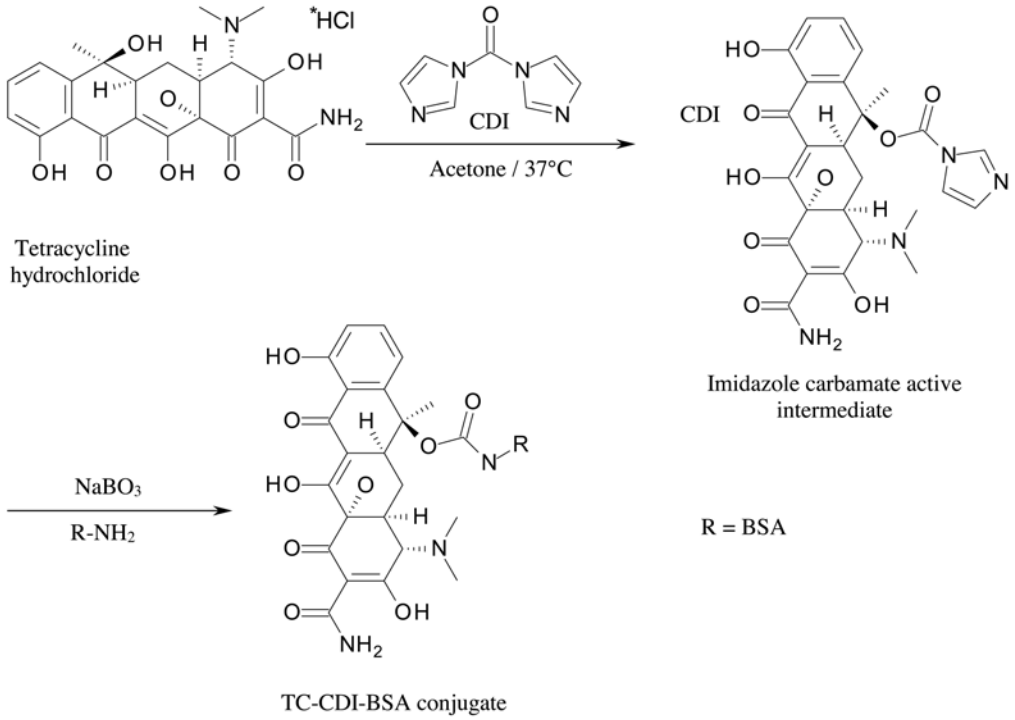


Figure 4.5: Synthesis of the TC-CDI-BSA conjugate through the CDI method, adapted from Zhang *et al.* [73].

### 4.4.3 Characterization of analyte-protein conjugates

The protein concentration after synthesis and purification was determined with the BCA Kit as described in Section 4.1. LDS-PAGE analysis was performed according to the description in Section 4.2. Further, the hapten to carrier protein coupling ratio was estimated with TNBSA as stated below.

#### 4.4.3.1 2,4,6-Trinitrobenzene sulfonic acid (TNBSA) assay

**Theory**—Habeeb [75] demonstrated that the TNBSA assay was a sensitive method to measure the free amino groups in proteins such as BSA and OVA. Molecules possessing primary amines can react with TNBSA to form a highly chromogenic derivative [67] (Figure 4.6). According to that, TNBSA colorimetric assay quantifies the number of lysine residues remaining free after conjugation with the hapten.

The reaction was performed as described by Hermanson [67]. Samples were diluted in the reaction buffer (0.1 M $NaHCO_3$, pH 8.5) to a final concentration of 0.02 µg mL$^{-1}$ to 0.2 µg mL$^{-1}$ and the

standard solutions for calibration were prepared from a stock solution of 2 mg mL$^{-1}$ BSA, OVA or KLH in the same buffer. To 1 mL sample or standard 0.5 mL of 0.01% (w/v) freshly prepared TNBSA solution in reaction buffer was added and mixed thoroughly. After incubation at 37 °C for 2 h, the reaction was stopped by adding 1 mL of 10% (w/v) SDS and 0.5 mL of 1 M hydrochloric acid. The absorbtion at 355 nm was measured. Prior to measurements, blanking was performed with a non-protein containing solution. The amount of free amine groups was calculated from the corresponding calibration curve. The coupling density was estimated by comparing the absorbance with the corresponding values of hapten-free proteins. Substation rate in percentage was calculated from absorbance values at 335 nm, using equation 4.1. Epitope density (number of hapten molecules per protein molecule) was determined by multiplying the substitution rate by the factor (f) 59, 20, or 2,000 in respect to the number of amino groups of BSA, OVA, and KLH, respectively [76].

$$SR(\%) = \frac{A_{reference} - A_{conjugate}}{A_{reference}} \times 100 \tag{4.1}$$

$$ED = \frac{SR}{100} \times f \tag{4.2}$$

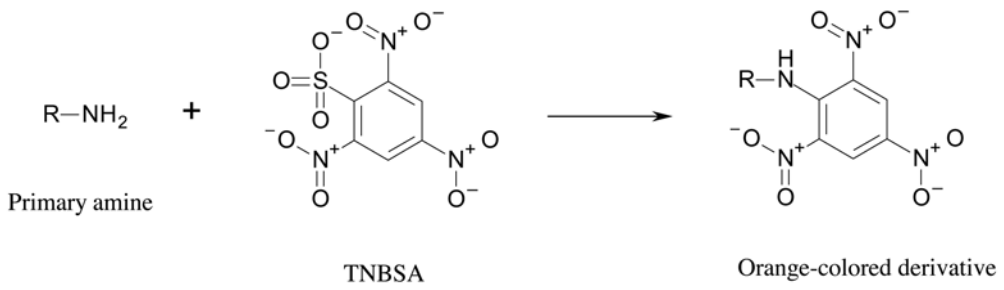


Figure 4.6: TNBSA assay [67].

## 4.5 Recombinant production of the PBP2x*-GST fusionprotein

**Theory**—The soluble derivative of PBP2x from *Streptococcus pneumoniae* was expressed as glutathione S-transferase (GST) fusionprotein (PBP2x*-GST fusionprotein) in *Escherichia coli* BL31(DE3) and purified by affinity chromatography. In the GST-fusion system, the target protein is fused to a GST-tag (26 kDa). The GST-tagged protein has a high binding affinity to glutathione and is therefore a convenient tool to purify GST-fusion proteins from

bacterial lysates. For this purpose, the glutathione ligand is coupled via a 10-carbon linker to highly cross-linked 4% agarose. The steps involved in the purification of GST fusion proteins from *E. coli* are described in detail in the manufacturer's instructions [77]. Here, a modified protocol published by Cacciatore *et al.* [1], Cacciatore [8], and Lamer [19] was used to produce PBP2x*-GST fusionprotein.

### 4.5.1 Host strain and vector

Plasmid pGEX-6P-1-tet-PBP2x* (Figure 4.7) was constructed by the working group of Prof. Hakenbeck. A short description of the cloning strategy should be given here. PCR was used to amplify the PBP2x* gene of pCG31, which encoded a soluble PBP2x derivative of *S. pneumonia* R6 with a deletion of the transmembranpeptid (aa 19-48) [36]. Initially, the PCR product was cloned into pGEM-T Easy (Promega) and inserts comprising the correct DNA sequence were subcloned into a pGEX-6P-1 (Amersham Biosciences) vector such that the PBP2x* gene is fused in-frame with the GST gene of *Schistosoma japonicum* [1]. A specific cleavage sequence in the pGEX-6P vector allows simple removal of the GST-tag with PreScission protease after purification of the fusionprotein [78]. Preventing $\beta$-lactams as selection marker in recombinant expression of PBP, the $\beta$-lactamase gene, originally encoded in the plasmid pGEX-6P-1, was replaced by the tetracycline resistance cassette from pBR322 [1, 19]. Thus, the expression of the GST-PBP2x* fusionprotein is under the control of the IPTG-inducible tac promotor. The $LacI^q$ gene product is a repressor protein that binds to the operator region of the tac promotor, preventing expression until induction by IPTG. Additionally, the plasmid contains a pBR322 origin for DNA replication in order to replicate independently from the chromosome. The *E. coli* BL21(DE3) strain is suitable for protein overexpression as this strain is deficient in both Ion and OmpT proteases which could induce proteolysis of overexpressed proteins [78]. Since the tac promotor is recognized by *E. coli* RNA polymerase, it does not need a DE3 strain. However, DE3 strains do not hamper expression form vectors (e.g. pGEX-6P-1) containing the tac promotor [79].

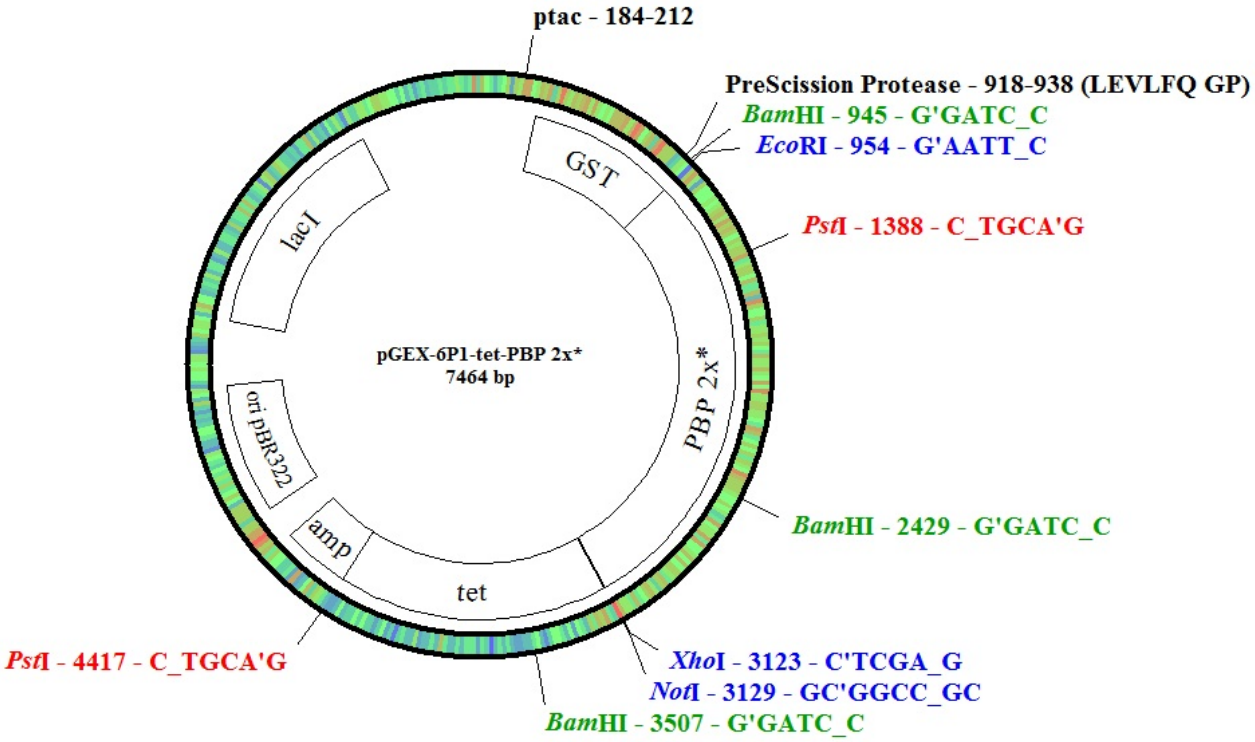


Figure 4.7: pGEX-6P1-tet-PBP2x* plasmid. Adapted from [19].

### 4.5.2 Transformation of *E. coli* cells

**Theory**—The pGEX-6P1-tetPBP2x* vector was transformed into *E. coli* BL21(DE3) cells in order to express the GST-tagged PBP protein. In principle, three steps are necessary for the introduction of plasmid DNA into *E. coli*: preparation of 'competent cells' (cells able to accept DNA), transformation of these competent cells, and selection of transformants. Commonly, high levels of $CaCl_2$ are used to alter the structure of the bacterial cell wall, facilitating the entry of plasmid DNA into *E. coli*, combined with heat shock treatment of these cells. A subsequent outgrowth step in selection marker-free media enables recovering and expressing the antibiotic resistance marker encoded by the plasmid. Selection of positive transformantes is performed by plating cells onto selective medium [80].

One µL of the plasmid and 100 µL of *E. coli* cells were mixed together and incubated on ice for 30 min. The cells were heat-shocked at 42 °C for 90 s, immediately placed on ice for 2 min, mixed with 800 µL of room-tempered SOC medium without tetracycline, and incubated for 60 min at 37 °C for 1 h with gentle shaking (250 rpm). Further, the *E. coli* cells were spinned down. 700 µL

of the supernatant were discarded, the *E. coli* pellet was resuspended in the remaining media by tapping the sides of the tube and spread on $LB_{tet}$ plates. Subsequently, the transformants were incubated overnight at 37 °C [54]. Once colonies had been grown on the transformation plate, three single colonies were picked using a sterile toothpick for each colony and the cells were transferred onto a fresh $LB_{tet}$ plate to form a master plate. Furthermore, each toothpick was embedded into the corresponding tube containing 2 mL of $LB_{tet}$ liquid media to prepare miniprep plasmid DNA. The chosen transformants were incubated overnight at 37 °C or at 37 °C at 100 rpm, respectively.

### 4.5.3 Isolation and agarose gel electrophoresis of plasmid DNA

**Theory**—In order to separate pure plasmid DNA from chromosomal DNA and from the rest of the cellular components the QIAprep® plasmid miniprep kit was used. This protocol is based on a modified alkaline lysis method of Birnboim and Doly [81] combined with silica-binding technology and the convenience of a spin column format. Briefly, SDS solubilizes phospholipid and protein components of the cell membrane, resulting in lysis and release of the cell content. Addition of NaOH leads to denatured chromosomal and plasmid DNA. During a subsequent neutralization step with potassium acetate, the ability of plasmid DNA to correctly renature and remain in solution in contrast to chromosomal DNA is exploited. Further, two purification steps are performed: (1) Denatured proteins, chromosomal DNA, and cellular debris are coprecipitated in potassium dodecyl sulfate complexes, and removed by centrifugation. (2) Remaining impurities are separated by selective adsorption of plasmid DNA to a silica membrane under high salt conditions. The pure plasmid DNA is obtained by elution under low salt conditions [82, 83]. Agarose gel electrophoresis [84] is an essential technique used to separate DNA fragments by size. Because of the consistent negative charge bestowed by their phosphate backbone, DNA molecules migrate toward the anode in an electric field (shorter molecules move faster and migrate farther than longer ones). Because DNA bands are invisible on gels, DNA is stained with ethidium bromide (EtBr), which fluoresces under UV light when it is bound to DNA [59].

QIAprep® plasmid miniprep kit was used according to the manufacturer´s instruction. Additionally, to the short user protocol [83], an incubation step (room temperature, 1 min) was operated after loading the cleared lysate into a binding column. The optional washing step with Buffer PB was not carried out. Agarose gel electrophoresis was performed in 1% agarose (suitable

for 0.5-10 kb DNA fragments) in TAE buffer, pH 8, containing 1% (v/v) ethidium bromide at 250 V.

### 4.5.4 Expression and purification of the recombinant PBP2x*-GST fusionprotein

The expression and purification of PBP2x*-GST fusionprotein were performed following a modified protocol published by Cacciatore *et al.* [1]. Precultures were grown in 250 mL baffled flasks each containing 50 mL of $2xTY_{tet}$ medium at 37 °C under vigorous shaking (250 rpm) overnight. Then, the starter-cultures were diluted 10-fold into a 5 L baffled flask containing 1.5 L $2xTYT_{tet}$ media. When the cells reached an absorbance of approx. 0.6 at 600 nm, the target PBP2x*-GST fusionprotein was expressed after IPTG induction (final concentration of 1 mM) for 4 h. Total cell concentration was determined by measuring the absorbance of the broth at 600 nm ($OD_{600}$) in a spectrophotometer. Samples were diluted with 0.9% NaCl at OD values exceeding 0.5. Bacteria cells were harvested by centrifugation (4,200 $x$ g, 20 min, 4 °C) washed once with 20 mL ice-cold 0.1 M PBS buffer and stored at −20 °C. The pellet was resuspended in 15 mL (about 3.5* cell weight) of ice-cold PBS supplemented with 5 mM dithiothreitol, 2 mM phenymethylsulfony fluoride and 10 mM $MgCl_2$. Cells were disrupted by three passages through a French press at 18,000 psi. The cell lyses was investigated under the microscope. To remove cell debris, two centrifugation steps were performed: at 4,700 $x$ g for 15 min followed by 20,000 $x$ g for 30 min at 4°C. The soluble fraction, containing the fusionprotein, was loaded onto a prepacked GSTrap FF column at a flow rate of 1 mL $min^{-1}$, previously equilibrated with 10 CV of binding buffer and subsequently, the column was washed with 12 bed volums of the same buffer at a flow rate of 5 mL $min^{-1}$. Then, the bound PBP2x*-GST fusionproteins were eluted with 14 mL of elution buffer and 2 mL fractions were collected and analyzed by SDS-PAGE. Protein containing fractions were pooled, purified by size exclusion chromatography using PD-10 desalting colums (see section 4.3), the protein content was determined, the protein solution was flash frozen, and stored at −80 °C.

### 4.5.5 Glycerol storage of bacterial cultures

For long-term storage of *E. coli* BL21(DE3) cells carrying the plasmid pGEX-6P-1 tet-PBP2x*, glycerol cultures are the method of choice. Glycerol functions as cryoprotectant which reduces damage from ice crystals. Additionally, plasmid DNA can be stored at −20 °C for further transformations. For a −80 °C *E. coli* glycerol culture, 500 µL of an *E. coli* overnight culture were mixed thoroughly with 500 µL of 40% glycerol solution (sterilized by autoclave; final glycerol

concentration: 20% (v/v)) in a 1.5 mL reaction tube and stored at −80 °C. In order to verify that the cells contain a plasmid construct (pGEX 6P-1 tet PBP2x), a mini-prep on a portion of the same culture medium that was used to prepare the glycerol culture had to be performed. These stocks could be reactivated by overnight growth at 37 °C on $LB_{tet}$ plates.

### 4.5.6 Ultrafiltration

In order to remove the seceded GST from the protein solution containing PBP2x* and PBP2x*-GST fusionprotein, ultrafiltration (MWCO 50 kDa, 7,500 *x* g) was performed. Three centrifugation steps á 3 min were carried out and the protein solution containing proteins greater than 50 kDa was each time diluted with 1 mL of 0.01 M PBS. The centrifugation was monitored by LDS-PAGE.

## 4.6 Use of colloidal gold as detector reagent

**Theory**—Immunogold conjugation is used to couple proteins to gold nanoparticles in order to produce an immunogold complex [41]. 40 nm AuC particles, commonly used in lateral-flow-devices, offer maximum visibility with the least steric hindrance in case of IgG conjugations [42], as shown in Figure 4.8. In LFDs, AuC is required for visualization of the interaction between the immunoreactive components. The gold particles are red in color due to the localized surface plasmon resonance effect [17]. Colloidal gold (AuC), a sol comprised of nanoparticles of $Au^0$, is produced by controlled reduction of tetrachloroauric(III) acid trihydrate with citrate [85], as described in chapter 4.6.1. The electron-dense negatively charged AuC particles [86] stay in solution through their mutual electrostatic repulsions [87, 88]. The net negative charge on their surface is generated by a layer of adsorbed negative ions arising from the reducing agent [43]. Negation of charge repulsion by cations in salt solutions triggers colloidal gold salt-mediated agglomeration [86, 88], which can be blocked by binding of proteins or other stabilizing agents to the nanoparticles´ surfaces by means of non-covalent electrostatic adsorption [88, 89]. The labeling of proteins with AuC is based on three major forces, as illustrated in Figure 4.9: First, charge attraction between the negative charges of the AuC particles´ surfaces and positively charged amino acids (e.g. lysine and arginine) of the protein contribute to the stability of the gold particle protein conjugate. Further, proteins will be strongly bound to the gold surface through hydrophobic interactions between the nanoparticle surface and the apolar amino acids (e.g. tryptophan, valine, leucine, isoleucine,

or phenylalanine). Additionally, the binding can be stabilized by dative bonds between sulfur atoms and gold particles, if sulfur-containing amino acids (e.g. cysteine and methionine) are present on the protein surface [43, 90]. The procedure for the determination of the optimum protein concentration for labeling antibodies with AuC (µg ab/ml AuC), as described in chapter 4.6.2, is based on the above mentioned salt induced agglomeration. If the protein concentration is too low and therefore, the entire negatively charged AuC nanoparticles surface are not coated with protein, the addition of positively charged sodium ions lead to agglomeration. Owing to this reaction, the absorbance maximum of the gold sol changes, whose evaluation allows an estimation of the optimal coupling ratio. After antibody gold labeling, the conjugate solution is stabilized against aggregation by blocking non-specific binding sites by means of BSA addition, as described in chapter 4.6.3.

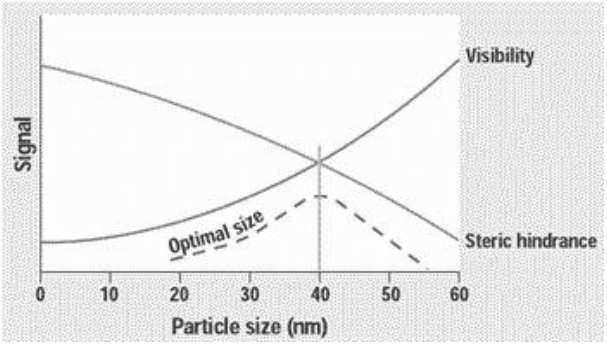


Figure 4.8: Relationship between particle size, visibility and steric hindrance of AuC. Figure taken from [41].

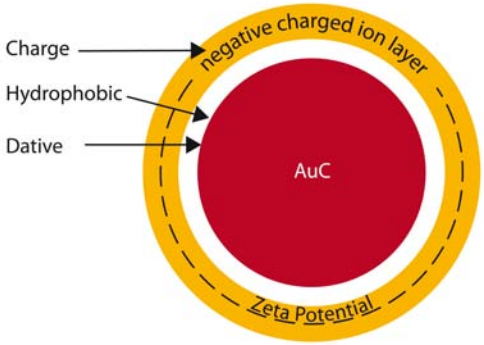


Figure 4.9: Binding forces between an antibody and a gold particle. Adapted from [43].

### 4.6.1 Synthesis of colloidal gold

Colloidal gold particles were prepared by controlled reduction of tetrachloroauric(III) acid trihydrate with citric acid trisodium salt [85] following a slightly modified procedure described by Frens [91], as previously described by Rudolf *et al.* [92]. 200 ml of 0.01% (w/v) $HAuCl_4$ solution was heated till boiling under reflux conditions and was further allowed to boil for 10 min under constant stirring. By adding a 1% (w/v) sodium citrate solution in a ratio of 1:100, the reduction process from $Au^{3+}$ to $Au^0$ was induced. During the reaction, the color of the yellow $HAuCl_4$ solution changed to colorless, black-blue and finally to wine-red (Figure 4.10), the colloidal gold solution was further boiled for 10 min and was then left to cool to room temperature. The solution was alkalized to pH 8.5 by addition of 0.2 M potassium carbonate and the UV/Vis absorption spectra (350 nm to 800 nm) of 1 ml gold sol was recorded. Colloidal gold was stored at the longest for one day at 4 °C until usage for titration and coupling.


Figure 4.10: Color reaction of the gold colloid production.

### 4.6.2 Titration of colloidal gold

Titration was performed as described by Rudolf *et al.* [92]. Briefly, antibody dilutions in a concentration range from 0 mg mL$^{-1}$ to 0.2 mg mL$^{-1}$ in 0.05 M PBS were prepared to a final volume of 65 µl. Then, 650 µl of the colloidal gold solution was added to each dilution and the mixture was thoroughly inverted and incubated for 15 min at room temperature. After adding 130 µl of 10% (w/v) sodium chloride, the mixture was allowed to react for 15 min. The adsorption was measured at the maximum absorption of the colloidal gold solution (e.g. 529 nm) and at 600 nm in triplicate on an ELISA plate reader. In order to evaluate the optimum ab/AuC coupling ratio, the antibody concentration (µg ab/ml AuC) was plotted against the absorption difference ($abs_{max}$ - $abs_{600}$). The subtraction of the absorbance at 600 nm from the absorbance at 529 nm was necessary to reduce the signal to noise ratio [93].

### 4.6.3 Protein-gold conjugation

For conjugation, 40 ml of AuC solution was compounded with the determined optimal amount of antibody solution by overhead-shaking at 7 rpm for 30 min at room temperature. The remaining binding sites were blocked by addition of a 1% (w/v) aqueous BSA solution in a ratio of 1:10 and incubation as stated before. Then, the solution was centrifuged (10,000 *x* g, 20 min, 4 °C) to separate unbound proteins form the gold colloid conjugate. The colorless supernatant was discarded and the dark-red conjugate was washed twice with distilled water. Finally, the pellet was resuspended in 400 µL of a 6% (w/v) BSA solution and 12 µL of 10% (w/v) sodium azide as preservative solutions was added. $OD_{529}$ was determined and the antibody-gold conjugate was stored at 4 °C until further use. Due to the fact that the AuC reacts very sensitively to ion impurties, the coupling reaction must be performed in deionized water [90].

## 4.7 Lateral flow devices

**Theory**—The assay under investigation was based on the competitive principle (Figure 2.9). Through the action of capillary forces, the sample and reporter particles were transported to the ligand sites. At the test line (TL), the gold-conjugated anti-$\beta$-lactam antibody bound to immobilized $\beta$-lactam-protein conjugate, forming a red line. The excess of the detector reagent migrated farther and the gold labeled antibody was trapped by the goat anti-sheep immunoglobulins to form the control line (CL).

### 4.7.1 Preparation of LFDs

CL and TL were sprayed with 0.5 µL cm$^{-1}$ onto the AE 99 nitrocellulose membrane (20 mm *x* 300 mm) employing a dispenser. Prior to application, both the Pen G-BSA (MCR 1:50) conjugate and the species-specific anti-sheep antibody were diluted to a concentration of 1 mg mL$^{-1}$ with 0.01 M PBS buffer. Membranes were dried at 37 °C for 2 d, and cut without blocking of the entire membrane into strips of 4.5 mm. The lateral flow dipsticks were stored under dry conditions at room temperature until use. Other preparation procedures are mentioned below.

### 4.7.2 Assay procedure

For the lateral flow assay procedure 30% (v/v) antibody–gold-conjugate was diluted in the SBGT assay buffer. 50 µL of the sample (e.g. milk or water) were mixed with an equal volume of gold mix in a well of a non-binding ELISA microtiter plate. One strip was dipped into the reaction mixture and incubated for 5 min. Results were either evaluated visually or with a photometric reflectance strip reader after drying with a blow dryer for 1 min.

### 4.7.3 Protein binding to nitrocellulose membranes

In Section 2.3.4 various factors that influence protein binding to nitrocellulose membranes are listed. The following experiments were carried out according to the suggestions by Jones [44, 45].

#### 4.7.3.1 Membrane effects

**Theory**—Six different membranes (FF 85/100, AE 98 Fast, AE 99, AE 100, Immunopore RP, and CN 95) were examined referring to their flow characteristics and their immobilization of the TL and CL. The membranes AE 98, AE 99, and AE 100 only distinguish in their pore size. Immunopore RP, and FF 85/100 have an integrated plastic backing for higher stability and better handling in assembling with an adhesive backing card. Each membrane consists of 100% nitrocellulose with no post-manufacture treatments except of Immunopore RP. It includes a proprietary polymer in the membrane matrix to ensure rapid rewetting and low background signal-eliminating protein-binding interferences commonly experienced with surfactants [94].

Assays were performed twice with all six membranes under following conditions. The CL and the TL (Pen G-BSA, MCR 1:50) were applied on each of the tested membrane as stated in Section 4.7.1. Since the standard blocking procedure (Section 4.7.3.3; blocking the entire membrane with 2% (w/v) BSA in 0.05 M PBS buffer containing 0.1% (w/v) $NaN_3$) removed the TL reagent during the blocking step from the NC membrane, and commonly used assay buffers as X-buffer and MTP led to false positive results because of their stripping effect, all test were performed by using non-blocked strip tests and the SBGT buffer according to the protocol mentioned above (Section 4.7.2).

#### 4.7.3.2 Evaluation of different hapten-protein conjugates and capture reagent application buffer compositions

**Theory**—Hoffman *et al.* [95] figured out that proteins that were bound to NC in acidic buffer were relatively resistant to milk stripping (displacement) form the NC membranes compared to proteins bound in pH 7. Further, coprecipitating agents or crosslinking agents (e.g., alcohol, glutaraldehyde) in the application buffer may improve protein binding to nitrocellulose [45].

Differences in the antibiotic coupled to the carrier protein were examined in the used carrier proteins and in the MCR. Both the TL and CL were applied onto the membrane CN 95 with a concentration of $1\,\mathrm{mg\,mL^{-1}}$. All conjugates listed in Table 5.1 were examined. Assays were performed as stated in Section 4.7.2 with water or milk as samples.

The Pen G-BSA (MCR 1:50) conjugate in 0.01 M PBS buffer was diluted in 0.1 M citric acid/$Na_2HPO_4$ (pH 2.6, 3.0, 5.0, and 7.0) or in 0.1 M sodium carbonate/sodium bicarbonate buffer (pH 9.2 or 10.1) (150 µL conjugate + 300 µL buffer) and 0.5 µL of each diluted conjugate (final conc. $1\,\mathrm{mg\,mL^{-1}}$) were applied as a drop on blank AE 99 test-strips, dried at 37 °C for 2 d, and examined in respect to the stripping effect of milk. Evaluation of the effective pH, was carried out by mixing 0.01 M PBS buffer pH 7 with the appropriate buffer in the same ratio as the conjugate. Assays were run using SBGT buffer with milk (0.9% fat content) or SGT buffer as sample.

Pen G-BSA (MCR 1:50) conjugate in 0.01 M PBS buffer was supplemented with 5% ethanol or 1% glutaraldehyde, sprayed on AE 99 membranes and dried at 37 °C for 2 d. The assays were performed as state in Section 4.7.2.

#### 4.7.3.3 Blocking of the membrane

**Theory**— Blocking may be necessary to reduce non-specific background signal and should be empirically determined for each test. If blocking is necessary, various blocking agents may be used, including various buffer compositions, proteins, and synthetic compounds [47]: gelatin, casein, BSA, IgG, PVP, and PVA [39]. Furthermore, the method employed for membrane blocking is also a crucial factor. Generally, there are two possibilities where a blocking agent can be applied: (1) blocking of the entire membrane after test and control line reagents have been applied and dried; (2) addition of blocking reagent in the assay buffer. In the latter case,

no redissolving of capture reagents may occur, but it is not as efficient as blocking the entire membrane [45]. Since the blocker might interfere with the capture reagent applied on the nitrocellulose membrane leading to false positive results, different blocking strategies has to be considered.

All blocking experiments were carried out using the AE 99 membrane, $1\,\mathrm{mg\,mL^{-1}}$ anti-sheep antibody as CL and $1\,\mathrm{mg\,mL^{-1}}$ Pen G-BSA (MCR 1:50) as test line reagent. After spraying CL and TL onto the NC membrane, membranes were dried at 37°C for 2d. Then, membranes were blocked in the blocking solution for 30 min and washed three times with 0.05 M PBS for 5 min and dried again as stated above. Following blocking agents were dissolved in 0.05 M PBS containing 0.1% (w/v) $NaN_3$: 2% (w/v) BSA, 0.5% (w/v) PVP, and 1% (w/v) Ficoll. The SGT assay buffer was used for assay performance. Alternatively, the blocking agent BSA was added to the SGT assay buffer to a final mass concentration of 2% and 4%.

#### 4.7.3.4 Influence of the assay buffer composition

**Theory**—If the binding-strength of the capture reagent onto the membrane is too low, or the surfactant level in the assay buffer is too high, the capture reagent may be physically removed from the membrane surface by the sample [45]. Hence, the optimal conditions must be figured out.

The assays were performed employing commonly used assay buffers such as X-buffer, MTP buffer, and SBGT buffer. Further, 1% SDS, 1% Span80, 0.2% Tween® 20, 0.51% Triton X-114, or 0.5% Brij 58 were added to the SBGT buffer without Triton. All experiments were carried out using test strips produced as stated in Section 4.7.1.

#### 4.7.3.5 Effect of drying conditions

**Theory**—As the binding of the protein to nitrocellulose is related to drying conditions, Jones [45] proposed to dry the membrane more vigorously after test line application. Increasing the drying temperature may reduce the chance of the capture reagent not being efficiently immobilized and therefore being removed by the sample or other agents.

Both the Pen G-KLH conjugate and the Pen G-BSA (MCR 1:50) were dried onto the AE 99 membrane under following conditions: at 24 °C for 4 d, at 37 °C for 4 d, and at 80 °C for 2 h. The

assays were performed as stated in Section 4.7.2.

#### 4.7.3.6 Evaluation of beta-lactam antibody

Stock solution of penicillin G potassium salt (8 mg mL$^{-1}$) was prepared in deionized water and then diluted in SGT buffer to receive a working solutions of 800 ng mL$^{-1}$. These working solutions were further diluted to obtain the desired concentrations (0.5, 1, 2, 4, 5, and 8 ppb) and stored for one hour at 4 °C prior to the assay procedure. Evaluation tests were performed in triplicate. Test strips were read out on a photometric reflectance strip reader (AgraStrip® XReader ) under the following assay conditions. Strip tests with immobilized anti-sheep IgG antibody (1 mg mL$^{-1}$) as control line and BSA-Pen G conjugate (1 mg mL$^{-1}$, MCR 1:50, in 0.01 M PBS) as test line on an AE 99 membrane were used. 30% (v/v) anti-$\beta$-lactam ab labeled gold sol was diluted in SBGT buffer. 50 µL spiked buffer were mixed with an equal volume of antibody-gold conjugate in SBGT buffer. One strip was dipped into the reaction mixture and incubated for 20 min. Results were quantified after drying for 1 min. The revised criteria of 657/2002/EC [52] for the validation of analytical methods introduces CC$\alpha$ and CC$\beta$ to replace the LOD and LOQ, respectively. In this thesis, the limit of detection (LOD) and the limit of quantification (LOQ) were calculated according to L´Hocine *et al.* [96]. The limit of detection (LOD) was calculated as the signal of the blank (n=3) plus three times the standard deviation (SD) of the blank. The limit of quantification (LOQ) is defined as the mean value of negative controls plus 3 SD of the mean.

# 5 Results and discussion

## 5.1 Characterization of analyte-protein conjugates

The analyte-protein conjugates prepared as stated in the Methods section 4.4 were characterized by BCA assay, TNBSA assay, UV/Vis spectrophotometry, and LDS-PAGE analysis.

### 5.1.1 Determination of the protein amount in conjugate solutions

All synthesized bioconjugates and standards were determined in triplicate. Standard curves were obtained by dilution of the appropriate protein (BSA, KLH, or OVA) in 0.01 M PBS buffer and a quadratic polynomial regression fit was calculated (Figure 5.1). The samples´ average values and the resulted standard deviations are outlined in Table 5.1. The dilutions were considered and a final standard concentration was specified for further experiments. Additionally, the measured protein concentration was used to calculate the total protein recovery from the synthesis reaction and the subsequent size exclusion purification in respect to the used amount of protein for preparation of conjugates. For example, the recovery rate regarding all $\beta$-lactam-BSA conjugates was greater than 94%. Summarizing, removing excess reagents of conjugation by employing disposable PD-10 desalting columns according to the protocol stated in Section 4.3 was acceptable.

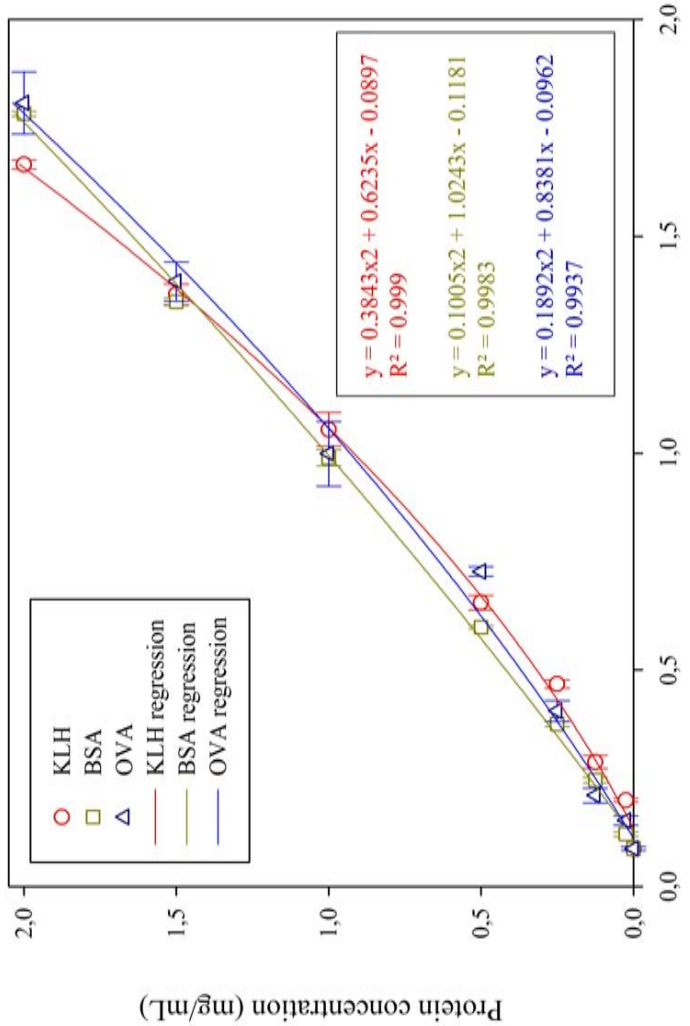


Figure 5.1: Calibration curves of BCA test with BSA, OVA, and KLH. The lines are 3-parameter polynomial regressions for the entire set of standard points.

Table 5.1: Calculated protein concentrations of synthesized bioconjugates and purification recovery rates.

| **Bioconjugates*** | **Mean abs.** | **Std. dev.** | **Dilution** | **Calculated conc. regarding dilution (mg mL$^{-1}$)** | **Final conc. (mg mL$^{-1}$)** | **Weighed mg/3.5 ml elution buffer** | **Recovery rate (%)** |
|---|---|---|---|---|---|---|---|
| BSA-Pen G 1:50 | 1.468 | 0.045 | 1:2 | 3.20 | 3.32 | 3.43 | 96.8 |
| | 0.733 | 0.003 | 1:5 | 3.43 | | | |
| | 0.422 | 0.006 | 1:10 | 3.32 | | | |
| BSA-Pen G 1:25 | 1.428 | 0.017 | 1:2 | 3.10 | 3.29 | 3.43 | 95.8 |
| | 0.672 | 0.013 | 1:5 | 3.08 | | | |
| | 0.455 | 0.006 | 1:10 | 3.68 | | | |
| BSA-Pen G 1:10 | 1.456 | 0.037 | 1:2 | 3.17 | 3.31 | 3.43 | 96.5 |
| | 0.765 | 0.013 | 1:5 | 3.62 | | | |
| | 0.405 | 0.014 | 1:10 | 3.13 | | | |
| OVA-Pen G | 1.572 | 0.087 | 1:2 | 3.38 | 3.31 | 3.43 | 96.6 |
| | 0.742 | 0.032 | 1:5 | 3.15 | | | |
| | 0.471 | 0.027 | 1:10 | 3.41 | | | |
| TC-CDI-BSA** | 1.282 | 0.054 | 1:10 | 13.61 | 13.03 | 13.33 | 97.8 |
| | 0.355 | 0.010 | 1:50 | 12.93 | | | |
| | 0.233 | 0.010 | 1:100 | 12.57 | | | |
| TC4-BSA | 0.938 | 0.010 | 1:5 | 4.66 | 4.81 | 5.71 | 84.1 |
| | 0.605 | 0.065 | 1:10 | 5.39 | | | |
| | 0.197 | 0.008 | 1:50 | 4.38 | | | |
| KLH-Pen G | 1.221 | 0.099 | - | 1.24 | 1.22 | 1.43 | 85.4 |
| | 0.736 | 0.035 | 1:2 | 1.16 | | | |
| | 0.433 | 0.011 | 1:5 | 1.26 | | | |

*continued on next page*

*continued from previous page*

| **Bioconjugates*** | **Mean abs.** | **Std. dev.** | **Dilution** | **Calculated conc. regarding dilution (mg mL$^{-1}$)** | **Final conc. (mg mL$^{-1}$)** | **Weighed mg/3.5 ml elution buffer** | **Recovery rate (%)** |
|---|---|---|---|---|---|---|---|
| BSA-Amp | 1.385 | 0.016 | 1:2 | 2.99 | 2.74 | 2.86 | 95.9 |
| | 0.623 | 0.023 | 1:5 | 2.80 | | | |
| | 0.342 | 0.011 | 1:10 | 2.44 | | | |
| BSA-Cef | 1.304 | 0.007 | 1:2 | 2.78 | 2.85 | 2.86 | 99.6 |
| | 0.611 | 0.046 | 1:5 | 2.73 | | | |
| | 0.396 | 0.008 | 1:10 | 3.03 | | | |
| BSA-Cef. in 0.1 M BB*** | 1.200 | 0.004 | 1:2 | 2.51 | 2.69 | 2.86 | 94.3 |
| | 0.669 | 0.016 | 1:5 | 3.06 | | | |
| | 0.348 | 0.004 | 1:10 | 2.51 | | | |

* Bioconjugates were purified with PD-10 columns and were dissovled in 0.01 M PBS
** Bioconjugate was dialysis against 0.01 M PBS buffer
*** Bioconjugate was dissovled in 0.1 M BB

### 5.1.2 Electrophoresis of the bioconjugates

LDS-PAGE analysis of BSA and OVA conjugates is shown in Figure 5.2. Smears on the gel could result from unwanted crosslinking of the proteins during the synthetic procedure, but also the unconjugated BSA used to prepare bioconjugates (not shown) had not a clear band at 67 kDa. All hapten-BSA conjugates have almost the same pattern on the gel. The Pen G-OVA conjugate has a smear between 40 kDa and 50 kDa compared to the BSA-conjugates. In order to visualize different coupling ratios, gels with a higher resolution can be used. Another possibility to characterize conjugates is MALDI-TOF, which was not performed in this thesis.

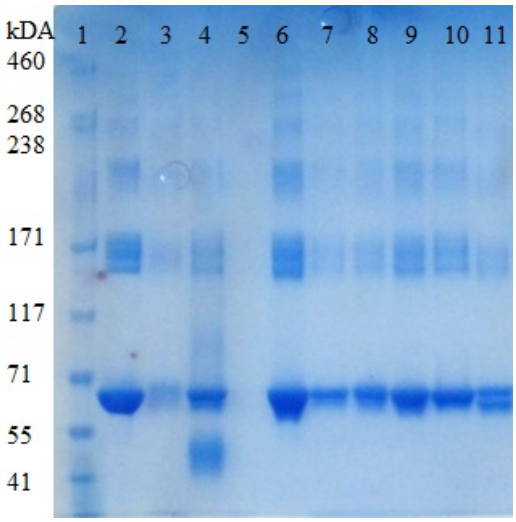


Figure 5.2: LDS-PAGE analysis (3-8% TA gel/TA buffer) of synthesized bioconjugates. Lane 1: HiMark™ prestained protein standard; lane 2: TC-CDI-BSA; lane 3: TC-4-BSA; lane 4: OVA-Pen G; lane 6: BSA-Pen G 1:50; lane 7: BSA-Pen G 1:25; lane 8: BSA-Pen G 1:10; lane 9: BSA-Cef; lane 10: BSA-Cef in 0.1 M BB; lane 11: BSA-Amp 1:50.

### 5.1.3 Determination of free amine groups

The extent of conjugation was evaluated by quantification of free amines in the bioconjugate sample, compared to a standard curve generated with unconjugated carrier proteins in series of known concentrations. Calibration curves for BSA, OVA, and KLH are shown in Figure 5.3. Linear ranges were achieved between $0.05\,\mathrm{mg\,mL^{-1}}$ to $0.5\,\mathrm{mg\,mL^{-1}}$, $0.01\,\mathrm{mg\,mL^{-1}}$ to $0.75\,\mathrm{mg\,mL^{-1}}$, and $0.1\,\mathrm{mg\,mL^{-1}}$ to $1\,\mathrm{mg\,mL^{-1}}$ for BSA, KLH, and OVA, respectively.

BSA contains 59 lysine residues of which only 30 to 35 are available for coupling reactions [67]. As outlined in Table 5.2, coupling saturation was achieved with a MCR of 1:50 (BSA:hapten).

Regarding Pen G-BSA conjugates, the decreasing substitution rate (SR) was accompanied by the decreasing MCR. Hence, the epitope density (number of hapten molecules per protein molecule) was varied by different MCRs. In case of the Pen G-OVA conjugate, only the dilution with a final concentration of 0.66 mg mL$^{-1}$ resulted in a detectable signal. The Pen G-OVA conjugate synthesis according to Knecht *et al.* [69], using a great molar excess of penicillin G, NHS, and EDC over the protein concentration (Section 4.4.1.2), resulted only in an epitope density of 5. With a coupling ratio of 1:50 the KLH protein (2,000 amines from lysine residues) was not saturated with penicillin G.

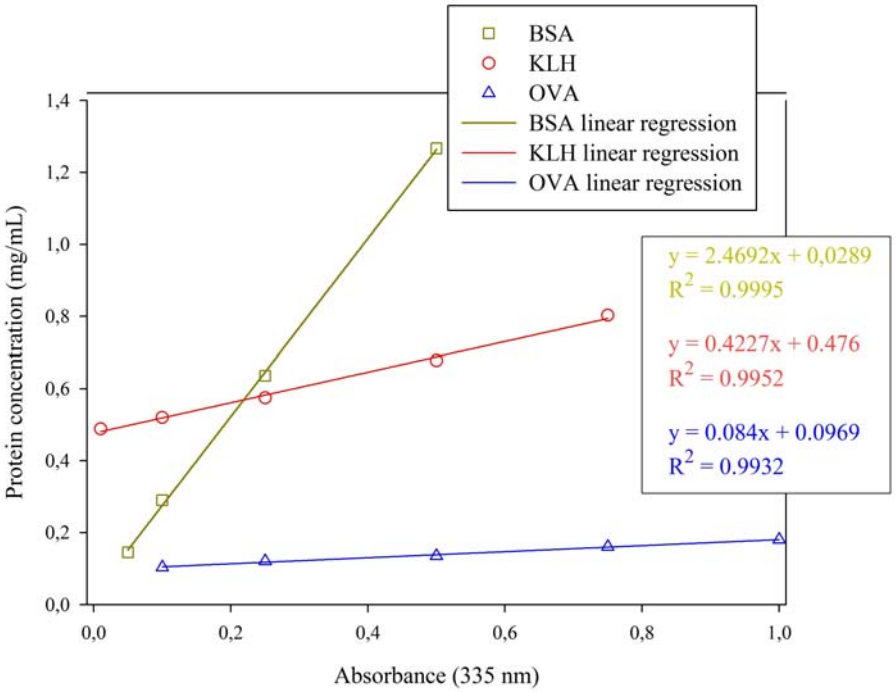


Figure 5.3: Calibration curves of the TNBSA assay. Standard deviations are smaller than 0.005 and hence, not shown.

Table 5.2: Determination of the coupling ratio by the TNBSA colorimetric assay.

| **Bioconjugates*** | **MCR** | **Working conc.** (mg mL$^{-1}$) | **Abs.$_{mean}$**** (nm) | **Std. dev.** (%) | **SR***** | **ED***** |
|---|---|---|---|---|---|---|
| BSA-PenG | 1:50 | 0.22 | 0.2550 | 0.0001 | 56 | 33 |
| BSA-PenG | 1:25 | 0.22 | 0.3766 | 0.0005 | 34 | 20 |
| BSA-PenG | 1:10 | 0.22 | 0.4163 | 0.0008 | 27 | 16 |
| TC-CDI-BSA | 1:30 | 0.26 | 0.4098 | 0.0009 | 39 | 23 |

*continued on next page*

*continued from previous page*

| **Bioconjugates** | **MCR*** | **Working conc.** ($mg\,mL^{-1}$) | **Abs.$_{mean}$**** (nm) | **Std. dev.** (%) | **SR***** | **ED***** |
|---|---|---|---|---|---|---|
| TC4-BSA | 1:50 | 0.19 | 0.2295 | 0.0002 | 54 | 32 |
| BSA-Amp | 1:50 | 0.18 | 0.2566 | 0.0001 | 47 | 27 |
| BSA-Cef | 1:50 | 0.19 | 0.2192 | 0.0001 | 56 | 33 |
| BSA-Cef in 0.1 M BB | 1:50 | 0.18 | 0.2481 | 0.0001 | 47 | 28 |
| KLH-PenG | 1:50 | 0.12 | 0.1935 | 0.0008 | 63 | 1268 |
| OVA-PenG | 1:240 | 0.66 | 0.1163 | 0.0008 | 24 | 5 |

* Molar coupling ratio (MCR) is defined as moles of hapten per mole of protein in the initial reaction mixture.
** n = 3.
*** Calculated according to equation given in Section 4.4.3.1.

### 5.1.4 UV/Vis spectra of TC-protein conjugates

In case of the TC-4-BSA conjugate, TC was modified by introduction of 4-aminobenzoic acid as diazo linkage to the ring D, prior to coupling with BSA (Figure 4.4). The synthetic procedure resulted in 7 and 9-(4´-carboxyphenylazo) products, which could not be separated. The TC-CDI-BSA conjugate was synthesized employing CDI as linking and activation agent (Figure 4.5). In the resulting conjugate, TC had been coupled to BSA via an one-carbon spacer. The UV spectra recorded from 250 nm to 600 nm for TC, BSA, TC-4-BSA, and TC-CDI-BSA is shown in Figure 5.4. It can bee seen that the BSA has a peak at 277 nm and TC has two peaks at 275 nm and 355 nm. The red shift in UV/Vis absorbance was observed for the TC-4-BSA bioconjugate (426 nm, 521 nm) as expected for diazo compounds. Similar results were obtained by Zhang *et al.* [73]. The UV/Vis pattern for TC-CDI-BSA differs from that obtained by Zhang *et al.* [73]. No obvious blue shift of the TC peak at 355 nm was measured, but a peak at 429 nm appeared.

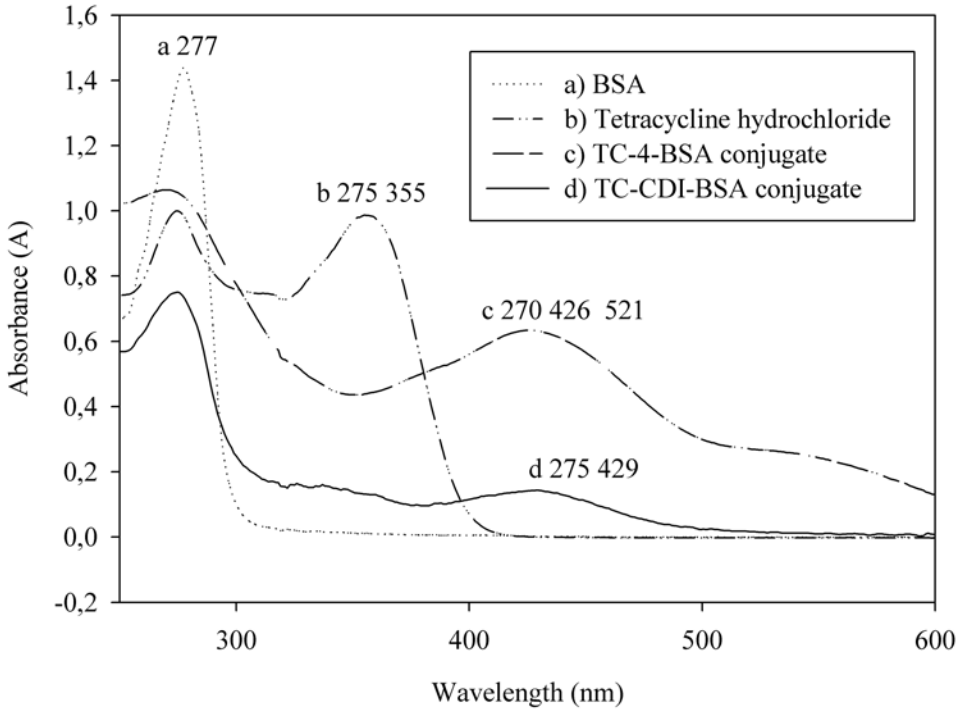


Figure 5.4: UV/Vis absorbance: a) BSA, b) TC, c) TC-CD4-BSA, and d) TC-CDI-BSA

## 5.2 Recombinant production of the PBP2x*-GST fusionprotein

### 5.2.1 Expression of PBP2x* as GST-fusion protein

The PBP2x*-GST fusionprotein expressed in *E. coli* BL21(DE3) from pGEX-tet-6P1-PBP2x* was composed of 954 aa (GST-tag: 220 aa, PreScission™ protease cleavage site: 14 aa, and PBP2x*: 720 aa). Compared to the PBP2x of *S. pneumoniae*, the soluble derivative PBP2x* lacks the transmembrane domain ($\Delta$ aa 19-48) [36], which was also demonstrated employing ClustalW for sequence alignment (Annex A.3). *E. coli* cells containing the pGEX-6P1-tet-PBP2x* expression vector were grown in 1.5 L of 2xTY broth supplemented with 15 µg mL$^{-1}$ tetracycline in a 5 L Erlenmeyer baffled flask at 37 °C with agitation at 250 rpm. The log phase cultures ($OD_{600}$ = 0.58) were induced by addition of 1 mM IPTG and allowed to express PBP2x*-GST fusionprotein for 4.75 h. Growth was measured by determination of the $OD_{600}$ of appropriate dilutions of the cultures. The corresponding growth curve is illustrated in Figure 5.5. After dilution of the preculture into fresh 2xTY medium (1:10), cell division was slow as the bacteria adapted to the fresh medium (lag phase). The bacteria then started to divide more rapidly and the culture entered logarithmic (log) phase (approx. 120 min after dilution). This fermentation followed a begin-log phase induction strategy, hence, no distinct exponential growth was obtained. Flattening of the growth curve was observed after addition of IPTG, because *E. coli* cells had grew slower after protein induction. The culture was harvested before entering the stationary phase.

### 5.2.2 Purification of PBP2x*-GST fusionprotein

The GST-PBP2x* was purified from the cell-free lysate by glutathione affinity chromatography and the procedure was monitored by LDS-PAGE (Figure 5.7). Since the GST-PBP2x* fusionprotein was not stable, several protein bands were observed in the eluted protein solution. In addition to one major band at the expected molecular mass for the fusionprotein of 102 kDa, two bands appeared at 78 kDa and 26 kDa, respectively. Both were in good agreement with the expected size for the PBP2x* protein and the GST-tag, respectively. Fractions (1 and 2; 6 and 7) were pooled and flash frozen, fractions 4, 5, and 6 were purified by size exclusion, aliquoted and flash frozen. Further experiments, e.g labeling AuC with PBP2x* and 50 kDa cut-off filtration were performed with fraction 3 or 4. 10.8 mg of protein (sum of PBP2x*-GST, GST, and PBP2x*) were obtained from 4.6 g cells (wet mass) yielding in 2.4 mg protein/g of wet weight of cell mass.

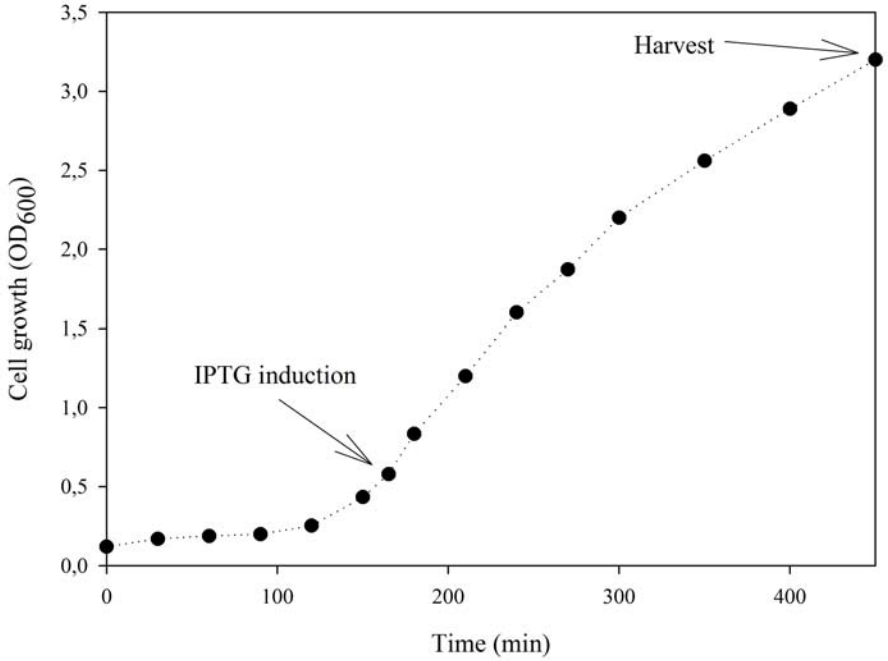


Figure 5.5: Growth curve of *E. coli* BL 21(DE3) containing pGEX-6P1-tet-PBP2x* in 2xTY medium.

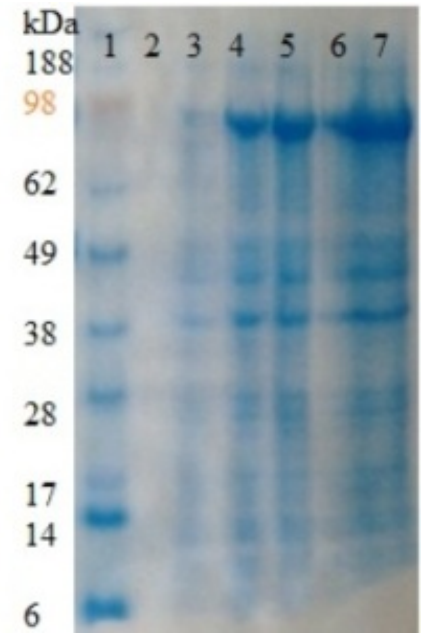


Figure 5.6: LDS-PAGE analysis of the expression of recombinant PBP2x*-GST fusionprotein using *E. coli* (4-12% Bis-Tris gel/MES buffer). Lane 1: SeeBlue® Plus2 prestained standard; lane 2: –; lane 3: bacterial pellet before IPTG induction; lane 4-7: bacterial pellet 1 h, 2 h, 3 h and 4.75 h after IPTG induction.

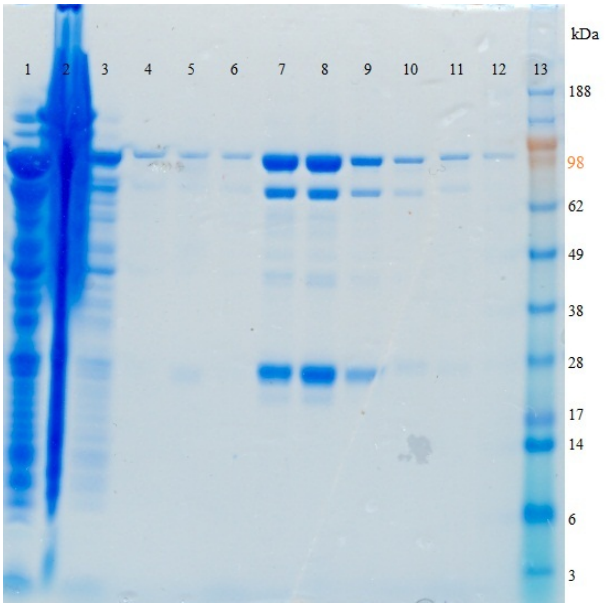


Figure 5.7: LDS-PAGE analysis of the purification of PBP2x* (4-12% Bis-Tris gel/MES buffer). Lane 1: cell-free lysate; lane 2: flow-through; lane 3: wash with 10 CV binding buffer; lane 4: wash with 10 ml binding buffer; lane 5-11: fraction 1-7; lane 12: wash with 10 ml binding buffer after elution; lane 13: SeeBlue® Plus2 pre-stained standard.

### 5.2.3 Plasmid isolation from *E. coli*

To amplify the plasmid for further transformations, miniprep was performed as stated in Section 4.5.3. The presence of the 7464 bp vector was proved by agarose gel electrophoresis (Figure 5.8). Additionally, glycerol stock cultures of *E. coli* BL21(DE3) cells containing the pGEX-6P1-tet-PBP2x* expression vector were made for further experiments.

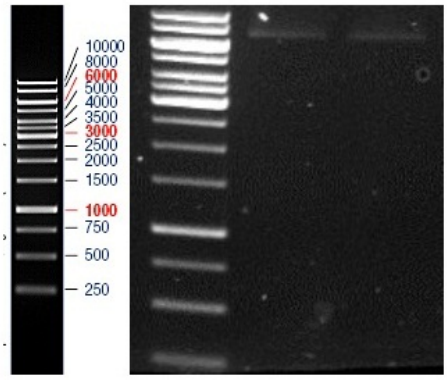


Figure 5.8: Agarose gel electrophoresis of the expression vector. GeneRuler™1 kb DNA ladder (left) and 1% agarose gel with pGEX-tet-PBP2x* 7464 bp (right). Lane 1: DNA Ladder; lane 2 and 3: expression vector.

## 5.3 LDS-PAGE of commercially obtained antibodies

The purity of both commercially obtained antibodies (anti-$\beta$-lactam ab and anti-TC ab) were verified by LDS-PAGE analysis. Both showed two bands of approximately 170 kDa and 160 kDa, being in conformity with the average molecular mass of about 150 kDa of IgG antibodies.

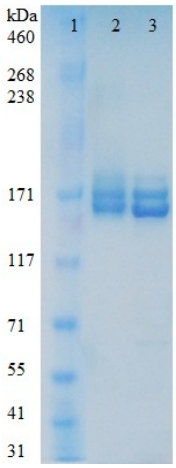


Figure 5.9: LDS-PAGE (3-8% Tris-actetate gel/Tris-acetate SDS buffer) of purchased antibodies. Lane 1: HiMark™ prestained protein standard; lane 2: anti-$\beta$-lactam antibody; lane 3: anti-TC antibody.

## 5.4 Gold conjugate

### 5.4.1 Colloidal gold characterization

Figure 5.10 shows the absorption spectra of the gold sol, which was prepared as described in Section 4.6.1. The plasmon absorbance peak in the visible region is representative for gold particles in red gold sol. Generally, absorption maximum red-shifts with increasing particle diameter [97] and therefore the correlation between particle size and absorbance maximum can be examined by employing UV/Vis spectrometry. In case of particles with a 40 nm mean diameter, the absorbance maximum correlates to approximately 529 nm under the stated assay conditions [98].

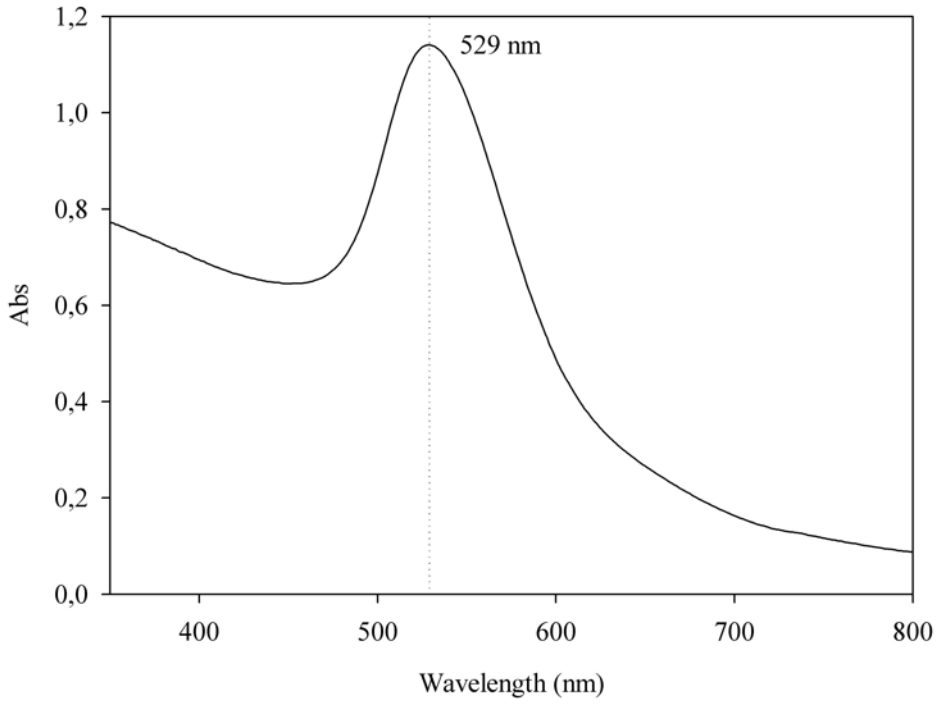


Figure 5.10: UV/Vis absorption spectrum of 40-nm gold nanoparticles in water.

### 5.4.2 Protein-gold sol titration

The determination of the optimum protein concentration for labeling AuC with the PBP2x*-GST fusionprotein, anti-$\beta$-lactam, or anti-TC antibodies was performed by addition of saturated sodium chloride solution, as stated in Section 4.6.2. The addition of positively charged sodium ions resulted in aggregation of insufficiently coated particles, which possessed remaining

negatively charged binding sites. In consequence of this reaction, the color changed from red to blue-gray (Figure 5.11), which was photometrically measured in order to estimate the optimal coupling ration. Commonly, a titration curve shows a strong rise at the lower concentrations and stays steady at higher concentrations of the protein or antibody coupled to AuC, as illustrated in Figure 5.12 for the anti-$\beta$-lactam antibody and the PBP2x*-GST fusionprotein. At about 6 µg anti-$\beta$-lactam antibody/mL AuC and at about 40 µg PBP2x*-GST fusionprotein/mL AuC the curves reached the beginning of the asymptotic region to the x-axis. Whereas, no saturation curve could be obtained with the protein A purified sheep anti-tetracycline antibody. Notwithstanding that, high amounts of antibody (20 µg antibody/mL AuC) were employed, it did not bind efficiently to the AuC surface. This phenomena was already described by Rudolf *et al.* [92] with Protein G affinity purified rabbit IgG. The PBP2x*-GST fusionprotein and the $\beta$-lactam antibody were conjugated to colloidal gold at a ratio of 45 µL/mL AuC and 8 µL/mL AuC, respectively, as described in section 4.6.3. The tetracycline antibody was not used in LDF system development.

Figure 5.11: Color change from blue-gray to red in titration experiments of PBP2x*-GST with colloidal gold at pH 8.5. The corresponding titration curve is given in Figure 5.12b.

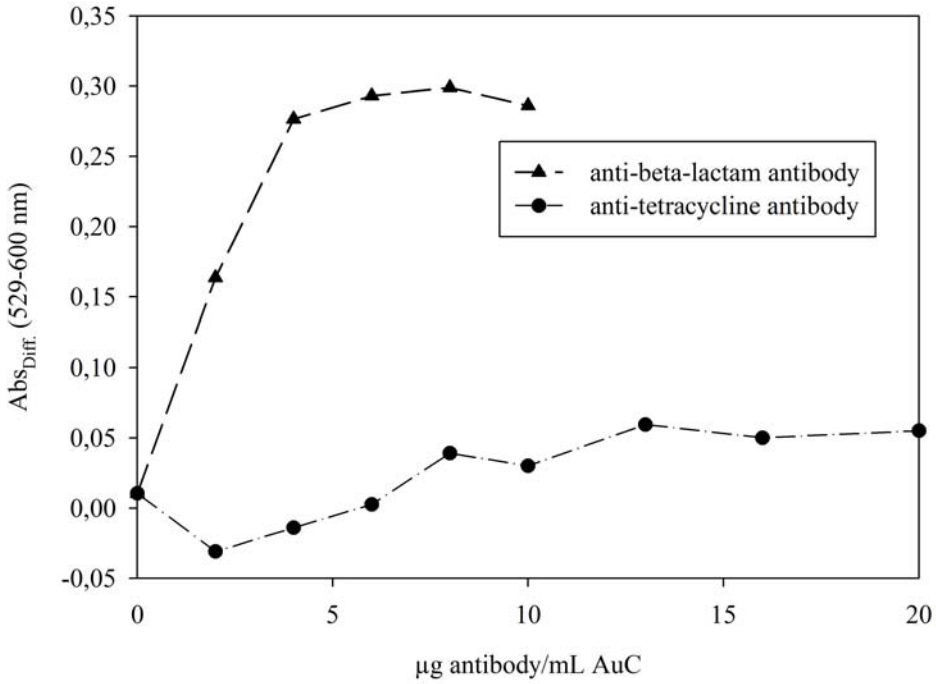


(a) Antibodies

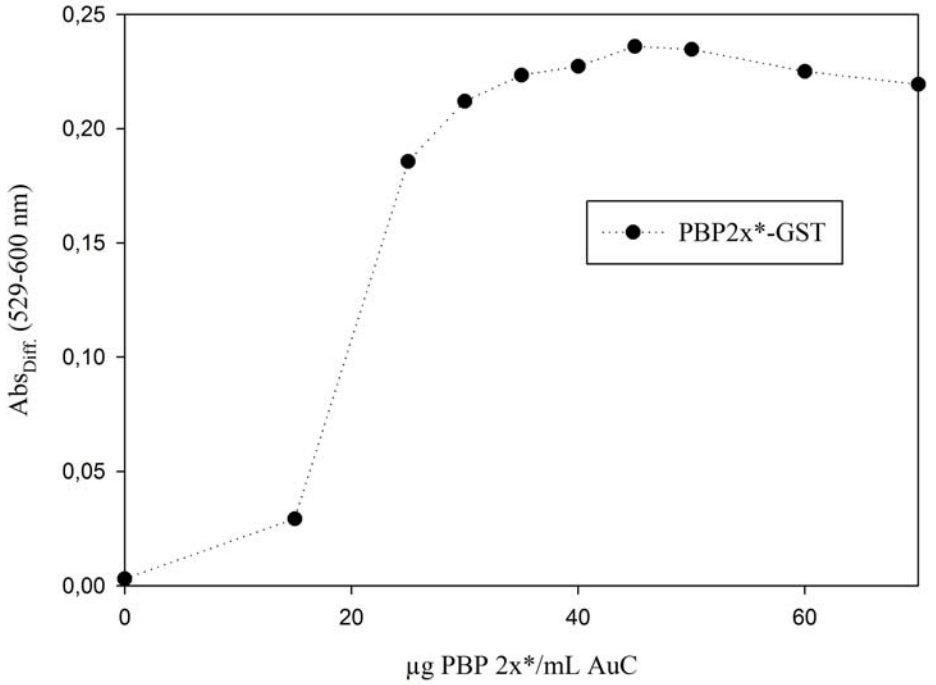


(b) Protein

Figure 5.12: Titration curves for AuC labeled with (a) $\beta$-lactam antibody or TC antibody and (b) PBP2x*-GST/GST/PBP2x* solution.

### 5.4.3 Labeling PBP2x* with AuC

At the outset, it was considered to use the entire PBP2x*-GST fusionprotein labeled with AuC in the competitive receptor-based assay format and the commercially available antibody raised against the glutathione-S-transferase (tag protein) as test line reagent.

Initial experiments were performed with the glutathione affinity chromatography purified proteins (Section 5.2). However, the fusionprotein was not stable, as LDS-PAGE analysis (Figure 5.7, lanes 5-11) revealed two faster migrating protein bands in addition to one major band at the expected apparent molecular mass of 102 kDa. Nevertheless, titration experiments were carried out with fraction 3 (Figure 5.7, lane 8) and resulted, as stated above, in an optimal coupling ratio of 45 µg PBP2x*-GST fusionprotein/mL AuC. Due to the fact that no visible test line appeared, when performing the test as described in Section 4.7.2, the supernatant after the coupling step to AuC was examined by LDS-PAGE analysis combined with silverstaining, as described in Section 4.2.3. The GST-tag predominantly attached to AuC and PBP2x* and PBP2x*-GST proteins remained in the supernatant (Figure 5.13, lanes 7,8, and 10).

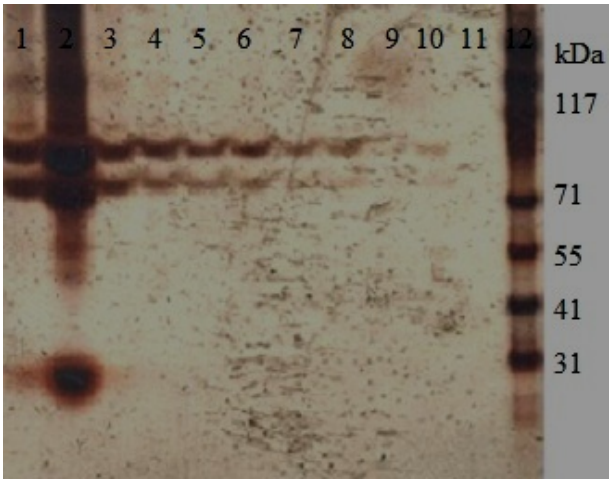


Figure 5.13: LDS-PAGE (4-12% Bis-Tris gel/MES running buffer) of the supernatant after labeling PBP2x*-GST fusionprotein with AuC and after cut-off filtration (MWCO 50 kDa). Lane 1: fraction 3; lane 2: fraction 4 (10 µg); lane 3-6: fraction 3 supernatant ultrafiltration; lane 7 and 8: 12 µL of AuC supernatant; lane 9: -; lane 10: 10 µL of AuC supernatant; lane 11: -; lane 12: HiMark™ protein standard; Concerning fraction 3 and 4 see Figure 5.7. For ultrafiltration see Section 4.5.6. For AuC supernatant see Section 4.2.3.

Robinson [41] suggested that those proteins with the highest level of the three amino acid residues that regulate protein binding (lysine, cysteine, and tryptophan) to the colloid will conjugate most

readily to the negatively charged gold nanoparticle. Table 5.3 outlines the amino acid distribution of the GST, PBP2x*, and PBP2x*-GST proteins regarding the three binding residues. GST possesses all three essential amino acids for coupling to AuC compared to PBP2x*. Although the fusionprotein contains both GST and PBP2x* binding residues, it does not apparently attach to AuC. Therefore, it can be suggested that the sole GST protein contained sufficient amounts of appropriately located lysine, tryptophan, and cysteine residues. Crystal structures of GST and PBP2x with highlighted binding residues are shown in Figure 5.14. The crystal structure of recombinant *Schistosoma japonicum* GST from pGEX vectors has been determined and it mathes that of the native protein [99]. No crystal structure of the fusionprotein expressed from pGEX-tet-6P1-PBP2x* has yet been available.

Table 5.3: Amino acid distribution of PBP2x*, GST, and PBP2x*-GST.

| | GST | PBP2x* | Fusionprotein |
|---|---|---|---|
| Lysine | 9.5% | 6.9% | 7.4% |
| Tryptophan | 1.8% | 0.8% | 1.1% |
| Cysteine | 0.8% | 0% | 0.42% |

Summarizing, a solution of PBP2x*, GST-tag, and PBP2x*-GST fusionprotein could not be employed in order to produce PBP2x* and/or PBP2x*-GST labeled AuC for its application in receptor-based strip tests to detect $\beta$-lactam antibiotic residues. In order to use the gold labeled PBP2x* protein in LFDs, it would be necessary to completely remove the GST-tag by digestion and subsequent affinity chromatography as it is performed by Cacciatore *et al.* [1] for PBP2x* protein´s application in an optical biosensor. In order to confirm the functionality of the recombinant expressed and purified protein prior to labeling with AuC, an enzymatic assay employing Bocillin™ could be performed according to Zhao *et al.* [100]. Additionally, the utilization of 20 nm colloid might be appropriate, because of the molecular weight less than 160 kDa [41].

### 5.4.4 Ultrafiltration of PBP2x*

Further, ultrafiltration (MWCO 50 kDa) was performed in order to remove GST. After several ultrafiltraion steps (Section 4.5.6, Figure 5.13), the free GST was removed. However, the remaining fusionprotein might break apart leading to PBP2x* (78 kDa) and free GST (26 kDa). Considering that, further experiments with the one-step purified PBP2x* were not performed.

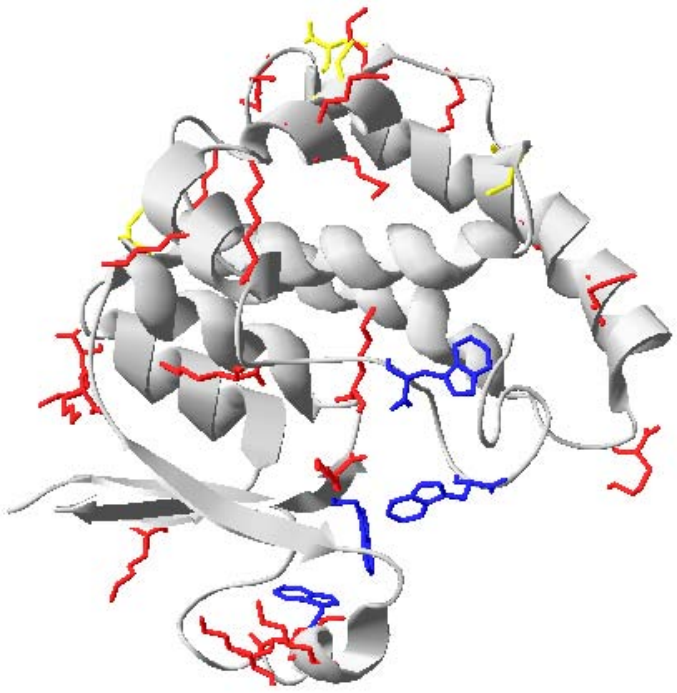

(a) GST

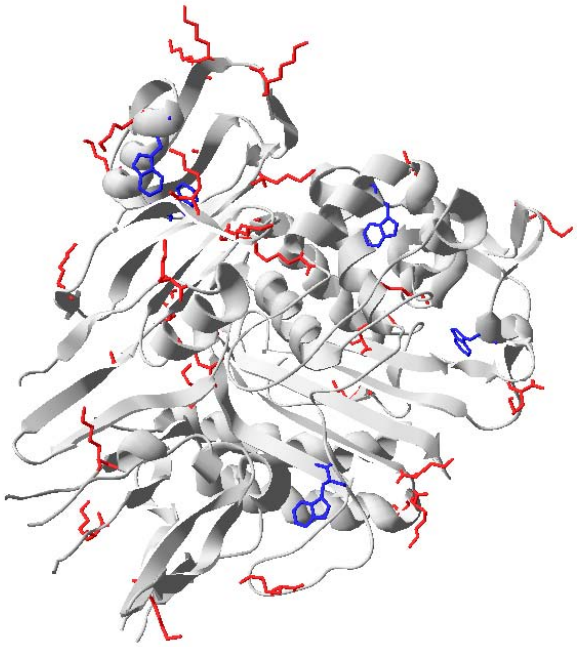

(b) PBP2x

Figure 5.14: Crystal structures of the 26 kDa glutathione S-transferase from *Schistosoma japonicum* (PDB-Code: 1M99) and the 78 kDa Penicillin binding protein 2x from *Streptococcus pneumoniae* (PDB-Code: 1QME). Amino acids which may play an important role in binding proteins to colloidal gold particles [42] are highlighted. Color code: Lysine, tryptophan and, cystein are accentuated in red, blue, and yellow, respectively.

## 5.5 Immunoassay development

### 5.5.1 Protein binding to nitrocellulose membranes

As already mentioned above the nitrocellulose membrane must irreversibly bind the TL and CL reagent, because the test results thoroughly depend on it. Here, different tasks for the development of the $\beta$-lactam lateral flow device in respect to used NC membranes, bioconjugates, assay buffer compositions, capture reagent application buffer compositions, membrane blocking, and drying conditions after spraying TL and CL onto the membrane are summarized. The assay conditions for each experiment is given in Section 4.7.3.

*The use of nitrocellulose membranes*, which differed in pore size and in post-manufacture treatment, led to false positive results with milk (fat content 0.9%) as sample and if MTP buffer or X-buffer was used as assay buffer, whereas employing the SBGT buffer did not.

*Evaluation of different hapten-protein conjugates:* $\beta$-lactam conjugates with difference in the antibiotic coupled to the carrier protein, in the used carrier proteins, and in the MCR were examined. In Figure 5.15, the effect of milk (0.9% fat) is illustrated. It seems that milk displaced proteins from NC or mask immobilized antibodies and the bioconjugate.

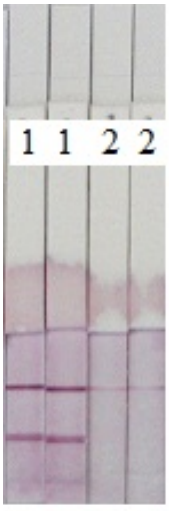


Figure 5.15: Influence of milk on the assay performance. Assay conditions: Membrane: CN 95; TL: 1 mg mL$^{-1}$ Cef-BSA in 0.01 M PBS; CL: 1 mg mL$^{-1}$ anti-sheep antibody; Assay buffer: SBGT; Sample 1: water; Sample 2: milk (fat content 0.9%).)

*Blocking* was performed as stated in Section 4.7.3.3. Displacement of the Pen G-BSA (cr 50:1) conjugate form the membrane was observed after blocking of the entire membrane with 1%

(w/v) BSA and 0.5% (w/v) PVP, both in 0.05 M PBS buffer. In case of PVP even the control line was removed. Employing Ficoll as blocking agent (1% (w/v) in 0.05 M PBS), CL and TL were visible after the assay was run as described in Section 4.7.2 with water as sample. Adding 4% (w/v) BSA to the SGT assay buffer resulted in false positive results, whereas adding 2% (w/v) BSA did not.

*The composition of the assay buffer* also had an influence of the assay procedure. As already mentioned above assay buffer containing Tween® (e.g. MTP buffer and X-buffer) led to false positive results. In case of SGB buffer containing 1% SDS both TL and CL are removed under the stated assay conditions (Section 4.7.2) using water as sample. Adding 1% Span80, 0.2% Tween® 20, 0.51% Triton X-114, or 0.5% Brij 58 to the SGB buffer leaded to visible TL and CL lines.

*Drying* of the test membranes after spraying was performed at various temperatures as stated in Section 4.7.3.5. However, the bioconjugate binding onto the membrane was not enhanced when the drying temperature was increased from 37 °C to 80 °C. Milk as sample leaded to false positive results.

*Changing the capture reagent application buffer.* Neither changing the pH nor the addition of coprecipitating agents ethanol and the crosslinking agent glutaraldeyhde resulted in enhancement of the protein binding in NC membranes.

The stripping effect of milk (fat content 0.9 %) might be based on the fact that milk contains fat globules and casein micelles which interfere with protein binding by inhibiting binding forces between the bioconjugate and the NC membrane. Hence, it may be necessary to treat the milk sample prior to testing. Disrupting of fat globules may be achieved by addition of detergents (surfactants such as Triton X-100 Triton X-114, sodium dodecyl sulfate and so on) or any other reagents (e.g. bile acids) to the assay buffer. Casein may be precipitated by acidifying milk below pH 4.3 using e.g. lactic acid, sulfuric acid, or vinegar [101]. It is also possible to apply those reagents onto a sample pad or a conjugate pad in case of developing a lateral flow device. Milk matrix effects have to be evaluated and overcome in further experiments, which will be published elsewhere.

### 5.5.2 Evaluation of the $\beta$-lactam antibody

The anti-$\beta$-lactam antibody was evaluated as stated in the Method section 4.7.3.6. Figure 5.16 shows the resulting calibration curve and the corresponding strip tests. The regression curve shows a satisfying linear relationship for low concentrations of penicillin G. LOD and LOQ were 0.3 ppb and 0.6 ppb, respectively. Since the MRL value for penicillin G in milk is 4 ppb, the commercially available anti-$\beta$-lactam antibody is suitable for its application in the detection of antibiotic residues.

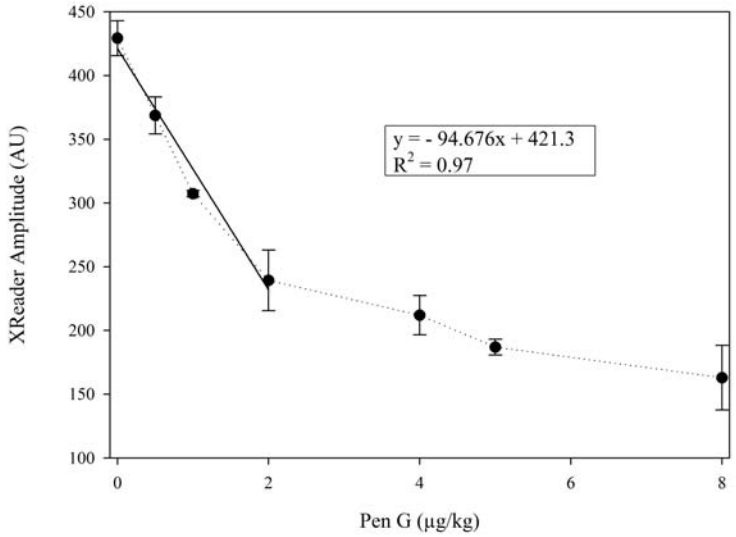


(a) Calibration curve. The line indicates the linear regression of Pen G dilutions form 0-2 ppb.

(b) Strip tests for evaluating the anti-$\beta$-lactam antibody.

Figure 5.16: Evaluation of the $\beta$-lactam antibody.

# 6 Conclusion

One part of this master thesis focused on the recombinant expression of the soluble derivative of the penicillin binding protein 2x of *Streptococcus pneumoniae*. The *E. coli* BL21(DE3) harboring the plasmid pGEX-6P1-tet-PBP2x* was used as host for the intracellular protein production. The PBP2x*-GST fusionprotein was purified with GST-affinity purification. The yield was 2.4 mg of protein per gram wet cell mass. LDS-PAGE analysis showed that the fusionprotein was not stable. The fusionprotein decomposed into PBP2x* and GST. An enzymatic cleavage employing the digestion enzyme PreScission™ combined with a further GST purification in order to get rid of the GST tag was not performed. Fractions containing PBP2x*-GST fusionprotein, PBP2x*, and the GST protein were used for labeling with colloidal gold. It was figured out that labeling PBP2x* (78 kDa) or PBP2x*-GST fusionprotein (102 kDa) with 40 nm gold particles employing those protein fractions was not feasible since mainly the 26 kDa GST-tag was attached to gold nanoparticles instead of the PBP2x* protein or the PBP 2x*-GST fusionprotein. Hence, it is suggested that either smaller molecules were preferentially coupled to 40 nm gold nanoparticles than larger proteins or the sole GST protein contained sufficient amounts of appropriately located lysine, tryptophan, and cysteine residues, which play a major role in protein binding to colloidal gold. Hence, the PBP2x* protein could not be evaluated in a lateral flow system for the detection of $\beta$-lactam residues.

The second part of this thesis was the synthesis of $\beta$-lactam-protein and tetracycline-protein conjugates. Penicillin G, ampicillin, and cefalexin were covalently bound to BSA via the active ester method. Furthermore, penicillin G molecules were covalently coupled through their carboxylic moiety to lysine residues of KLH. A diazospacer arm was coupled to TC to introduce a carboxylic acid group and then the modified TC was coupled to BSA by means of the active ester method. Another TC-BSA conjugate was prepared using CDI as linking reagent. The total protein recovery, after synthesis and size exclusion chromatography, were determined for each conjugate. It was figured out that the different synthesis procedures and the removal of excess reagents of conjugation led to an average protein recovery of 94%. For evaluation of

the extent of conjugation the TNBSA assay was performed and it was evaluated that each conjugation procedure was successful.

In the third part of the thesis, a commercially purchased antibody was used to set up a lateral flow device for the detection of $\beta$-lactam residues in milk. The use of commonly used buffers (e.g. MTP and X-buffer) resulted in false positive results, because of their high surfactant content. Due to that, an appropriate buffer was tested out and the evaluation of the antibody was performed with assay buffer as sample. For the developed strip test a detection limit of 0.3 ppb and a quantification limit of 0.6 ppb was obtained for penicillin G. Tests with milk was not performed, because milk is abundant in fat and casein and these influenced the test system. It was shown that these milk components need to be separated in a pretreatment step for further testing. In order to develop a rapid and simple test system, agents which destroy or withhold casein and fat components may be applied on a sample pad compiled of glass fiber.

Summarizing, the preferable format of the strip test will consist of two components: the lyophilized receptor-gold conjugate contained in microwells and the strip tests, which are comprised of a short sample pad incorporating casein and fat restraining-agents, followed by a layered membranes with a test line and a control line, and a wicking pad.

# Bibliography


[1] G. Cacciatore, M. Petz, S. Rachid, R. Hakenbeck, and A.A. Bergwerff. Development of an optical biosensor assay for detection of ß-lactam antibiotics in milk using the penicillin-binding protein 2x*. *Anal. Chim. Acta*, 520(1-2):105–115, 2004.

[2] E. Gustavsson. *SPR biosensor analysis of β-lactam antibiotics in milk*. PhD thesis, Swedish University of Agricultural Sciences, Uppsala, 2003.

[3] A.G. Rico, editor. *Drug residues in animals*, chapter - Allergenicity of antibacterial drug residues, pages 33–49. Academic Press, 1986.

[4] A.D. Dayan. Allergy to antimicrobial residues in food: assessment of the risk to man. *Vet. Microbiol.*, 35(3-4):213–226, 1993.

[5] J.M. Dewdney and R.G. Edwards. Penicillin hypersensitivity - is milk a significant hazard: a review. *J. R. Soc. Med.*, 77(10), 1984.

[6] M.E. Torrence and R.E. Isaacson, editors. *Microbial food safety in animal agriculture*, chapter 38 - Antimicrobial residues and residue detection in milk and dairy products. Blackwell Publishing, 2008.

[7] J.M. Dewdney, L. Maes, J.P. Raynaud, F. Blanc, J.P. Scheid, T. Jackson, S. Lens, and C. Verschueren. Risk assessment of antibiotic residues of β-lactams and macrolides in food products with regard to their immuno-allergic potential. *Food Chem. Toxicol.*, 29(7):477–483, 1991.

[8] G. Cacciatore. *Screening auf Rückstände von β-Lactam-Antibiotika in Milch: Entwicklung eines optischen Biosensor-Assays mit Penicillin-bindenden Proteinen.* PhD thesis, Universität Wuppertal, 2005.

[9] Commission Regulation (EU) No 37/2010 of 22 December 2009 on pharmacologically active substances and their classification regarding maximum residue limits in foodstuffs of animal origin. *Off. J. Eur. Comm.*, L 15.

[10] W. Reybroeck. *Screening for residues of antibiotics and chemotherapeutics in milk and honey.* PhD thesis, Universiteit Gent, 2010.

[11] Y.W. Park, editor. *Bioactive components in milk and dairy products*, chapter 2 - Bioactive components in bovine milk. Wiley-Blackwell, 2009.

[12] Regulation (EC) No 853/2004 of the European Parliament and of the Council of 29 april 2004 laying down specific hygiene rules for on the hygiene of foodstuffs. *Off. J. Eur. Comm.*, L 139.

[13] Regulation (EC) No 1774/2002 of the European Parliament and of the Council of 3 October 2002 laying down health rules concerning animal by-products not intended for human consumption. *Off. J. Eur. Comm.*, L 273.

[14] Food Standards agency. Information and guidance on the testing of milk for antibiotic residues. *http://www.food.gov.uk*, 2009.

[15] Council Directive 96/23/(EC) of 29 April 1996 on measures to monitor certain substances and resides thereof in live animals and animal products and repealing Directives 85/358/EEC and 86/469/EEC and Decisions 89/187/EEC and 91/664/EEC. *Off. J. Eur. Comm.*, L 125.

[16] Regulation (EC) No 470/2009 of the European Parliament and of the Council of 6 May 2009 laying down Community procedures for the establishment of residue limits of pharmacologically active substances in foodstuffs of animal origin, repealing Council Regulation (EEC) No 2377/90 and amending Directive 2001/82/EC of the European Parliament and of the Council and Regulation (EC) No 726/2004 of the European Parliament and of the Council. *Off. J. Eur. Comm.*, L 152.

[17] J. Wang, J.D. MacNeil, and J.F. Kay. *Chemical analysis of antibiotic residues in food.* John Wiley & Sons, 2011.

[18] P. Navrátilová. Screening methods used for the detection of veterinary drug residues in raw cow milk – a review. *Czech J. Food Sci.*, 2008.

[19] J. Lamer. *Entwicklung, Optimierung und Validierung eines rezeptorproteingestützten Mikrotiterplatten-Test zur Rückstandsanalytik von β-Lactam-Antibiotika.* PhD thesis, Bergische Universität Wuppertal, 2007.

[20] AGES. Antibiotika-Vertriebsmengen in der Veterinärmedizin in Österreich. *http://www.ages.at*, 2011.

[21] N. Moeller. *Entwicklung eines optischen Biosensors-Assays mit Elementen aus der Resistenzforschung zum Screening auf Tetracyclin-Rückstande in Lebensmitteln.* PhD thesis, Bergische Universität Wuppertal, 2007.

[22] I.E. Alcamo. *Microbes and society.* Jones and Bartlett Publishers, Inc., 2003.

[23] D.L. Mayers, editor. *Antimicrobial drug resistance - Mechanisms of drug resistance*, chapter 13 - Penicillin-binding proteins and $\beta$-lactam resistance. Humana Press Inc., 2009.

[24] R. Hakenbeck, M. Tarpay, and A. Tomasz. Multiple changes of penicillin-binding proteins in penicillin-resistant clinical isolates of *Streptococcus pneumoniae. Antimicrob. Agents Chemother.*, 17(3):364–371, 1980.

[25] J.M. Ghuysen. Serine $\beta$-lactamases and penicillin-binding proteins. *A. Rev. Microbiol.*, 45(1):37–67, 1991.

[26] C. Goffin and J.-M. Ghuysen. Multimodular penicillin-binding proteins: an enigmatic family of orthologs and paralogs. *Microbiol. Mol. Biol. R.*, 62(4):1079–1093, 1998.

[27] H. König, H. Claus, and A. Varma, editors. *Prokaryotic cell wall compounds - Structure and biochemistry.* Springer, 2010.

[28] E. Sauvage, F. Kerff, M. Terrak, J.A. Ayala, and P. Charlier. The penicillin-binding proteins: structure and role in peptidoglycan biosynthesis. *FEMS Microbiol. Rev.*, 32(2):234–258, 2008.

[29] G. Fuchs and H.G. Schlegel. *Allgemeine Mikrobiologie.* Thieme, 2006.

[30] M. Schaechter, editor. *The desk encyclopedia of microbiology*, chapter - Peptidoglycan, pages 827–843. Academic Press, 2 edition, 2009.

[31] O.A. Mascaretti. *Bacteria versus antibacterial agents.* ASM Press, 2003.

[32] R. Hakenbeck, T. Briese, and H. Ellerbrok. Antibodies against the benzylpenicilloyl moiety as a probe for penicillin-binding proteins. *Eur. J. Biochem.*, 157(1):101–106, 1986.

[33] R. Hakenbeck and M. Kohiyama. Purification of penicillin-binding protein 3 from *Streptococcus pneumoniae. Eur. J. Biochem.*, 127(2):231–236, 1982.

[34] G. Laible, R. Hakenbeck, M. A. Sicard, B. Joris, and J.-M. Ghuysen. Nucleotide sequences of the pbpX genes encoding the penicillin-binding proteins 2x from *Streptococcus pneumoniae* R6 and a cefotaxime-resistant mutant, C506. *Mol. Microbiol.*, 3(10):1337–1348, 1989.

[35] N. Mouz, A.M. Di Guilmi, E. Gordon, R. Hakenbeck, O. Dideberg, and T. Vernet. Mutations in the active site of penicillin-binding protein PBP2x from *Streptococcus pneumoniae*. *J. Biol. Chem.*, 274(27):19175–19180, 1999.

[36] G. Laible, W. Keck, R. Lurz, H. Mottl, J.M. Frère, M. Jamin, and R. Hakenbeck. Penicillin-binding protein 2x of *Streptococcus pneumoniae*. *Eur. J. Biochem.*, 207(3):943–949, 1992.

[37] M. Jamin, R. Hakenbeck, and J.M. Frère. Penicillin binding protein 2x as a major contributor to intrinsic ß-lactam resistance of *Streptococcus pneumoniae*. *FEBS Letters*, 331(1-2):101–104, 1993.

[38] M. Jamin, C. Damblon, S. Millier, R. Hakenbeck, and J.M. Frère. Penicillin-binding protein 2x of *Streptococcus pneumoniae*: Enzymic activities and interactions with beta-lactams. *Biochem. J.*, 292(3):735–741, 1993.

[39] Millipore. Rapid lateral flow test strips - considerations for product development. Technical report, 2008.

[40] GE Healthcare. Clinical diagnostics without boundaries. Technical report, 2010.

[41] N. Robinson. Immunogold conjugation for IVD applications. *IVD Technol.*, March, 2002.

[42] J. Chandler, T. Gurmin, and N. Robinson. The place of gold in rapid tests. *IVD Technol.*, 6(2):37–49, 2000.

[43] J. Chandler, N. Robinson, and K. Whiting. Handling false signals in gold-based rapid tests. *IVD Technol.*, 7(2):34–45, 2001.

[44] K. Jones. Troubleshooting protein binding in nitrocellulose membranes, part 1: Principles. *IVD Technol.*, 5(2):32–41, 1999.

[45] K. Jones. Troubleshooting protein binding in nitrocellulose membranes, part 2: Common problems. *IVD Technol.*, 5(3):26–35, 1999.

[46] G.A. Posthuma-Trumpie, J. Korf, and A. van Amerongen. Lateral flow (immuno)assay: its strengths, weaknesses, opportunities and threats. A literature survey. *Anal. Bioanal. Chem.*, 393(2), 2009.

[47] G. Shan, editor. *Immunoassays in agricultural biotechnology.* John Wiley & Sons, Inc., 2011.

[48] R.C. Wong and H.Y. Tse, editors. *Lateral flow immunoassay.* Humana Press, 2009.

[49] A. Weiss. Concurrent engineering for lateral-flow diagnostics. *IVD Technol.*, 7:48–57, 1999.

[50] S. Baumgartner, I. Fürtler-Leitzenberger, E. Drs, A. Molinelli, R. Krska, U. Immer, K. Schmitt, M. Bremer, W. Haasnoot, Ch. Danks, Romkies. V., P. Reece, Ph. Wilson, M. Kiening, M. Weller, R. Niessner, E. Corsini, and S. Mendonça. *European surey for hidden allergens in food: a case study with peanut ad hazelnut*, chapter 24, pages 370–381. 2008.

[51] L.E. Lindler and F.J. Lebeda, editors. *Biological weapons defense - Infectious diseases and counterbioterrorism*, chapter 25 - Concepts for the development of immunodiagnostic assays for detection and diagnosis of biothreat agents. Humana Press, 2005.

[52] Commission Decision 2002/657/EC of 12 August 2002 implementing Council Directive 96/23/EC concerning the performance of analytical methods and the interpretation of results. *Off. J. Eur. Comm.*, L 221.

[53] Community reference laboratories residues (CRLs) 20/1/2010 — guidelines for the validation of screening methods for residues of veterinary medicines (initial validation and transfer), 2010.

[54] J. Sambrook and D.W. Russel. *Molecular cloning - A laboratory manual.* Cold Spring Harbor Laboratory Press, 3 edition, 2001.

[55] M.M Franse, I.J. Blankwater, and M. Valentine. Lateral flow binding assay. Patent application number: 20080227220, 09 2008.

[56] P.K. Smith, R.I. Krohn, G.T. Hermanson, A.K. Mallia, F.H. Gartner, M.D. Provenzano, E.K. Fujimoto, N.M. Goeke, B.J. Olson, and D.C. Klenk. Measurement of protein using bicinchoninic acid. *Anal. Biochem.*, 150:76–85, 1985.

[57] K.J. Wiechelman, R.D. Braun, and J.D. Fitzpatrick. Investigation of the bicinchoninic acid protein assay: identification of the groups responsible for color formation. *Anal. Biochem.*, 175:231–237, 1988.

[58] Thermo Scientific. *Pierce® BCA Protein Assay Kit*, 2011.

[59] B. Alberts, A. Johnson, J. Lewis, M. Raff, K. Roberts, and W.P. Peter. *Molecular biology of the cell.* Garland Science, 4 edition, 2002.

[60] U.K. Laemmli. Cleavage of structural proteins during the assembly of the head of bacteriophage T4. *Nature*, 277:680–685, 1970.

[61] Invitrogen. *NuPAGE® Technical Guide - General information and protocols for using the NuPAGE® electrophoresis system*, 2010.

[62] V. Neuhof, editor. *Free SH-groups are important for the polychromatic staining of proteins with silver nitrat*, page 328–330. Verlag Chemie Weinheim, 1984.

[63] A.S. Bommarius and B.R. Riebel. *Biocatalysis: fundamentals and applications.* Wiley-VCH Verlag GmbH & Co, 2004.

[64] J.M. Walker, editor. *The proteomics protocols handbook*, chapter 18 - Silver Staining of 2-D Gels. Humana Press Inc., 2005.

[65] H. Rehm and T. Letzel. *Der Experimentator: Proteinbiochemie/Proteomics.* Spektrum Akademischer Verlag, 2010.

[66] J. Heukeshoven and R. Dernick. Improved silver staining procedure for fast staining in phastsystem development unit - staining of sodium dodecyl sulfate gels. *Electrophoresis*, 9(1):28–32, 1988.

[67] G.T. Hermanson. *Bioconjugate Techniques.* Academic Press, 2 edition, 2008.

[68] N. Pastor-Navarro, Á. Maquieira, and R. Puchades. Review on immunoanalytical determination of tetracycline and sulfonamide residues in edible products. *Anal. Bioanal. Chem.*, 395:907–920, 2009.

[69] B.G. Knecht, A. Strasser, R. Dietrich, E. Märtlbauer, R. Niessner, and M.G. Weller. Automated microarray system for the simultaneous detection of antibiotics in milk. *Anal. Chem.*, 76(3):646–654, 2004.

[70] A.C. Strasser. *Entwicklung eines Biosensors zum Nachweis von Antibiotika und Sulfonamiden in Milch - Herstellung der immunchemischen Komponenten.* PhD thesis, LMU München, 2003.

[71] E. Usleber, S. Litz, and E. Märtlbauer. Production and characterization of group-specific antibodies against penicillin antibiotics. *Food Agr. Immunol.*, 10(4):317–324, 1998.

[72] A. Williams and I.T. Ibrahim. Carbodiimide chemistry: recent advances. *Chem. Rev.*, 81(6):589–636, 1981.

[73] Y. Zhang, S. Lu, W. Liu, C. Zhao, and R. Xi. Preparation of anti-tetracycline antibodies and development of an indirect heterologous competitive enzyme-linked immunosorbent assay to detect residues of tetracycline in milk. *J. Agric. Food Chem.*, 55(2):211–218, 2007.

[74] N. Pastor-Navarro, S. Morais, Á. Maquieira, and R. Puchades. Synthesis of haptens and development of a sensitive immunoassay for tetracycline residues: application to honey samples. *Anal. Chim. Acta*, 594(2):211–218, 2007.

[75] A.F. Habeeb. Determination of free amino groups in proteins by trinitrobenzenesulfonic acid. *Anal. Biochem.*, 1966.

[76] S. Pauillac, J. Naar, B. Mouratou, and J.L. Guesdon. Application of a modified version of habeeb's trinitrophenylation method for the characterization of hapten-protein conjugates in a reversed micellar medium. *J. Immunol. Meth.*, 263(1-2):75–83, 2002.

[77] GE Healthcare. *Recombinant protein purification handbook - Principles and methods.*

[78] GE Healthcare. *GST gene fusion system handbook*, 2010.

[79] N.H. Tolia and L. Joshua-Tor. Strategies for protein coexpression in *Escherichia coli. Nat. Meth.*, 3(1), 2006.

[80] J.M. Becker, G.A. Caldwell, and E.A. Zachgo. *Biotechnology - A laboratory course.* Academic Press, 2 edition, 1996.

[81] H.C. Birnboim and J. Doly. A rapid alkaline lysis procedure for screening recombinant plasmid DNA. *Nucleic Acids Res.*, 7:1513–1522, 1979.

[82] S. Carson, H. Miller, and D.S Witherow. *Molecular biology techniques - A classroom laboratory manual.* Academic Press, 2 edition, 2006.

[83] Qiagen. *QIAprep® Miniprep Handbook*, 2006.

[84] R.C. Ogden and D.A. Adams. Electrophoresis in agarose and acrylamide gels. *Meth. Enzymol.*, 152:61–87, 1987.

[85] A. Molinelli, K. Grossalber, M. Führer, S. Baumgartner, M. Sulyok, and R. Krska. Development of qualitative and semiquantitative immunoassay-based rapid strip tests for the detection of T-2 toxin in wheat and oat. *J. Agric. Food Chem.*, 56:2589–2594, 2008.

[86] S.L. Goodman, G.M. Hodges, L.K. Trejdosiewicz, and D.C. Livingston. Colloidal gold probes - a further evaluation. *Scan. Electron. Micros.*, 3:619–628, 1979.

[87] F. Daumas, H. Mazarguil, C. Millot, Á Lopez, and L. Salomé. Probing functionalized gold colloids for single particle tracking experiments. *Biochem. Biophys. Res. Commun.*, 295(3):610–615, 2002.

[88] G.F. Paciotti, L. Myer, D. Weinreich, D. Goia, N. Pavel, R.E. McLaughlin, and L. Tamarkin. Colloidal gold: a novel nanoparticle vector for tumor directed drug delivery. *Drug Deliv.*, 11(3):169–183, 2004.

[89] S. L. Goodman, G. M. Hodges, L. K. Trejdosiewicz, and D. C. Livingston. Colloidal gold markers and probes for routine application in microscopy. *J. Micros.*, 123(2):201–213, 1981.

[90] W. Luttmann, K. Bratke, M. Küpper, and D. Myrtek. *Immunology.* Academic Press, 2006.

[91] G. Frens. Controlled nucleation for the regulation of the particle size in monodisperse gold suspensions. *Nat. Phys. Sci.*, 241:20–22, 1973.

[92] J. Rudolf, M. Führer, B. Galler, P. Ansari, C. Hasenhindl, and S. Baumgartner. Differences in usability of rabbit IgG and chicken IgY after clean-up and impact on gold labelling properties. *J. Immunol. Meth.*, 350(1-2):79–88, 2009.

[93] M. Helmel. Development of a lateral flow device for T-2 toxin and HT-2 toxin in wheat and oats. Master's thesis, Vienna University of Technology, 2009.

[94] Diagnostic membranes for lateral flow assays. *http://www.whatman.com*, 2011.

[95] W.L. Hoffman, A.A. Jump, P.J. Kelly, and A.O. Ruggles. Binding of antibodies and other proteins to nitrocellulose in acidic, basic, and chaotropic buffers. *Anal. Biochem.*, 198(1):112–118, 1991.

[96] L. L´Hocine, J.I. Boye, and C. Munyana. Detection and quantification of soy allergens in food: study of two commercial enzyme-linked immunosorbend assays. *J. Food Sci.*, 72(3):145–153, 2007.

[97] S. Link and M.A. El-Sayed. Size and temperature dependence of the plasmon absorption of colloidal gold nanoparticles. *J. Phys. Chem. B*, 103(21):4212–4217, 1999.

[98] B. Cvak, D. Pum, A. Molinelli, and R. Krska. Synthesis and characterization of colloidal gold particles as labels for antibodies as used in lateral flow devices. *Analyst*. First published on the web 02 March 2012.

[99] GE Healthcare. Glutathione S-transferase gene fusion system. Technical Report 28-9622-84 AA, 2009.

[100] G. Zhao, T.I. Meier, S.D. Kahl, K.R. Gee, and L.C. Blaszczak. Bocillin FL, a sensitive and commercially available reagent for detection of penicillin-binding proteins. *Antimicrob. Agents Chemother.*, 43(5):1124–1128, 1999.

[101] W.M. Wondu. Method for simultaneous detection of multiple microbial antigens in biological specimens from mastitic animals. United States Patent No. US 6,720,160 B2.

# A Annex

## A.1 DNA sequence of pGEX-6P1-tet-PBP2x*

The sequence of pGEX-6P1-tet-PBP2x* was provided from Prof. Hackenbeck (TU Kaiserslautern).

acgttatcga ctgcacggtg caccaatgct tctggcgtca ggcagccatc ggaagctgtg gtatggctgt gcaggtcgta aatcactgca taattcgtgt cgctcaaggc gcactcccgt tctggataat gttttttgcg ccgacatcat aacggttctg gcaaatattc tgaaatgagc tgttgacaat taatcatcgg ctcgtataat gtgtggaatt gtgagcggat aacaatttca cacaggaaac agtattcatg tcccctatac taggttattg gaaaattaag ggccttgtgc aacccactcg acttcttttg gaatatcttg aagaaaaata tgaagagcat ttgtatgagc gcgatgaagg tgataaatgg cgaaacaaaa agtttgaatt gggtttggag tttcccaatc ttccttatta tattgatggt gatgttaaat taacacagtc tatggccatc atacgttata tagctgacaa gcacaacatg ttgggtggtt gtccaaaaga gcgtgcagag atttcaatgc ttgaaggagc ggttttggat attagatacg gtgtttcgag aattgcatat agtaaagact ttgaaactct caaagttgat tttcttagca agctacctga aatgctgaaa atgttcgaag atcgtttatg tcataaaaca tatttaaatg gtgatcatgt aacccatcct gacttcatgt tgtatgacgc tcttgatgtt gttttataca tggacccaat gtgcctggat gcgttcccaa aattagtttg ttttaaaaaa cgtattgaag ctatcccaca aattgataag tacttgaaat ccagcaagta tatagcatgg cctttgcagg gctggcaagc cacgtttggt ggtggcgacc atcctccaaa atcggatctg gaagttctgt tccaggggcc cctgggatcc ccggaattca tgaagtggac aaaaagagta atccgttatg cgaccaaaaa tcggaaatcg ccggggacag gcactcgctt tggaacagat ttagcgaagg aagctaagaa ggttcatcaa accacccgta cagttcctgc caaacgtggg actatttatg accgaaatgg agtcccgatt gctgaggatg caacctctta taatgtctat gcggtcattg atgagaacta taagtcagca acgggtaaga ttctttacgt agaaaaaaca caatttaaca aggttgcaga ggtctttcat aagtatctgg acatggaaga atcctatgta agagagcaac tctcgcaacc taatctcaag caagtttcct ttggagcaaa gggaaatggg attacctatg ccaatatgat gtctatcaaa aaagaattgg aagctgcaga ggtcaagggg attgatttta caaccagtcc caatcgtagt tacccaaacg gacaatttgc ttctagtttt atcggcctag ctcagctcca tgaaaatgaa gatggaagca agagcttgct gggaacctct ggaatggaga gttccttgaa cagtattctt gcagggacag acggcattat tacctatgaa aaggatcgtc tgggtaatat tgtacccgga acagaacaag tttcccaacg aacgatggac ggtaaggatg tttatacaac catttccagc cccctccagt cctttatgga aacccagatg gatgcttttc aagagaaggt aaaaggaaag tacatgacag cgactttggt cagtgctaaa acaggggaaa ttctggcaac aacgcaacga ccgacctttg atgcagatac aaaagaaggc attacagagg actttgtttg

gcgtgatatc ctttaccaaa gtaactatga gccaggttcc actatgaaag tgatgatgtt ggctgctgct attgataata
ataccttttcc aggaggagaa gtctttaata gtagtgagtt aaaaattgca gatgccacga ttcgagattg ggacgttaat
gaaggattga ctggtggcag aatgatgact ttttctcaag gttttgcaca ctcaagtaac gttgggatga ccctccttga
gcaaaagatg ggagatgcta cctggcttga ttatcttaat cgttttaaat ttggtgttcc gacccgtttc ggtttgacgg
atgagtatgc tggtcagctt cctgcggata atattgtcaa cattgcgcaa agctcatttg gacaagggat ttcagtgacc
cagacgcaaa tgattcgtgc ctttacagct attgctaatg acggtgtcat gctggagcct aaatttatta gtgccattta
tgatccaaat gatcaaactg ctcggaaatc tcaaaaagaa attgtgggaa atcctgtttc taaagatgca gctagtctaa
ctcggactaa catggttttg gtagggacgg atccggttta tggaaccatg tataaccaca gcacaggcaa gccaactgta
actgttcctg ggcaaaatgt agccctcaag tctggtacgg ctcagattgc tgacgagaaa aatggtggtt atctagtcgg
gttaaccgac tatattttct cggctgtatc gatgagtccg gctgaaaatc ctgattttat cttgtatgtg acggtccaac
aacctgaaca ttattcaggt attcagttgg gagaatttgc caatcctatc ttggagcggg cttcagctat gaaagactct
ctcaatcttc aaacaacagc taaggctttg gagcaagtaa gtcaacaaag tccttatcct atgcccagtg tcaaggatat
ttcacctggt gatttagcag aagaattgcg tcgcaatctt gtacaaccca tcgttgtggg aacaggaacg aagattaaaa
acagttctgc tgaagaaggg aagaatcttg ccccgaacca gcaagtcctt atcttatctg ataaagcaga ggaggttcca
gatatgtatg gttggacaaa ggagactgct gagacccttg ctaagtggct caatatagaa cttgaatttc aaggctcggg
ctctactgtg cagaagcaag atgttcgtgc taacacagct atcaaggaca ttaaaaaaat tacattaact ttaggagact
aactcgagcg gccgctcatg tttgacagct tatcatcgat aagctttaat gcggtagttt atcacagtta aattgctaac
gcagtcaggc accgtgtatg aaatctaaca atgcgctcat cgtcatcctc ggcaccgtca ccctggatgc tgtaggcata
ggcttggtta tgccggtact gccgggcctc ttgcgggata tcgtccattc cgacagcatc gccagtcact atggcgtgct
gctagcgcta tatgcgttga tgcaatttct atgcgcaccc gttctcggag cactgtccga ccgctttggc cgccgcccag
tcctgctcgc ttcgctactt ggagccacta tcgactacgc gatcatggcg accacacccg tcctgtggat cctctacgcc
ggacgcatcg tggccggcat caccggcgcc acaggtgcgg ttgctggcgc ctatatcgcc gacatcaccg atggggaaga
tcgggctcgc cacttcgggc tcatgagcgc ttgtttcggc gtgggtatgg tggcaggccc cgtggccggg ggactgttgg
gcgccatctc cttgcatgca ccattccttg cggcggcggt gctcaacggc ctcaacctac tactgggctg cttcctaatg
caggagtcgc ataagggaga gcgtcgaccg atgcccttga gagccttcaa cccagtcagc tccttccggt gggcgcgggg
catgactatc gtcgccgcac ttatgactgt cttctttatc atgcaactcg taggacaggt gccggcagcg ctctgggtca
ttttcggcga ggaccgcttt cgctggagcg cgacgatgat cggcctgtcg cttgcggtat tcggaatctt gcacgccctc
gctcaagcct tcgtcactgg tcccgccacc aaacgtttcg gcgagaagca ggccattatc gccggcatgg cggccgacgc
gctgggctac gtcttgctgg cgttcgcgac gcgaggctgg atggccttcc ccattatgat tcttctcgct tccggcggca
tcgggatgcc cgcgttgcag gccatgctgt ccaggcaggt agatgacgac catcagggac agcttcaagg atcgctcgcg
gctcttacca gcctaacttc gatcactgga ccgctgatcg tcacggcgat ttatgccgcc tcggcgagca catggaacgg
gttggcatgg attgtaggcg ccgccctata ccttgtctgc ctccccgcgt tgcgtcgcgg tgcatggagc cgggccacct
cgacctgaat ggctgcagca atggcaacaa cgttgcgcaa actattaact ggcgaactac ttactctagc ttcccggcaa

caattaatag actggatgga ggcggataaa gttgcaggac cacttctgcg ctcggccctt ccggctggct ggtttattgc
tgataaatct ggagccggtg agcgtgggtc tcgcggtatc attgcagcac tggggccaga tggtaagccc tcccgtatcg
tagttatcta cacgacgggg agtcaggcaa ctatggatga acgaaataga cagatcgctg agataggtgc ctcactgatt
aagcattggt aactgtcaga ccaagtttac tcatatatac tttagattga tttaaaactt cattttaat ttaaaaggat
ctaggtgaag atccttttg ataatctcat gaccaaaatc ccttaacgtg agttttcgtt ccactgagcg tcagaccccg
tagaaaagat caaaggatct tcttgagatc ctttttttct gcgcgtaatc tgctgcttgc aaacaaaaaa accaccgcta
ccagcggtgg tttgtttgcc ggatcaagag ctaccaactc tttttccgaa ggtaactggc ttcagcagag cgcagatacc
aaatactgtc cttctagtgt agccgtagtt aggccaccac ttcaagaact ctgtagcacc gcctacatac ctcgctctgc
taatcctgtt accagtggct gctgccagtg gcgataagtc gtgtcttacc gggttggact caagacgata gttaccggat
aaggcgcagc ggtcgggctg aacgggggt tcgtgcacac agcccagctt ggagcgaacg acctacaccg aactgagata
cctacagcgt gagctatgag aaagcgccac gcttcccgaa gggagaaagg cggacaggta tccggtaagc ggcagggtcg
gaacaggaga gcgcacgagg gagcttccag ggggaaacgc ctggtatctt tatagtcctg tcgggtttcg ccacctctga
cttgagcgtc gatttttgtg atgctcgtca gggggggcgga gcctatggaa aaacgccagc aacgcggcct ttttacggtt
cctggccttt tgctggcctt ttgctcacat gttctttcct gcgttatccc ctgattctgt ggataaccgt attaccgcct ttgagtgagc
tgataccgct cgccgcagcc gaacgaccga gcgcagcgag tcagtgagcg aggaagcgga agagcgcctg atgcggtatt
ttctccttac gcatctgtgc ggtatttcac accgcataaa ttccgacacc atcgaatggt gcaaaacctt tcgcggtatg
gcatgatagc gcccggaaga gagtcaattc agggtggtga atgtgaaacc agtaacgtta tacgatgtcg cagagtatgc
cggtgtctct tatcagaccg tttcccgcgt ggtgaaccag gccagccacg tttctgcgaa aacgcgggaa aaagtggaag
cggcgatggc ggagctgaat tacattccca accgcgtggc acaacaactg gcgggcaaac agtcgttgct gattggcgtt
gccacctcca gtctggccct gcacgcgccg tcgcaaattg tcgcggcgat taaatctcgc gccgatcaac tgggtgccag
cgtggtggtg tcgatggtag aacgaagcgg cgtcgaagcc tgtaaagcgg cggtgcacaa tcttctcgcg caacgcgtca
gtgggctgat cattaactat ccgctggatg accaggatgc cattgctgtg gaagctgcct gcactaatgt tccggcgtta
tttcttgatg tctctgacca gacacccatc aacagtatta ttttctccca tgaagacggt acgcgactgg gcgtggagca
tctggtcgca ttgggtcacc agcaaatcgc gctgttagcg ggcccattaa gttctgtctc ggcgcgtctg cgtctggctg
gctggcataa atatctcact cgcaatcaaa ttcagccgat agcggaacgg gaaggcgact ggagtgccat gtccggtttt
caacaaacca tgcaaatgct gaatgagggc atcgttccca ctgcgatgct ggttgccaac gatcagatgg cgctgggcgc
aatgcgcgcc attaccgagt ccgggctgcg cgttggtgcg gatatctcgg tagtgggata cgacgatacc gaagacagct
catgttatat cccgccgtca accaccatca aacaggattt tcgcctgctg gggcaaacca gcgtggaccg cttgctgcaa
ctctctcagg gccaggcggt gaagggcaat cagctgttgc ccgtctcact ggtgaaaaga aaaaccaccc tggcgcccaa
tacgcaaacc gcctctcccc gcgcgttggc cgattcatta atgcagctgg cacgacaggt ttcccgactg gaaagcgggc
agtgagcgca acgcaattaa tgtgagttag ctcactcatt aggcacccca ggctttacac tttatgcttc cggctcgtat
gttgtgtgga attgtgagcg gataacaatt tcacacagga aacagctatg accatgatta cggattcact ggccgtcgtt
ttacaacgtc gtgactggga aaaccctggc gttacccaac ttaatcgcct tgcagcacat ccccctttcg ccagctggcg

taatagcgaa gaggcccgca ccgatcgccc ttcccaacag ttgcgcagcc tgaatggcga atggcgcttt gcctggtttc cggcaccaga agcggtgccg gaaagctggc tggagtgcga tcttcctgag gccgatactg tcgtcgtccc ctcaaactgg cagatgcacg gttacgatgc gcccatctac accaacgtaa cctatcccat tacggtcaat ccgccgtttg ttcccacgga gaatccgacg ggttgttact cgctcacatt taatgttgat gaaagctggc tacaggaagg ccagacgcga attatttttg atggcgttgg aattt

## A.2 Sequence alignment - HSA and BSA

Clustal multiple sequence alignment results in 76% sequence homology between HSA and BSA. Protein sequences of ovine serum albumin of bos taurus (GenBank: CAA76847.1) and albumin of homo sapiens (GenBank: AAA98797.1) were aligned.

```
Homo        MKWVTFISLLFLFSSAYSRGVFRRDAHKSEVAHRFKDLGEENFKALVLIAFAQYLQQCPF 60
Bos         MKWVTFISLLLLFSSAYSRGVFRRDTHKSEIAHRFKDLGEEHFKGLVLIAFSQYLQQCPF 60
            **********:**************:****:**********:**.******:********

Homo        EDHVKLVNEVTEFAKTCVADESAENCDKSLHTLFGDKLCTVATLRETYGEMADCCAKQEP 120
Bos         DEHVKLVNELTEFAKTCVADESHAGCEKSLHTLFGDELCKVASLRETYGDMADCCEKQEP 120
            ::*******:************  .*:**********:**.**:******:***** ****

Homo        ERNECFLQHKDDNPNLPRLVRPEVDVMCTAFHDNEETFLKKYLYEIARRHPYFYAPELLF 180
Bos         ERNECFLSHKDDSPDLPKLK-PDPNTLCDEFKADEKKFWGKYLYEIARRHPYFYAPELLY 179
            *******.****.*:**:*  *: :.:*  *: :*:.*  ********************:

Homo        FAKRYKAAFTECCQAADKAACLLPKLDELRDEGKASSAKQRLKCASLQKFGERAFKAWAV 240
Bos         YANKYNGVFQECCQAEDKGACLLPKIETMREKVLTSSARQRLRCASIQKFGERALKAWSV 239
            :*::*:..* ***** **.******:: :*::  :***:***:***:*******:***:*

Homo        ARLSQRFPKAEFAEVSKLVTDLTKVHTECCHGDLLECADDRADLAKYICENQDSISSKLK 300
Bos         ARLSQKFPKAEFVEVTKLVTDLTKVHKECCHGDLLECADDRADLAKYICDNQDTISSKLK 299
            *****:******.**:**********.**********************:***:******

Homo        ECCEKPLLEKSHCIAEVENDEMPADLPSLAADFVESKDVCKNYAEAKDVFLGMFLYEYAR 360
Bos         ECCDKPLLEKSHCIAEVEKDAIPENLPPLTADFAEDKDVCKNYQEAKDAFLGSFLYEYSR 359
            ***:***************:* :* :**.*:***.*.******* ****.*** *****:*

Homo        RHPDYSVVLLLRLAKTYETTLEKCCAAADPHECYAKVFDEFKPLVEEPQNLIKQNCELFE 420
Bos         RHPEYAVSVLLRLAKEYEATLEECCAKDDPHACYSTVFDKLKHLVDEPQNLIKQNCDQFE 419
            ***:*:* :****** **:***:***  *** **:.***::* **:**********: **

Homo        QLGEYKFQNALLVRYTKKVPQVSTPTLVEVSRNLGKVGSKCCKHPEAKRMPCAEDYLSVV 480
Bos         KLGEYGFQNALIVRYTRKVPQVSTPTLVEVSRSLGKVGTRCCTKPESERMPCTEDYLSLI 479
            :**** *****:****:***************.*****::**.:**::****:*****::

Homo        LNQLCVLHEKTPVSDRVTKCCTESLVNRRPCFSALEVDETYVPKEFNAETFTFHADICTL 540
Bos         LNRLCVLHEKTPVSEKVTKCCTESLVNRRPCFSALTPDETYVPKAFDEKLFTFHADICTL 539
            **:***********::******************  ******* *: : **********

Homo        SEKERQIKKQTALVELVKHKPKATKEQLKAVMDDFAAFVEKCCKADDKETCFAEEGKKLV 600
Bos         PDTEKQIKKQTALVELLKHKPKATEEQLKTVMENFVAFVDKCCAADDKEACFAVEGPKLV 599
            .:.*:***********:*******:****:**::*.***:*** *****:*** ** ***

Homo        AASQAALGL 609
Bos         VSTQTALA- 607
            .::*:**.
```

Figure A.1: Sequence alignment of HSA and BSA.

## A.3 Sequence alignment - PBP2x and PBP2x*

Clustal multiple sequence alignment show that the soluble derivative of PBP2x (PBP2x*) leaks aa 19-48. Protein sequences of PBP2x (Swiss-Prot: P59676.1) and PBP2x* (Section A.1) were aligned.

```
gi|PBP2x        MKWTKRVIRYATKNRKSPAENRRRVGKSLSLLSVFVFAIFLVNFAVIIGTGTRFGTDLAK 60
gi|PBP2x*       MKWTKRVIRYATKNRKSP----------------------------GTGTRFGTDLAK 30
                ******************                              ************

gi|PBP2x        EAKKVHQTTRTVPAKRGTIYDRNGVPIAEDATSYNVYAVIDENYKSATGKILYVEKTQFN 120
gi|PBP2x*       EAKKVHQTTRTVPAKRGTIYDRNGVPIAEDATSYNVYAVIDENYKSATGKILYVEKTQFN 90
                ************************************************************

gi|PBP2x        KVAEVFHKYLDMEESYVREQLSQPNLKQVSFGAKGNGITYANMMSIKKELEAAEVKGIDF 180
gi|PBP2x*       KVAEVFHKYLDMEESYVREQLSQPNLKQVSFGAKGNGITYANMMSIKKELEAAEVKGIDF 150
                ************************************************************

gi|PBP2x        TTSPNRSYPNGQFASSFIGLAQLHENEDGSKSLLGTSGMESSLNSILAGTDGIITYEKDR 240
gi|PBP2x*       TTSPNRSYPNGQFASSFIGLAQLHENEDGSKSLLGTSGMESSLNSILAGTDGIITYEKDR 210
                ************************************************************

gi|PBP2x        LGNIVPGTEQVSQRTMDGKDVYTTISSPLQSFMETQMDAFQEKVKGKYMTATLVSAKTGE 300
gi|PBP2x*       LGNIVPGTEQVSQRTMDGKDVYTTISSPLQSFMETQMDAFQEKVKGKYMTATLVSAKTGE 270
                ************************************************************

gi|PBP2x        ILATTQRPTFDADTKEGITEDFVWRDILYQSNYEPGSTMKVMMLAAAIDNNTFPGGEVFN 360
gi|PBP2x*       ILATTQRPTFDADTKEGITEDFVWRDILYQSNYEPGSTMKVMMLAAAIDNNTFPGGEVFN 330
                ************************************************************

gi|PBP2x        SSELKIADATIRDWDVNEGLTGGRMMTFSQGFAHSSNVGMTLLEQKMGDATWLDYLNRFK 420
gi|PBP2x*       SSELKIADATIRDWDVNEGLTGGRMMTFSQGFAHSSNVGMTLLEQKMGDATWLDYLNRFK 390
                ************************************************************

gi|PBP2x        FGVPTRFGLTDEYAGQLPADNIVNIAQSSFGQGISVTQTQMIRAFTAIANDGVMLEPKFI 480
gi|PBP2x*       FGVPTRFGLTDEYAGQLPADNIVNIAQSSFGQGISVTQTQMIRAFTAIANDGVMLEPKFI 450
                ************************************************************

gi|PBP2x        SAIYDPNDQTARKSQKEIVGNPVSKDAASLTRTNMVLVGTDPVYGTMYNHSTGKPTVTVP 540
gi|PBP2x*       SAIYDPNDQTARKSQKEIVGNPVSKDAASLTRTNMVLVGTDPVYGTMYNHSTGKPTVTVP 510
                ************************************************************

gi|PBP2x        GQNVALKSGTAQIADEKNGGYLVGLTDYIFSAVSMSPAENPDFILYVTVQQPEHYSGIQL 600
gi|PBP2x*       GQNVALKSGTAQIADEKNGGYLVGLTDYIFSAVSMSPAENPDFILYVTVQQPEHYSGIQL 570
                ************************************************************

gi|PBP2x        GEFANPILERASAMKDSLNLQTTAKALEQVSQQSPYPMPSVKDISPGDLAEELRRNLVQP 660
gi|PBP2x*       GEFANPILERASAMKDSLNLQTTAKALEQVSQQSPYPMPSVKDISPGDLAEELRRNLVQP 630
                ************************************************************

gi|PBP2x        IVVGTGTKIKNSSAEEGKNLAPNQQVLILSDKAEEVPDMYGWTKETAETLAKWLNIELEF 720
gi|PBP2x*       IVVGTGTKIKNSSAEEGKNLAPNQQVLILSDKAEEVPDMYGWTKETAETLAKWLNIELEF 690
                ************************************************************

gi|PBP2x        QGSGSTVQKQDVRANTAIKDIKKITLTLGD 750
gi|PBP2x*       QGSGSTVQKQDVRANTAIKDIKKITLTLGD 720
                ******************************
```

Figure A.2: Sequence alignment of PBP2x and PBP2x*.